"MOLECULAR CHAMELEONS": DESIGN AND SYNTHESIS OF A SECOND SERIES OF FLEXIBLE NUCLEOSIDES.

A Dissertation
Presented to
The Academic Faculty

By

Samer Salim

In Partial Fulfillment
Of the Requirement for the Degree
Doctor of Philosophy in Chemistry

Georgia Institute of Technology
December, 2004

"MOLECULAR CHAMELEONS": DESIGN AND SYNTHESIS OF A SECOND SERIES OF FLEXIBLE NUCLEOSIDES

Approved by:

Dr. Katherine L. Seley, Advisor
School of Chemistry

Dr. David M. Collard
School of Chemistry

Dr. Donald F. Doyle
School of Chemistry

Dr. Suzzane B. Shuker
School of Chemistry

Dr. Harish Radhakrishna
School of Biology

Date Approved: November 2004

"Read! And thy Lord is Most Bountiful - He who taught (the use of) the Pen, Taught the human that which he knew not." *Al-Qur'an [96:3-5]*

DEDICATION

To my beloved parents Dr. Abu Salim and Zarrin Salim, and my dear sisters Zeba Aisha Salim and Sofia Almas Salim.

ACKNOWLEDGEMENT

I would like to thank Professor Katherine L. Seley for being an exceptional research advisor and mentor. She has provided immense support, guidance and leadership throughout my graduate career. Furthermore, she has allowed me to excel and reach new heights that I may have deemed unimaginable.

I am thankful to my thesis committee members: Professors David M. Collard, Donald F. Doyle, Suzanne B. Shuker, and Harish Radhakrishna for their precious time and support.

I am extremely appreciative towards Dr. Liang Zhang for his helpful advice on different synthetic approaches. I am grateful to Lauren Schwimmer and Peter O'Daniel for their guidance with molecular modeling.

I would also like to thank Dr. Les Gelbaum for NMR assistance as well as David Bostwick and Sarah Shealy for mass spectrometry assistance.

I would like to give many special thanks to the scientific community at the University of Maryland, Baltimore County for their excellent resources and amazing support throughout the final year of graduate school.

It gives me great pleasure to thank the Seley Research Group members, past and present, Dr. Liang Zhang, Dr. Asmerom M. Hagos, Sylvester L. Mosley, Peter I. O'Daniel, Joshua M. Sadler, and Naresh K. Sunkara for all their helpful advice and assistance with editing and proof reading. I will always look back on our friendship within the group with fond memories.

Moreover, I would like to thank my best friend Munir J. Huq for his guidance and wisdom throughout my high school, undergraduate and graduate career.

And, finally, I would like to thank my dear friends and family members for their love and support.

TABLE OF CONTENTS

LIST OF TABLES

LIST OF FIGURES

LIST OF SCHEMES

LIST OF ABBREVIATIONS

3TC……...…Lamivudine

ADA……..…….adenosine deaminase

Ado……...adenosine

AIDS…….. .....Acquired Immunodeficiency Syndrome

ara-A……...….arabinosyladenosine

ara-C……...arabinosylcytidine

Arg……..arginine

Ari…….…….aristeromycin

Asn…….…….…….asparigine

Asp……...……aspartic acid

ATP…….……adenosine triphosphate

AZT…….…….……..……zidovudine

BSA……..…..N,*O*-bis(trimethylsilyl)acetamide

CTP…….……..…..……cytidine triphosphate

cff……...…….consistent force field

cvff……..…….constant valence force field

d4T……..……..……stavudine

dba…….……dibenzylideneacetone

ddC……..……....zalcitabine

ddI……..……..…didanosine

DME…….……..…1,2-dimethoxyethane

DMF……..…….……..….*N*,*N*-dimethylformamide

DNA……..…..…….…….deoxyribonucleic acid

dppf……1’,1’ bis(diphenylphosphino)ferrocene

DTNB……...…...……..5,5’-dithiobis-2-nitrobenzoic acid

FUDR……...……..5’-fluoro-2’-deoxyuridine

GA……genetic algorithm

Glu……..……...glutamic acid

Hcy…….……...……homocysteine

His……..……histidine

HIV…….....……Human Immunodeficiency Virus

HIV-RT…….……..……...HIV-reverse transcriptase

HMDS…….……..……....……hexamethyldisilazane

HSV……..……....……Herpes Simplex Virus

isoG……..…..……..…isoguanosine

Lys……..……..……..…lysine

MCM……..…..……Monte Carlo minimazation

MD…….....….……...molecular dynamics

MeTase…….....……...…methyltransferase

mRNA…….……..……messenger RNA

MSNI……...minimization with shifted nonbonded interactions

MUSIC…….....…multi-unit search for interacting conformers simulations

NADH……...…..……...….nicotinamide adenine dinucleotide

NpcA…….……..……...……...…neplanocin A

PNP……...……purine nucleoside phophorylase

PPh_3……...……triphenylphosphine

RNA……...……ribonucleic acid

SAH……...……...…*S*-adenosylhomocysteine

SAHase…….*S*-adenosylhomocysteine hydrolase

SAM…… *S*-adenosylmethionine

SARS……Sudden Acute Respiratory Syndrome

TBAI……tetrabutylammonium iodide

THF…….……tetrahydrofuran

Thr…….……threonine

TK……thymidine kinase

TMSOTf…….……trimethylsilyl triflate

TNB……2-nitro-5-thiobenzoic acid

Tyr……...……...……...tyrosine

WHO……World Health Organization

SUMMARY

It has recently been shown that the binding site of SAHase, an enzyme critical in the replication mechanism of viruses, is quite flexible and exhibits a large difference between the "open" and "closed" conformations, thus presenting an obstacle towards design efforts. As a possible solution to this dilemma, we have strategically designed and synthesized a series of structurally innovative nucleosides possessing a heteroaromatic purine ring split into its two components (for example, an imidazole and pyrimidine ring), thereby conferring additional degrees of conformational freedom and torsional flexibility to the ligand. As a result, these molecular "chameleons" can adapt to the environment of the flexible binding site in order to maximize and complement structural interactions, without losing the integrity of the crucial contacts involved in the enzyme's mechanism of action. The synthesis of several proximal analogues is presented herein.

CHAPTER I

BACKGROUND AND SIGNIFICANCE

According to Alfred Burger,[1] medicinal chemistry "remains a challenging science, which provides satisfaction to its practitioners. It intrigues those of us who like to solve problems posed by nature. It verges increasingly on biochemistry and on all the physical, genetic and chemical riddles in animal physiology which bear on medicine. Medicinal chemists have a chance to participate in the fundamentals of prevention, therapy and understanding of diseases and thereby to contribute to a healthier and happier life." Medicinal chemistry is defined as an interdisciplinary science situated at the interface of organic chemistry and the life sciences such as biochemistry, pharmacology, molecular biology, immunology, pharmacokinetics and toxicology on one side and chemistry-based disciplines such as physical chemistry, crystallography, spectroscopy and computational modeling on the other.[2]

Medicinal chemistry has been practiced for several thousand years as was indicative from *Pen-t'sao*, a book of herbs by the Chinese Emperor Shen Nung. [2] The root *Dichroa febrifuga*, known as *Ch'ang Shan* during the emperor's reign, was prescribed for the treatment of fevers.[2] Ironically, this root contains alkaloids, a natural product containing a basic nitrogen, which is now found in pharmaceutical drugs for malaria. *Ma Huang*, now known as *Ephedra sinica*, was used as a heartstimulant, diaphoretic agent and cough suppressant. *Ma Huang* contains ephedrine which is used to treat bronchial asthma and raise blood pressure.

In this "prescientific" period, the majority of remedies were discovered by chewing on cinchona bark, roots, leaves and berries, as evidenced by the written records of the Chinese, Indian, South American, Middle Eastern and Mediterranean cultures.[2] Only within the last 150 years have scientists searched for the active components of these medicinal agents.[2] Although little of modern-drug therapy is based on these "prescientific" remedies, it is fascinating to observe that the approach to the practice of medicinal chemistry has developed from such a fundamental process.

Development of drug therapy progressed rapidly after the discovery of DNA as the primary genetic material in 1944 and subsequent elucidation of the physical structure in 1953.[3] Since the nucleic acids DNA and RNA are the initial precursors in the formation of proteins that are responsible for many biological and physiological processes, it is logical that these molecules could be viewed as potential targets for drug design and development.[4] DNA and RNA are biopolymers composed of nucleosides held together by phosphodiester linkages, as a result, the nucleosides can also be considered as potential targets.[3,4]

In 1909, the term "nucleoside" was proposed by Levene and Jacobs to describe carbohydrate derivatives of purines and pyrimidines.[5] The nucleoside constituents of RNA and DNA are composed of a sugar moiety, β-D-ribofuranose and 2'-deoxyribose-β-D-ribofuranose respectively, linked to either a purine (adenine or guanine) or pyrimidine (cytosine, thymine or uracil) heterocyclic base via a glycosidic bond, through the N-9 of the purine or the N-1 of the pyrimidine base (Figure 1). The purine bases adenine and guanine, as well as the pyrimidine base

cytosine, are common to both DNA and RNA whereas the pyrimidine base thymine only occurs in DNA and uracil in RNA.

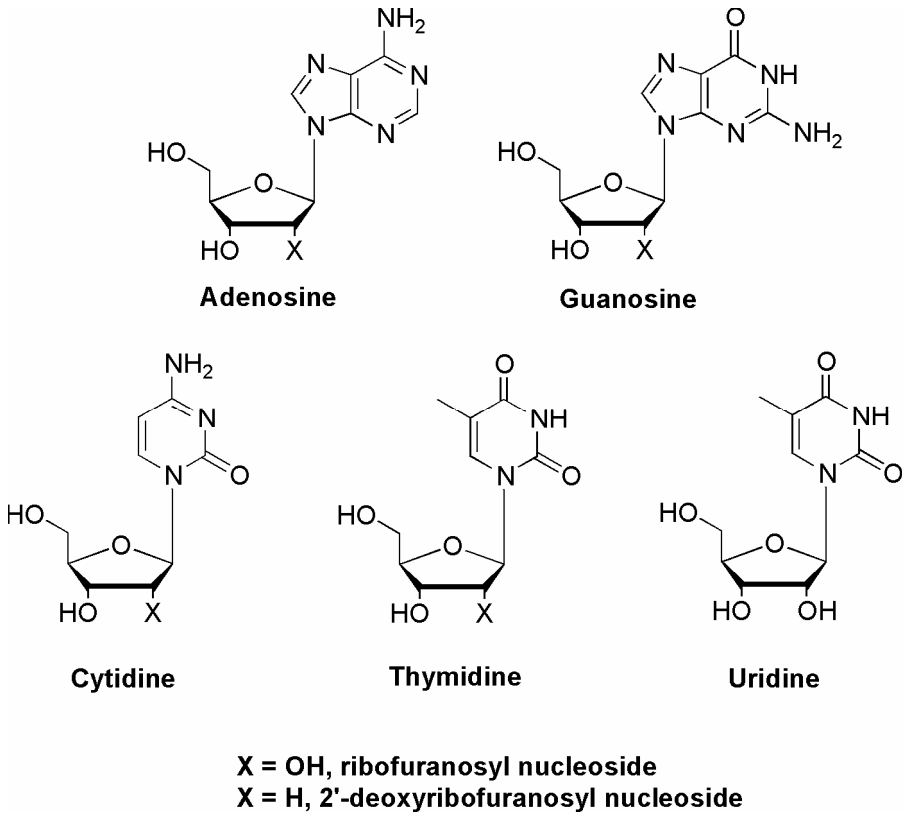

Figure 1. The naturally-occurring nucleosides in DNA and RNA.

It was not until the 1960's, that chemistry involving nucleosides and nucleotides provided the fundamental infrastructure and synthetic methodology necessary to produce numerous biologically active naturally occurring and structurally modified nucleosides. The biological activity of anticancer agents such as 5-fluoro-2'-deoxyuridine (FUDR), arabinosylcytidine (ara-C), 8-azainosine, along with the discovery of a potent antiviral nucleoside, arabinosyladenosine (ara-A), and

antitumor agent, toyocamycin revealed the potential value of modified nucleoside analogues as chemotherapeutic agents (Figure 2).[6,7]

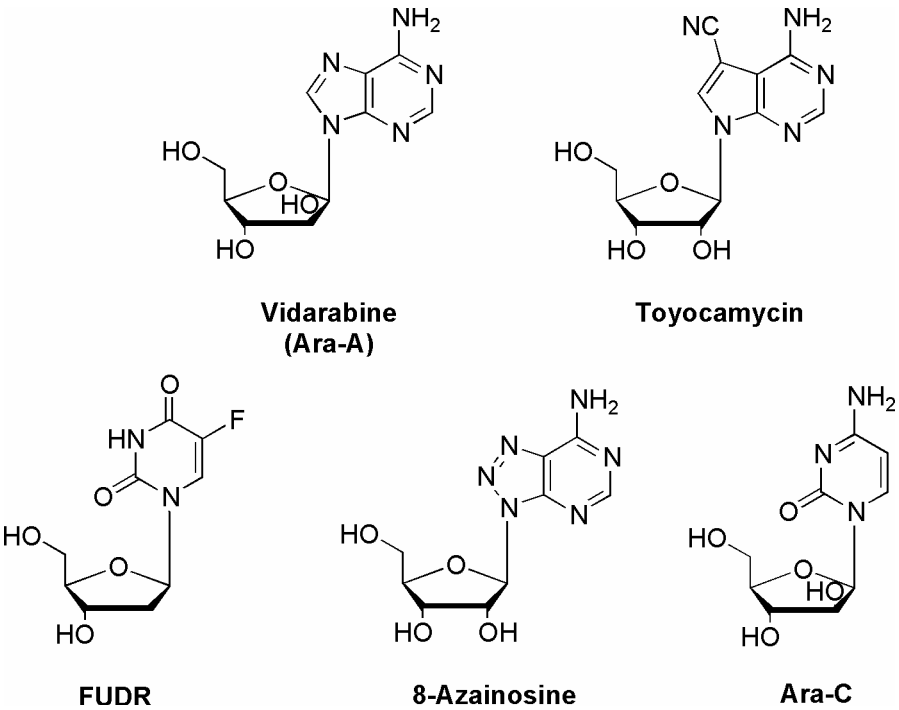

Figure 2. Some FDA-approved nucleoside drugs.

The importance of these nucleoside analogues was later confirmed with the emergence of HIV as the main etiological agent of AIDS.[8] The first drug approved for the treatment of HIV was the modified nucleoside AZT which inhibits HIV-1 reverse transcriptase.[9] Furthermore, several other nucleoside analogues involved in inhibition of HIV-1 reverse transcriptase, namely ddC, ddI, d4T and 3TC, have provided even more significance to the use of nucleoside analogues as biologically potent chemotherapeutic agents (Figure 3 on the next page).[8,10,11]

Despite these examples, clinical use of these drugs is limited due to several factors, including toxicity, the wide range of side effects, problems with lipophilicity

and crossing cell membranes, and susceptibility to enzymatic cleavage.[11] This has prompted researchers to search for more advanced chemotherapeutic agents that could address these issues. Some of the approaches pursued for "second generation" nucleosides included structural modifications to either the sugar moiety or to the purine or pyrimidine heterocyclic base.

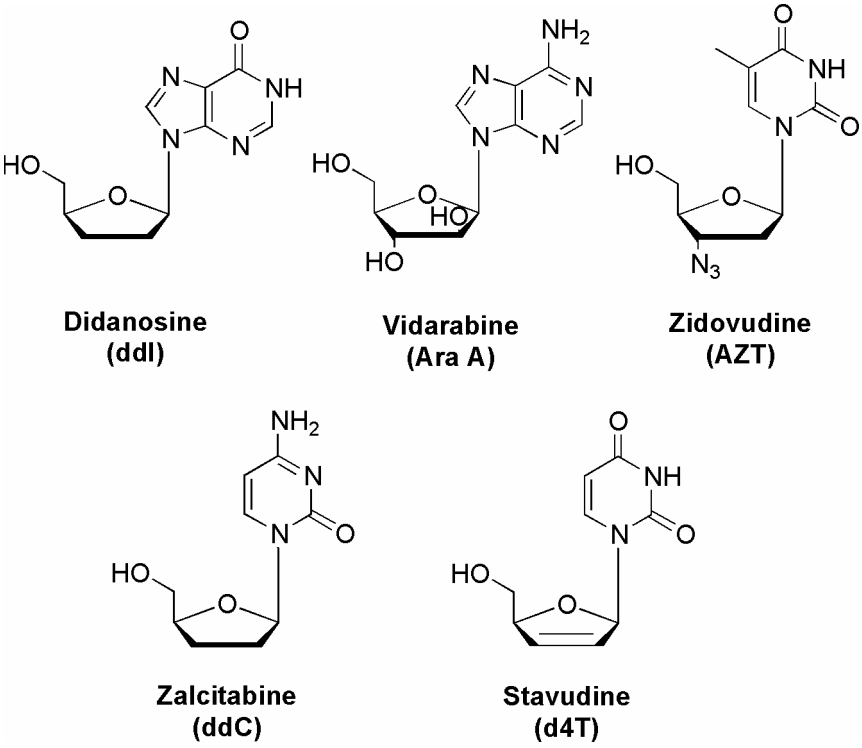

Figure 3. Some potent nucleoside-based inhibitors of HIV-1 RT.

One structural modification that has proven valuable is the replacement of nitrogen atom or atoms, within the heterocyclic ring scaffold, with a methine group to form for example, 1-deaza, 3-deaza, 7-deaza or 9-deazapurine nucleoside analogues (Figure 4). The deazapurine modified nucleosides have been extensively studied and have shown to have anticancer and antiviral properties.

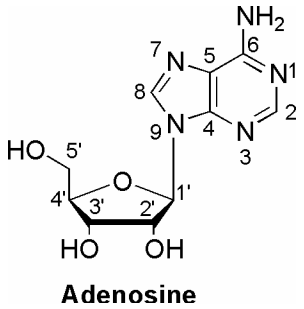

Figure 4. Heteroaromatic purine ring and ribosyl numbering.

Montgomery *et al* first synthesized 3-deazaadenosine,[12] which exhibited potent biological activity and surprisingly, did not undergo phosphorylation at the 5' position. Moreover, 3-deazaadenosine has been shown to inhibit *S*-adenosylhomocysteine hydrolase,[13] a widely recognized enzymatic target for antiviral, antiparasitic and anticancer agents. Some of the 7-deazanucleosides such as tubericidin, toyocomycin and sangivamycin have exhibited significant antitumor activity *in vivo* (Figure 5 on the next page).[11,14] The 7-deazanucleosides have potential advantages over conventional purine nucleosides, as in the case of tubercidin. These advantages include stability towards both adenosine deaminase (ADA) and purine nucleoside phosphorylase (PNP), enzymes which are involved in biologically important pathways.[15,16] Hence, these modified purine-based nucleosides have become potential chemotherapeutic agents for a variety of antiviral based diseases.

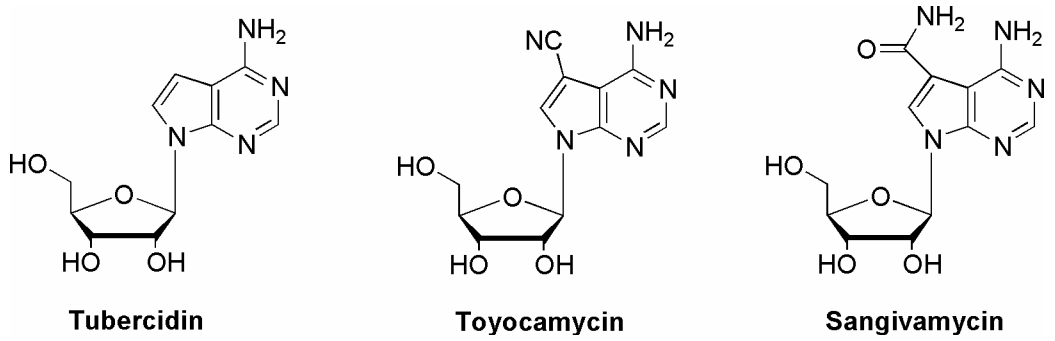

Figure 5. Examples of biologically significant 7-deazapurine nucleosides.

Modification of N-1 to a methine group within the heteroaromatic purine affords the 1-deazapurines which disrupts the hydrogen-bonding within Watson-Crick base pair and ultimately disturbs protein synthesis. 1-Deazaadenosine and its analogues have shown to possess potent antitumor activity[17] as well as to be an inhibitor of ADA[18] and blood platelet aggregation.[19]

Another purine modification that has been extensively studied is the replacement of the methine groups, especially at C-2 and C-8, with a nitrogen atom resulting in 2-azaadenosine and 8-azaadenosine respectively (Figure 6). 8-Azaadenosine, as well as 8- azainosine and 8-azaguanosine, have exhibited potent anticancer activity *in vivo* (Figure 7 on the next page).[20]

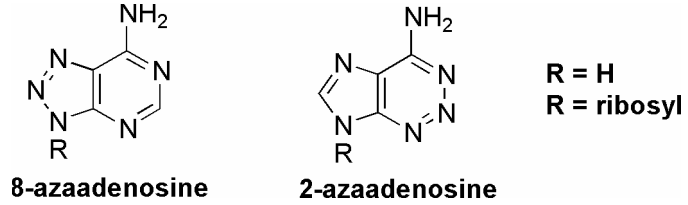

Figure 6. Modification of the C-8 and C-2 position of adenosine.

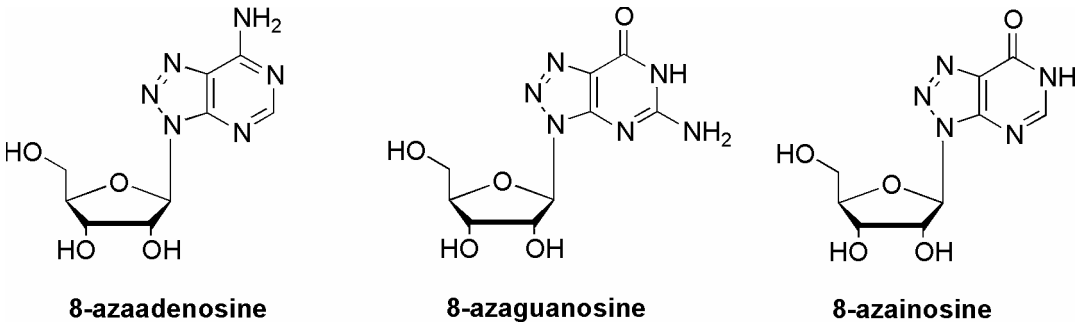

Figure 7. Biologically potent 8-azapurines.

Furthermore, when these 8-azanucleosides are phosphorylated by kinases into their respective monophosphate forms, they are incorporated into RNA thereby disrupting protein synthesis.[7] 2-Azaadenosine, a fluorescent nucleoside, has displayed modest *in vivo* activity against both murine L1210 leukemia cells and rat mammary tumor cell lines.[21]

Combining both deaza and aza components in a heterocyclic purine moiety has resulted in other biologically potent purine modified nucleosides. For instance, 8-aza-7-deazaadenosine resulted in moderate activity against PNP. Additionally, 8-aza-1-deaza-6-chloropurine nucleosides are known to inhibit PNP as well as to exhibit moderate antiviral activity against the polio (Sb-1) virus (Figure 8). [22]

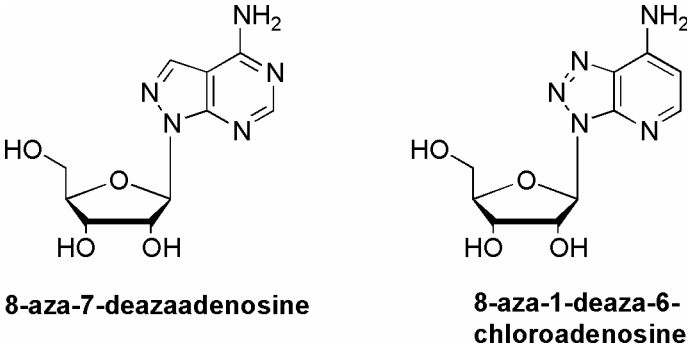

Figure 8. Biologically potent modified nucleosides.

Further approaches to the modifications of purines have involved the incorporation of other heteroatoms such as sulfur or oxygen, which allows the heterocyclic moiety to retain its aromaticity. Modifications involving other heteroaromatic bases such as pyrimidines have not been as extensively studied as purines, however, their modifications have primarily resulted in aza/deaza pyrimidine-based nucleosides and extended pyrimidine ring systems. 5-Azacytidine, along with its 2'-deoxy analogue, has displayed significant biological activity against L1210 leukemia cells and is presently used clinically in the treatment of acute leukemia.[23] 3-Deazauridine, another modified pyrimidine-based nucleoside, has also shown significant biologically activity against leuekemia[24] and as well as inhibitory activity against CTP synthetase,[25] an enzyme involved in cytosine nucleotide metabolism (Figure 9).

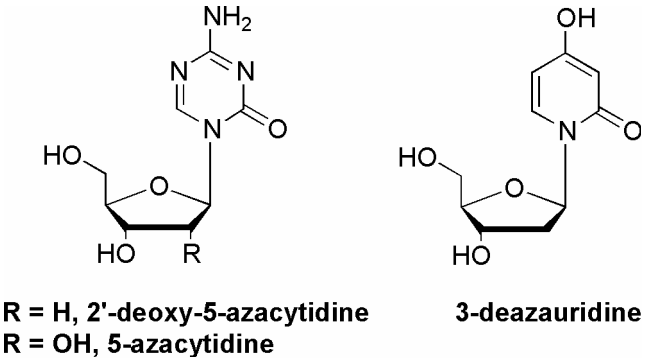

Figure 9. Biologically potent modified pyrimidine-based nucleosides.

Another structural modification that has been extensively used is the isosteric replacement of the furanose oxygen of the sugar moiety with a methylene subunit (where X = CH_2) resulting in a carbocyclic nucleoside (Figure 10 on the next page).

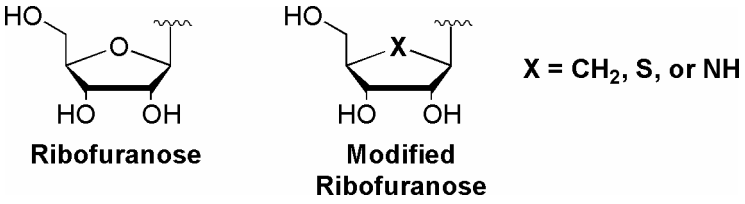

Figure 10. Some modifications of the ribose moiety.

This modification transforms the glycosidic bond from an unstable hemiaminal to a more stable tertiary amine which endows the nucleoside with the ability to resist cleavage by phosphorylases, as well as to increase its overall lipophilicity.[26] The naturally occurring carbocyclic nucleosides aristeromycin and neplanocin A and their 4',5'-unsubstituted analogues have shown significant biological activity against both SAHase and DNA MeTase, another important enzymatic target for antiviral, antiparasitic and anticancer agents (Figure 11).[27,28] Although the carbocylic nucleosides are synthetically challenging, a generation of extremely potent antiviral carbocyclic nucleosides such as carbovir, abacavir and lobucavir have been produced (Figure 12 on the next page).

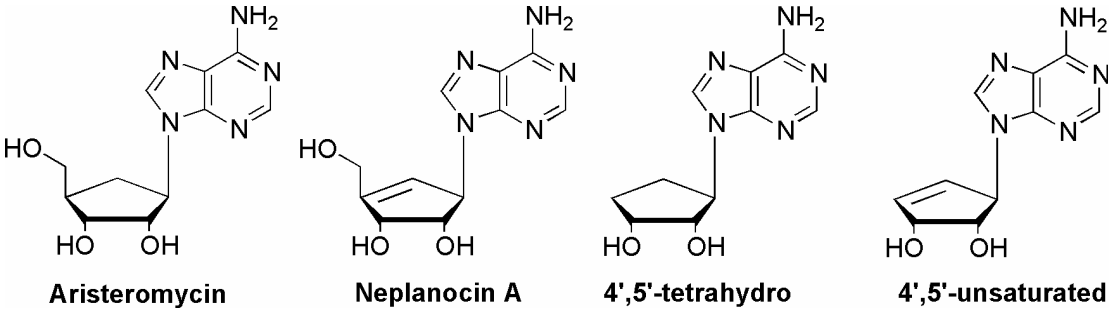

Figure 11. Naturally occurring carbocyclic analogues (Ari and NpcA) and their synthetic analogues (4',5'-tetrahydro and 4',5'-unsaturated).

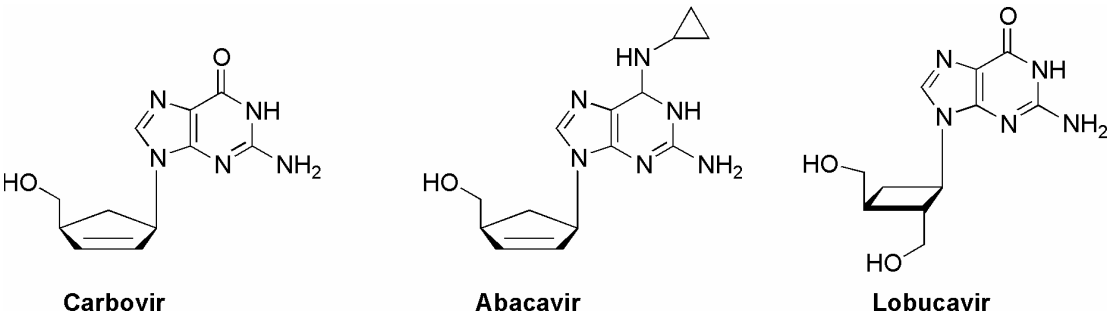

Figure 12. Extremely potent antiviral carbocylic nucleosides.

Approaches to Drug Development and Design

In order to design a "perfect" drug it is essential to identify the cause for the disease since most diseases result from one of these major causes; one, an imbalance of certain chemicals in the body, two, from the invasion of a virus or a foreign organism, or three, from abnormal cell growth.[2] This imbalance can often times be overcome by inhibition of a particular enzyme, interference with DNA replication or inhibition of certain biosynthetic pathways within the virus.

Once the pertinent biochemical system is identified, a prototypical or lead compound, is sought which has exhibited desirable biological and pharmacological effects but may have some unfavorable properties such as toxicity, insolubility, or metabolism problems.[2] There are several traditional approaches to the identification of a lead compound; these include random screening or nonrandom screening of various types of compounds, drug metabolism studies or even clinical observations of the affects of a drug.[2] Once a lead compound is identified, systematic structural modifications are undertaken which include homologation, chain branching, ring chain transformations and bioisosterism resulting in a structure-activity relationship study.

For instance, a homologous series of compounds, where each successive compound differs by a simple structural unit, generally a $–CH_2$ group, is synthesized to hopefully produce an increased pharmacological response.[4] Another variation that can be made is the "transformation" of straight chains into branched chains which will inherently affect the lipophilic relationship and ultimately alter the potency of a compound. Another common modification of a side chain is the conversion of alkyl substituents into their corresponding cyclic analogues.[4] The potential for this approach was clearly observed in the development of the highly potent HIV-RT inhibitor Abacavir, in which the C-6 amino group was alkylated with a cyclopropyl as opposed to an *n*-propyl group, thereby increasing the potency significantly (Figure 12 on the previous page). Finally, bioisosterism is a technique that is widely used to modify lead compounds into safer and more clinically effective chemotherapeutic agents by exchanging an atom or group of atoms with a similar atom or group of atoms.[4] Bioisoteres are classified as either classical or nonclassical bioisosteres. Classical bioisosteres are those groups which have similar steric and electronic features but may or may not have a different number of atoms as compared to the structural moiety for which they are used as a replacement.[4] In contrast, nonclassical bioisosteres do not obey the strict steric and electronic definition of classical isosteres, and they do not have the same number of atoms as the moiety for which they are used as a replacement.[4] These isosteres are capable of maintaining similar biological activity by imitating the spatial arrangement, electronic properties, or some other physiochemical property of the structural piece or functional group that is critical for the retention of biological activity. Regardless of the type of modification,

it is expected that successful structural modifications to a lead compound will lead to greater biological activity as well as to eliminate any undesirable characteristics.

Since the interaction of a drug with an enzyme is extremely specific, usually only a small fragment of the lead compound, known as the pharmacophore, may be involved in the necessary interactions which lead to biological activity.[2] Further systematic structural manipulation of the pharmacophore results in second generation analogues of lead compounds, usually provides useful information regarding structure-activity relationships.[2] This information can then be exploited to construct an even better drug with an improved therapeutic index which is a measure of the ratio of the undesirable to desirable drug effects.

As straightforward as it may seem to develop new inhibitors for known enzymes, there are many factors to consider when designing potential inhibitors for a particular enzyme binding site. These include variable energies for an enzyme's conformations, multiple binding modes and even differential solvation effects.[2,4] More importantly, it is necessary to consider the conformational changes of not only the inhibitor, but the enzyme to predict optimal binding, which, even if achieved does not guarantee activity.

The first attempt to explain the specificity of enzyme interactions was formulated by Emil Fischer in 1894.[3] Fischer termed his hypothesis as a "lock and key" mechanism (Figure 13 on the next page),[29,30] and stated "the specificity of an enzyme (the lock) for its substrate (the key) arises from their geometrically complementary shapes." This theory was ultimately shown to be flawed since it suggested that enzymes only have one optimal substrate and other substrates, as

similar as they might seem, do not "fit" as well and therefore catalyze reactions less efficiently. Therefore, the drawback is that if the active site has a rigid structure, it cannot fit both the substrate and the products of a reversible reaction in an optimum fashion.

(a)

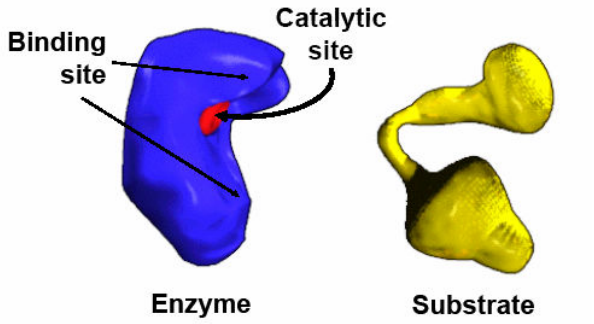

(b)

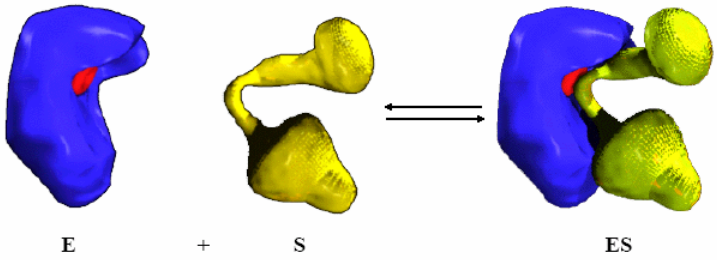

Figure 13. (a) The enzyme's active site and the substrate. (b) The lock and key model.

Obviously, this is not true for all cases since some enzymes can catalyze reactions for a range of different substrates. In order to explain this observation, Daniel Koshland proposed that the enzyme does not have to be in the appropriate conformation required for the substrate to bind, rather the enzyme is forced into a conformational change in order to adopt the optimal shape to accommodate the

binding of substrates to the active site. This mode of action, termed as "induced fit", explains why enzymes can accommodate a range of substrates (Figure 14).[31-33] A related model to the "induced fit" theory is "conformational selection" theory which hypothesizes that a particular conformation of the binding site exists that has the appropriate geometry for biological activity, but that conformation is only a small percentage of the various conformations that the enzyme is capable of, therefore not highly populated.[34-36] Overall, the induced fit and conformational selection models are significantly different from the "lock and key" model since they both display the importance of protein flexibility. Flexibility may play an active role in binding specificity due to the interactions produced upon binding structurally distinct molecules to structurally distinct protein conformations.

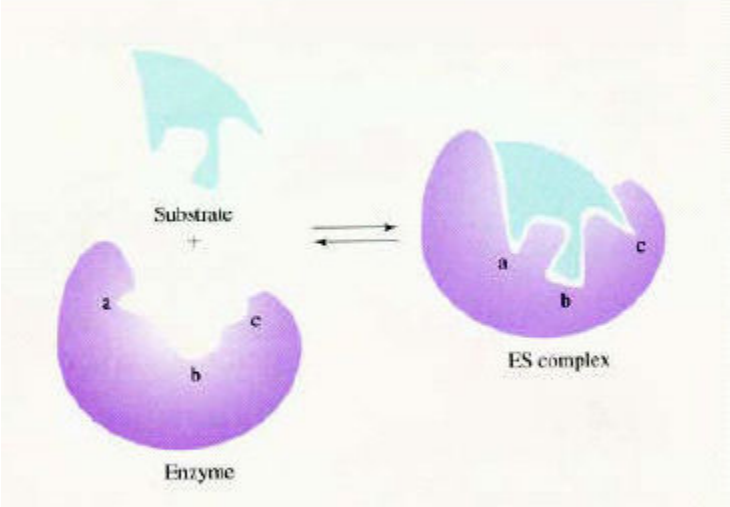

Figure 14. The induced fit model.

Historically, prior to the availability of sophisticated instrumentation, structural information such as highly resolved X-ray crystal structures or high field solution NMR structures of enzymes and enzyme-ligand binding complexes, scientists were forced to elucidate the parameters of active sites by several methods.[2,4] One such approach involved the synthesis and biological testing of large numbers of potential inhibitors that closely resembled the basic structure of the natural substrate of an enzyme. Once the natural substrate or lead compound was identified, systematic alterations of the functional groups on the molecule were done in order to develop more potent chemotherapeutic agents.[2]

Another approach involved the systematic modification of the dimensional parameters of a ligand to analyze the enzyme's active site. Leonard *et al* introduced this innovative approach[37-40] to the nucleoside community by expanding the purine ring system, whereby a spacer ring (or rings) was inserted in some fashion between the two rings of the purine heterocycle, or, extended out from a pyrimidine nucleoside. This led to a variety of shape-modified heterocycles, most notably his *lin*-, *dist*-, and *prox*-benzo-separated heterobases and nucleosides (Figure 15).[37-42]

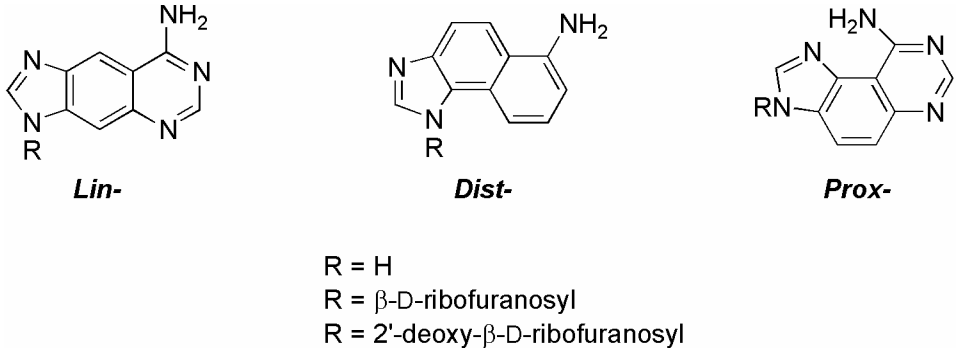

Figure 15. Leonard's benzo-separated adenine analogues.

His pioneering work with extended and expanded purine and pyrimidine nucleosides and nucleotides provided an excellent foundation for using shape-modified nucleosides as dimensional bioprobes to help elucidate structural information about enzymes, as well as to study recognition and binding properties.

Enzymes such as purine nucleoside phophorylase, phosphoryl transfer enzymes such as adenosine kinase, adenylate kinase and pyruvate kinase, hydrolyzing enzymes such as ATPase, as well as other enzymes such as adenosine deaminase and xanthine oxidase, were explored, since purines are recognized in these enzymatic systems. [37-41] Unfortunately, these analogues ultimately proved limited in their utility, partially due to their inherent rigidity.[42]

Although this approach to drug design was rational, it remained random, tedious and of course, expensive. The explosion of cutting-edge computer technology and methodologies to calculate molecular properties have made it increasingly possible to use computer techniques to aid the drug discovery process. If the three-dimensional structure of the target enzyme is available from X-ray crystallography, preferentially co-crystallized with a ligand so that the interactions of the binding site with the ligand are known, it is reasonable to investigate the enzyme-ligand complex by computational molecular modeling. In this way, a detailed knowledge of the interactions between the ligand and the enzyme may be obtained. Potential candidate ligands can then be docked into the binding site in order to predict if the new structure can interact with the enzyme in an optimal way.

Today, crystal structures for many enzymes are readily available, and this has facilitated a more sophisticated approach to the design of new drugs. Computer-

assisted structure-based drug design has emerged as a new tool in medicinal chemistry. The drug design cycle approach shown in Figure 16 begins with creating a computer model of an enzyme-binding site based on known crystallographic data. Next, potential inhibitors or ligands are then docked into the binding site; the computer model of the enzyme- substrate complex is subjected to energy minimization using innovative computer modeling programs. Based on the computational analysis of structural interactions between the enzyme and several different potential substrates; the most promising inhibitors are then synthesized.

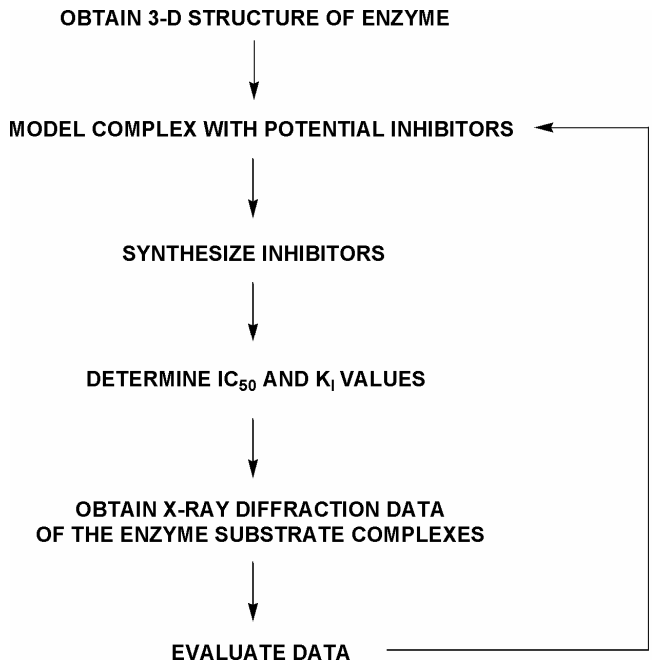

Figure 16. Computer-assisted structure-based drug design.

Each of the targets is then assayed to determine the levels of affinity (K*i*) for the enzyme and the activity against the enzyme (IC_{50}). Additionally, potential inhibitors may also be "soaked" into a preformed crystal of the enzyme to determine

enzyme-substrate interactions via X-ray crystallography. All the collected data is then evaluated, fed back into the algorithm, and used to design a second generation of inhibitors.

Despite the significant advances made in recent years, this approach is still in its formative years and not without numerous failures. For example, it is not uncommon that the "best guess" inhibitor analogues predicted by sophisticated computer modeling programs ultimately prove to be biologically inactive. One early example of this was the work carried out by Ealick *et al* with purine nucleoside phosphorylase (PNP),[43,44] an enzyme involved in the purine salvage pathway of cells. PNP exists as a homotrimer of approximately 100 kDa subunits with three identical active sites (Figure 17).[45]

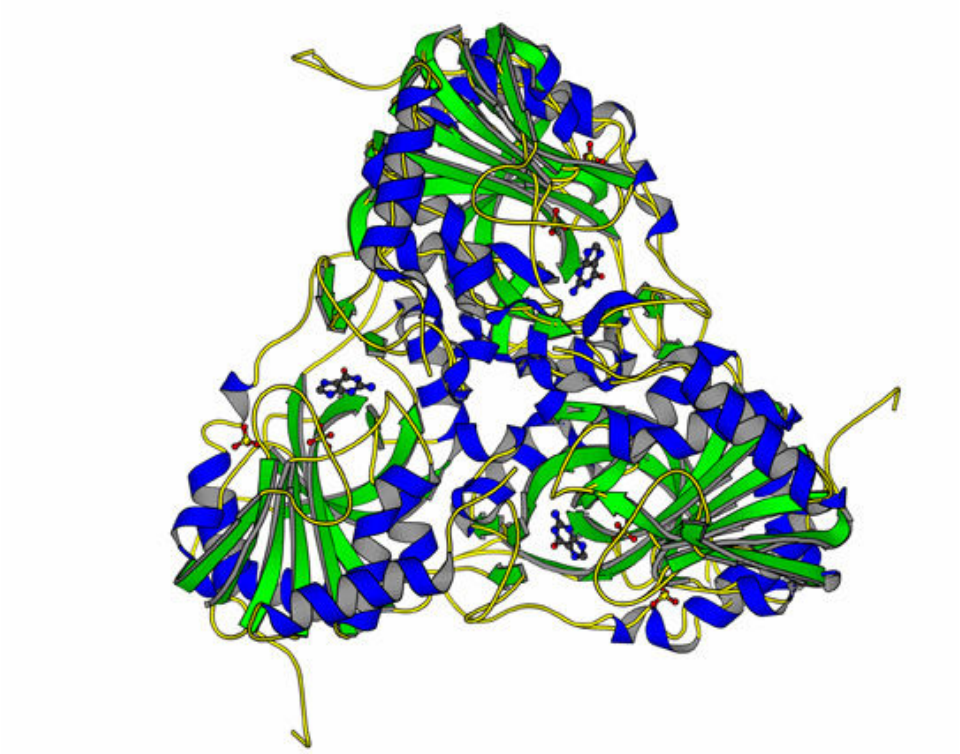

Figure 17. Purine Nucleoside Phosphorylase.[45]

The nucleophilicity of the phosphate ion of PNP assists in cleaving the nucleoside into a free purine base and a phosphorylated sugar. The free purine moiety can then be destroyed or recycled by the cell (Figure 18).[45] The design of PNP inhibitors is extremely vital to the stability of antiviral and anticancer agents as well as to the suppression of T-cell activity. Since many nucleoside-based anticancer and antiviral agents are similar to their natural purine nucleoside, they are recognized by PNP, thereby undergoing cleavage into their cellular components and hence diminishing their therapeutic value. Furthermore, recent compelling evidence has led researchers to believe that PNP is required for the proper functioning of T-cells, however, it does not affect other cellular components of the immune system. Many autoimmune disorders such as psoriasis, rheumatoid arthritis, multiple sclerosis, systemic lupus erythematosus, and insulin-dependent diabetes have abnormally elevated levels of T cell activity.

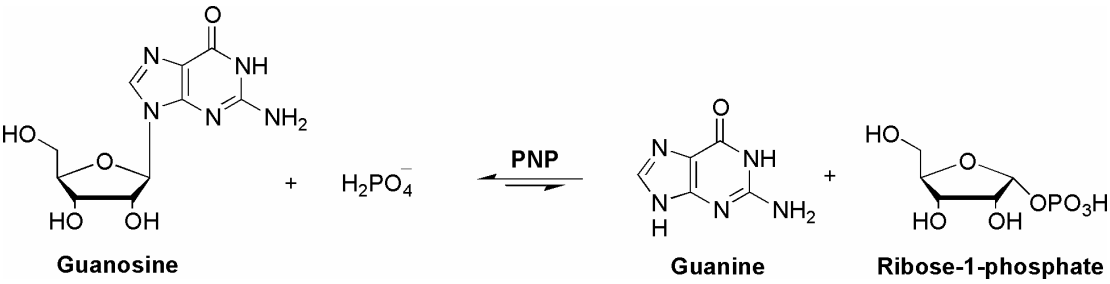

Figure 18. Mechanism of Purine Nucleoside Phosphorylase.

Using molecular modeling programs, Montgomery and coworkers[46] designed several ligands that appeared to have the greatest binding affinity for the crystalline

structure of PNP which is essentially identical to human forms of the enzyme. Unfortunately, the "ideal" ligand, identified by molecular modeling proved to be biologically inactive for PNP.[46] Further studies finally revealed that the binding site of PNP was not static, but rather, underwent significant conformational changes upon binding different ligands.[46] PNP possessed a "swinging gate" of residues that would open to allow a wide variety of ligands to bind, at which point the "gate" would then close, thereby giving the appearance of a perfect fit, when in reality, it was not.[46]

While most programs on the market today have the ability to consider ligand flexibility, few programs are capable of accurately predicting the consequences of flexibility when modeling enzyme binding sites.[47-49] This is a direct consequence of the limitations of the structural information utilized by the program; the origin of this structural information is the X-ray crystallographic coordinates of the crystallized enzyme, which in reality is merely a static "snapshot" of the enzyme-ligand complex. Furthermore, until quite recently, it was believed that only one ideal conformation of the complex was responsible for the biological activity, however, the ever-increasing availability of crystallographic structures has now revealed that many enzymes are capable of adapting a variety of conformations.[50-55] This may offer forth more than just increased inhibitory activity; this also presents unique prospects towards the optimization of other desirable properties for potential drugs such as metabolic stability, bioavailability, and formulation. Given these findings, it is clear that new and more innovative approaches for identifying chemotherapeutically viable enzyme-ligand conformations are vital to the design of new and more potent inhibitors.

Prior to the development of sophisticated docking programs that take into account flexibility of both the enzyme as well as the ligand and the absence of highly resolved X-ray crystal structures of various enzymes, scientists were forced to use very fundamental approaches to study enzyme-ligand interactions.

Approximately 60 years elapsed since the first computation of the steric energy calculation in terms of nonbonded interactions. Westheimer and Mayer[56] calculated the steric contribution as a means to rationalize the rates of racemization of optically active diphenyl compounds. They used mathematical functional forms, and the idea of calculating molecular energy from them was suggested by Hill.[57] Approximately 40 years ago, the first use of an electronic computer to calculate and optimize the molecular energy was made by Hendrickson.[58] He evaluated simple energy functions for angle bending, torsional twisting, and nonbonded contributions to perform functional analysis and find minimum energy geometries for cycloalkanes most notably, cyclopentane, cyclohexane, and cyclohexane.[58]

The impetus for much of the thinking about drug design in the late 1970s and early 1980s was the perception that random screening – so successful in the early days of antibiotics – was no longer likely to be an efficient strategy for drug discovery due to the process being extremely tedious and expensive.[58] Two technological advances of this period have had major impact on the discovery of new therapeutic agents: routine determination of macromolecular structures and the application of molecular biology to produce large quantities of high-purity proteins for assays and structural use. The interest in structure-based or structure-assisted design came from the early ideas of Ehrlich and Fischer, who proposed a geometric –

lock and key analogy – for drug action.[29,30] This powerful idea has been the model of receptor fitting, pharmacophore matching, and database searching, despite general acknowledgement that it has many shortcomings, including failure to account for the multiple conformational states possible in ligands and enzymes.

In the past few years, investigators using three-dimensional search methods have begun to explore the conformational flexibility of potential ligands.[59] Whereas storing multiple conformations of a single molecule is conceptually simple, it is limited by the amount of storage space and by the linear increase in search time with the number of molecules to be searched. It is impossible to ensure that the conformation being sought will be among those stored, even with systematic search algorithms, because of the chance that the conformation of the bound ligand is not a minimum-energy structure in the absence of the enzyme.[59] Instead of storing multiple conformations, some approaches encode the distances accessible to pairs of atom centers. These accessible distances are used during the search to select molecules that could match a particular query, and the matching conformations are generated for only those compounds. Other approaches adjust torsional angles to match the query. Unfortunately, flexible searching has been shown to significantly increase the amount of computer time required for searching.[59]

Initial attempts to accommodate enzyme flexibility in drug design were through a technique deemed “soft docking”, which was introduced by Jiang and Kim.[60] The flexible enzyme is immobilized and a “soft”-scoring function is used to determine enzyme-ligand affinity. Scoring functions are used for two purposes; one, they optimize the placement of the ligand and, two, rank each ligand in the database

for which a docking solution has been found.[48,61] On the other hand, soft-scoring functions provide some insight into the flexibility of the enzyme by allowing a small amount of overlap between the ligand and enzyme.[62] However, this technique only accommodates for small conformational changes of the enzyme;[48,62] hence the search for a more effective algorithm continued.

During the mid 1990s, several plausible solutions, using multiple protein structures, to overcome ligand flexibility and docking were introduced.[63-66] One such solution was a "grid" approach was developed that precalculate grids on interaction energy based on the enzymatic target.[63] By extrapolation of the adjacent grid points, the interaction energy for a specific conformation is then calculated.[63,67] Programs such as Autodock or DOCK then perform simulated annealing in the space of the flexible ligand.[63,67] Although grid-based method has shown to calculate binding energies efficiently, it is still remained ambiguous as far as introducing enzyme flexibility to the system.[67]

Another approach involves an incremental construction algorithm, which is based on genetic algorithms (GAs) and a tree-search technique, was created to hinder the flexibility of the ligand as well as the enzymatic binding site thereby significantly reducing the time required for these calculations.[67,68] GAs are based on Darwinian selection and utilize the operators selection, crossover, and mutation. The algorithm is based on a known compound (i.e. a chromosome) and proceeds in generations where some molecules are selected and modified using the crossover or mutation operators.[67,68] Crossover involves swapping fragments between molecules that occupy the same volume of space. Mutations include translation, rotation, rotation

about a bond, changing a bond type, adding or removing a fragment, and changing an atom type.[67,68] In each generation, there is a greater likelihood that the fittest members will be selected for modifications. For example, the chromosomes used in the GA of Jones *et al* encode the orientation of the ligand via hydrogen bonding interactions with the enzyme. However, randomly changing the torsional degrees of freedom of side chain residues could lead to overlapping structures with extremely poor energy.[68]

Due to the high demands in procedures for docking flexible ligands in a flexible enzymatic binding site, Apostolakis *et al*[69] developed a novel approach that relies on Monte Carlo minimization (MCM) and combination of minimization with shifted nonbonded interactions (MSNI). The algorithm is designed such that Monte Carlo minimization runs are executed on the low energy enzyme-ligand conformers.[69] Their model had some significant advantages which include allowing unrestricted flexibility in the enzymatic binding site and a more rigorous determination of the solvation free energy in the evaluation of structures.[69]

Recently, Calson *et al*[48,70-72] presented a new "dynamic" pharmacophore model based on multiple protein structures that incorporate the inherent flexibility of the enzymatic active site and reduces the propagation of errors in an individual protein conformation. The flexibility of the active site is determined by collecting an ensemble of conformational models from molecular dynamics (MD) simulation, several crystal structures or multiple NMR structures which can be referred to as multiple "snapshots" of the active site.[48,70-72] Each of these "snapshots" are subjected to a series of multi-unit search for interacting conformers (MUSIC) simulations, a

Monte-Carlo simulation that calculates multiple, gas-phase minimizations for numerous ligands within the enzyme's active site.[48,70-72] The abundant conformations of the enzyme were overlaid to reveal the specific regions of the binding site that interact with the functional groups of the ligands to ultimately define a pharmacophore model for potential inhibitors.[48,70-72]

Although these new approaches and programs are promising,[72] they still have major limitations, especially regarding the programs inability to incorporate the flexibility of both the ligand and enzyme. Therefore, it was our hypothesis that pairing a flexible ligand into a flexible binding site would provide an ideal match to aid in investigating the structural requirements of various enzyme binding sites. By permitting both the flexible enzyme and flexible ligand to adjust to each other, the best possible fit would most likely be achieved and maintained, since both the enzyme and the inhibitor would naturally want to achieve their lowest energy state. The lowest energy for the enzyme-inhibitor complex may then also be the most highly populated state, which was most likely to be the conformation that would crystallize. By crystallizing the most highly populated conformation of the enzyme-inhibitor complex, it should provide vital information with regards to the interactions between the ligand and the active site of the enzyme, and thereby aid in the design of more powerful inhibitors.

That said, one problem logically could be anticipated would be the unfavorable entropic cost that would result from binding. In an enzymatic reaction where the enzyme is inherently flexible, it will most likely distort to bind the ligand. The favorable binding energy between the "perfect" ligand and the flexible enzyme is

used to compensate for the conversion to the entropically unfavorable, yet active enzyme-ligand conformation. If the enzyme is more rigid, the initial binding of the ligand will most likely be energetically unfavorable because (i) the enzyme is disordered and (ii) it is beneficial for the active site of the enzyme to be complementary to the structure of the transition. Despite the possible energetic loss in entropy, we believed the potential for new or more stable hydrogen bonding interactions between a flexible ligand and the structurally flexible binding site would compensate for any entropic cost.

_S_-Adenosyl-L-homocysteine hydrolase

Recently, the threat of biological terrorism has drawn attention to our inherent vulnerability to a variety of diseases, both old and new. Pathogens most likely to be used in such weapons must possess certain characteristics; facile transmission, longevity outside of the human body, and most importantly, a high mortality rate. One such example is smallpox, a particularly virulent member of the orthopox viruses. Smallpox has plagued mankind for centuries, but in 1977, the last confirmed case of smallpox was diagnosed and in 1980, the World Health Organization (WHO) announced that the orthopox virus genus had been eradicated after an aggressive 50-year international campaign of vaccination. Since then very few cases have been reported and vaccinations have ceased, making the general population vulnerable to variola due to its high mortality rate, which is greater than 60%. While immunizations were recently reinstated, albeit in a very limited capacity, there is still no agent available that can be used to treat already infected individuals and the

current vaccine cannot be used in immunocompromised individuals. As a result, millions could be infected within a short period of time since, as the recent outbreak of Sudden Acute Respiratory Syndrome (SARS) has shown, mankind is more mobile than ever and as a result, an outbreak can spread rapidly from one side of the globe to the other.

Some newer emerging pathogens include the filoviruses Ebola and Marburg viruses present serious challenges to medicinal chemists.[73] These viruses cause severe hemorrhagic fevers, and mortality has been in nearly 90% of the reported cases. Ebola virus was first identified in Africa in 1976, but little is known about the histories of these viruses. There are no specific treatments available, and Ribavarin, a nucleoside antiviral agent that has seen success in many diseases, has no effect on either Marburg or Ebola.[73,74] As a result, the development of an effective chemotherapeutic target is crucial.

One approach to the design of chemotherapeutic agents active against viral pathogens is to target steps central to viral replication. An ideal enzymatic target is one in which there is (i) no equivalent in the normal cell, (ii) the cellular analogue is not inhibited within the range of concentrations that would inhibit the viral enzymatic target, or (iii) the virally encoded enzyme differs significantly in structure from the normal analogue. An additional issue that must be considered is the development of resistant viral stains, which can quickly render a previously potent inhibitor useless. The commonly used reverse transcriptase inhibitors, AZT and 3TC are perfect examples of this problem; recent studies have shown that drug resistant viral strains are becoming increasingly problematic for patients treated with these drugs even after

a few days of treatment.[50,51,53,75] More recent investigations with tenofovir, an acyclic nucleoside RT inhibitor, as well as another RT inhibitor, etravirine, have both remained active against a variety of mutant viral strains. Arnold *et al* have shown that if an inhibitor has the ability to be flexible, it endows the inhibitor with a greater capacity to adapt to viral mutations, thereby retaining potency against viral resistance mechanisms. Therefore, an additional requirement for design chemotherapeutic agents must be to consider options to overcome drug resistance mechanisms.[50,51,53,75]

In that regard, S-adenosyl-L-homocysteine hydrolase (SAHase) is an important cellular target for antiviral drug development.[13,27,73,76,77] Inhibitors of SAHase can indirectly inhibit DNA methyltransferase by a biofeedback mechanism.[78-80] The byproduct of all *S*-adenosylmethionine (SAM)-promoted methyltransferase reactions is *S*-adenosylhomocysteine (SAH) (Figure 19), therefore SAH is a potent competitive inhibitor of all methylation reactions dependent upon SAM as the methyl donor, including DNA MeTase.[78-80] SAM is the most ubiquitous methyl donor thus SAM dependent methylations are considered to be the most important biologically. Moreover, SAHase is the only known enzyme able to remove SAH in mammals.

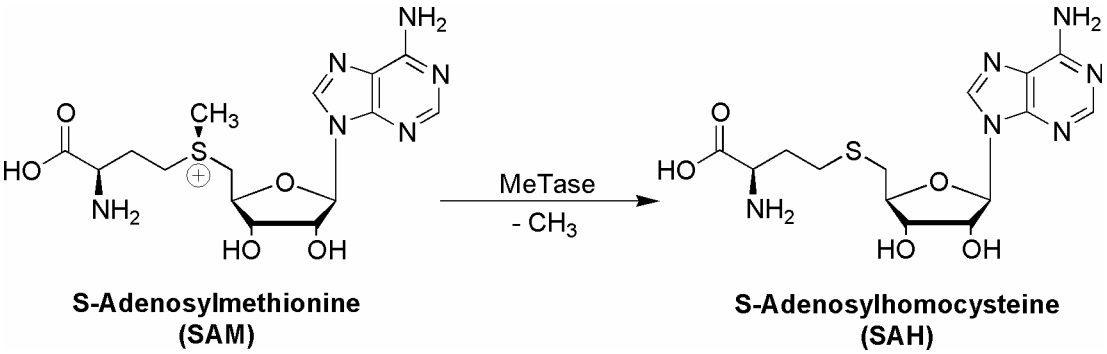

Figure 19. Conversion of S-Adenosylmethionine to S-Adenosylhomocysteine.

As depicted in Figure 20, following the methyl transfer, SAM is readily converted into SAH, which is subsequently hydrolyzed by SAHase into its two cellular components, adenosine (Ado) and homocysteine (Hcy), requiring assistance from an enzyme-bound cofactor, NADH.[80] Inhibition of SAHase by nucleoside analogues involves depletion of the NADH cofactor, which causes an intracellular accumulation of SAH, thereby significantly elevating the SAH/SAM ratio.[80] This imbalance in the SAH/SAM ratio results in cessation of SAM-dependent methylations which leads to hyper- and hypo-methylated DNA.[80] As a result, methylation reactions important for viral replication can be considered potential targets.[81,82]

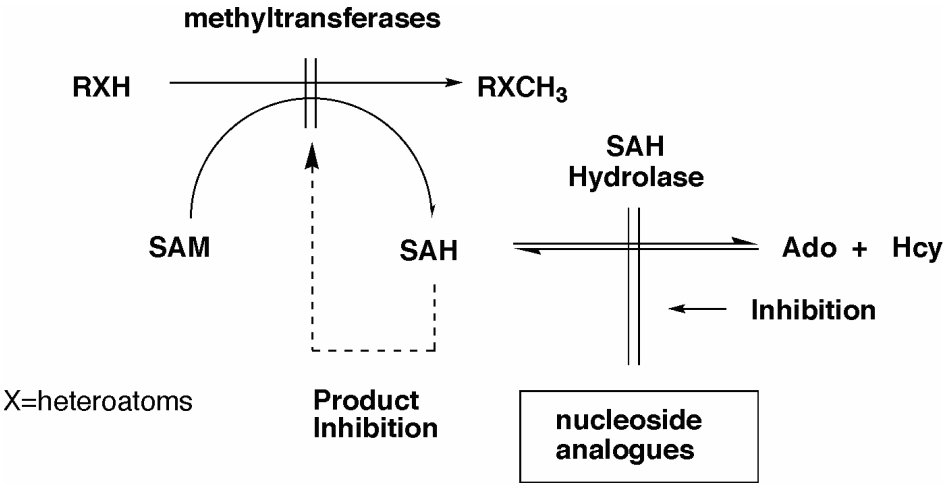

Figure 20. Inhibition of SAHase and its effect on methyltransferases.

More evidence of the biological significance of methylations is that a eukaryotic messenger RNA (mRNA) must possess a methylated 5'-cap for stability against phosphorylases and ribonucleases.[83,84] This "capped" structure is also

required for proper binding to ribosomes, and for the promotion of splicing. [83,84] Therefore, an improperly "capped" mRNA is much less likely to be translated into its respective protein, and replication is disrupted. In particular, the 5'-terminal guanosine nucleotide, as well as the penultimate nucleotide residue are subsequently methylated by mRNA nucleoside N-7-guanine- and 2'-O-methyltransferases; if these transferases are inhibited, incomplete methylation of the cap structure occurs and replication is inhibited (Figure 21). [81-84]

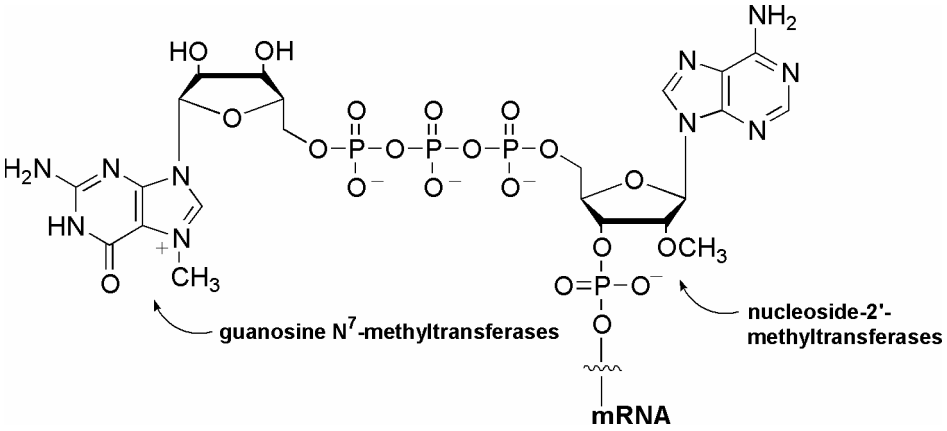

Figure 21. Methylated 5' cap of mRNA.

Palmer and Abeles have determined the mechanism of catalysis of SAH (depicted in Scheme 1 on the next page).[85] The hydrolysis of SAH is an equilibrium reaction favors the formation of SAH with a K_{eq} of 10^{-6} M.[85] The overall reaction proceeds in the hydrolysis direction due to the cellular removal of adenosine by its conversion into ATP and inosine, as well as the conversion of homocysteine into methionine and cystathionine. The mechanism begins with the oxidation of 3'hydroxyl group of SAHase by an enzyme bound NAD^+. Lysine, a basic amino acid

bound within the enzyme, deprotonates at the C-4 position from the 3'-keto-Ado form to afford a carbanion that subsequently eliminates the C-5' homocysteine group in order to form an exocyclic π-bond. The resulting 3'-keto-4',5'-dehydro-Ado undergoes a Michael-type addition of H_2O to produce the 5'-hydroxy group. Next, the 3'-keto functionality is reduced by enzyme bound NADH to afford adenosine and the newly regenerated NAD^+ such that the process may restart.[85]

Scheme 1

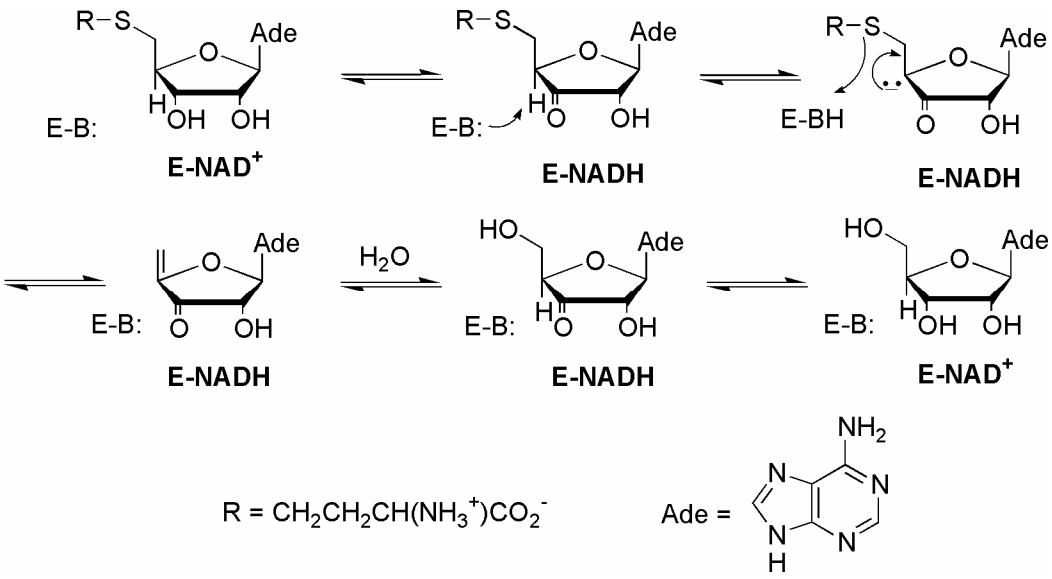

Mammalian SAHase is a homotetramer of approximately 48,000 kDa molecules (432 amino acid residues per subunit), each of which is complexed with a cofactor, NAD^+.[86-88] Four virtually spherical subunits are arranged to afford a flat, square tetramer with an opening in the center allowing for a potential substrate to dock (Figure 22 on the next page). The SAHase monomer is structurally similar to

NAD^+-dependent dehydrogenases with the substrate, SAH, and cofactor, NAD^+, binding sites located in a cleft between two domains. The significant difference between SAHase and NAD^+-dependent dehydrogenases is representative in the NAD^+ binding site of SAHase since NAD^+ requires significant interactions from two protein monomers, specifically amino acid residues Tyr430 and Lys426.[88]

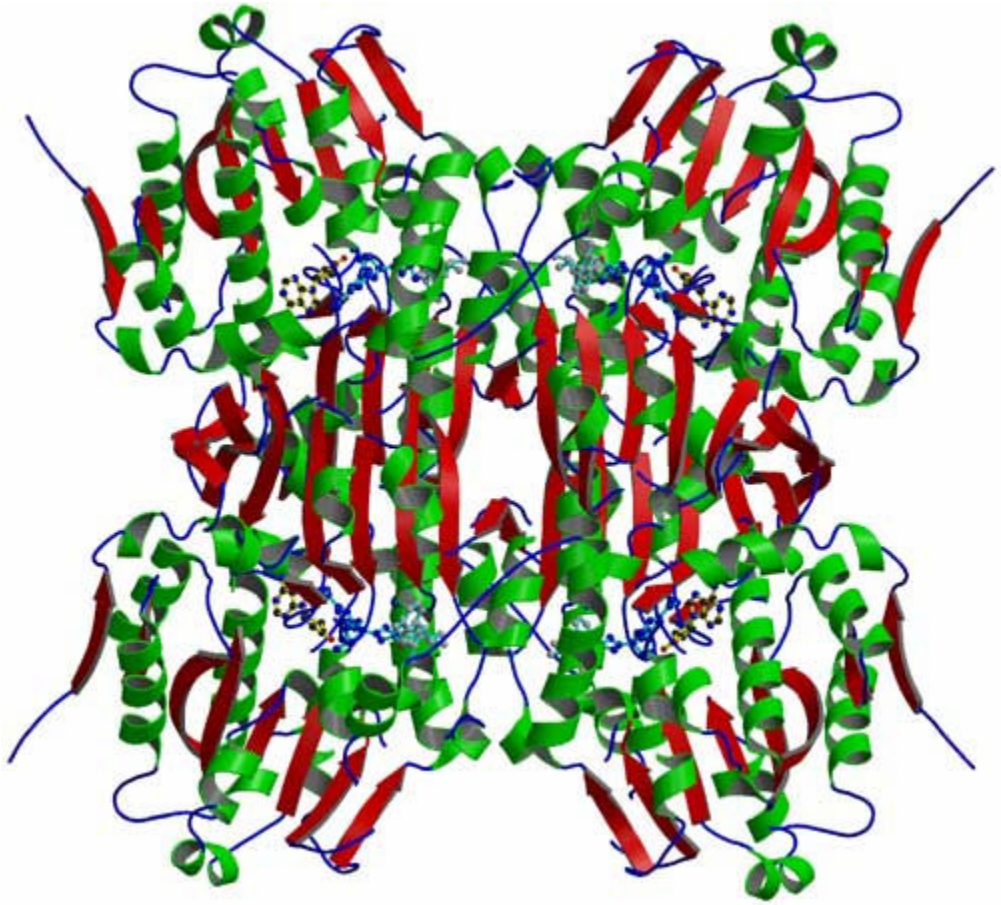

Figure 22. *S*-Adenosylhomocysteine hydrolase.[88]

SAHase undergoes a significant conformational change between the NAD^+ and NADH forms of the enzyme within each catalytic cycle.[89] NADH and its oxidized form, NAD^+, show considerable differences in their hydrodynamic

properties which suggests that SAHase will most likely adopt a far more compact conformation on NAD^+ reduction and substrate oxidation.[90,91] From the crystal structure resolved by Turner *et al*,[88] the inhibitor, 3'-keto-DHCeA, is immersed deeply within the active site located in a cleft between two domains of each subunit in the NADH form. However, in the recently solved crystal structure of rat SAHase, the NAD^+ form shows an open catalytic site in the absence of an inhibitor.[92] It has been shown that there exists a hinged motion associated within domain I of each subunit of SAHase during the enzymatic reaction, since domain II of each subunit is mainly involved with the adjacent subunits, thus creating a conformational change between the "open" and "closed" forms of SAHase (Figure 23 on the next page).[93]

Based on Turner's crystal structure of SAHase[88] complexed with the inhibitor, it has been noticed that domain I and II are interconnected by two bent linkers; linker I, amino acid residues 184-186 and linker II, amino acid residues 350-360). Since amino acid residues Lys186, Asp190, His353, and Met358 within linkers I and II are involved in binding to the oxidized C4' position inhibitor in the enzymatic site, it is plausible that this binding induces "bending" of the two linkers, hence the mobile domain I moves towards the stationary domain II thereby sealing the active site to enclose the substrate. In the "closed" conformation, two histidine residues; His55 (domain I) and His301 (domain II) may possibly act collectively for the enzymes hydrolytic activity.[88]

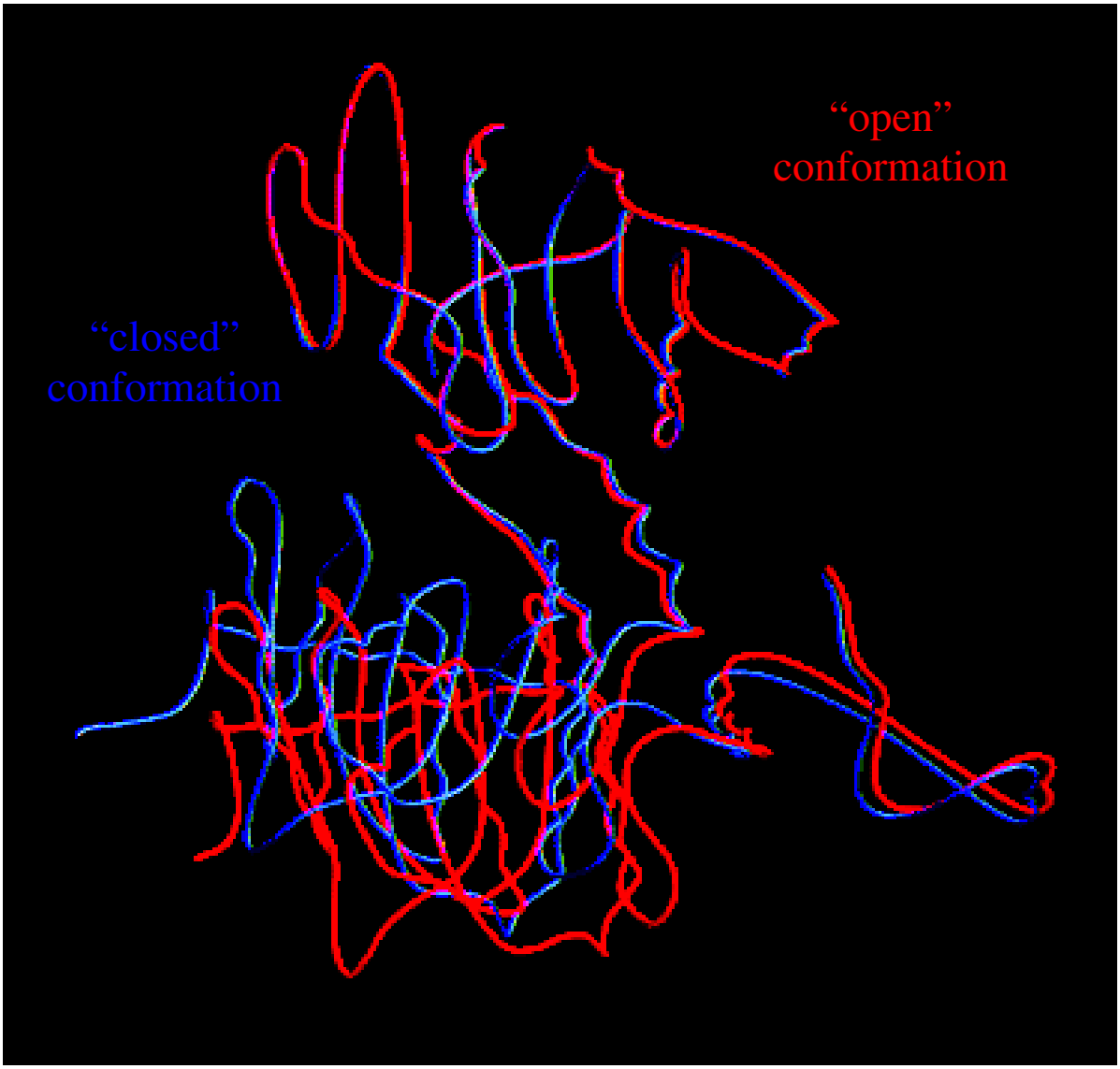

Figure 23. Open and closed conformations of SAHase.[94]

In the past 20 years there have been many SAHase inhibitors identified, many of which structurally resemble adenosine since it is the natural substrate of SAHase. These have since been separated into three categories; first, second and third generation inhibitors, based on their record of discovery. First and second generation inhibitors are also termed *type I mechanism-based inhibitors*, which inhibit the enzyme by serving as substrates for the 3'-oxidative activity of SAHase and converting it from the active form (NAD^+) to the inactive form (NADH). Alternatively, third generation inhibitors are defined as *type II mechanism-based inhibitors* which are activated by the SAHase and irreversibly inactivate the enzyme through covalent modification. Throughout the many years of searching for a "magic" inhibitor of SAHase, these subsequent generations of inhibitors have become increasingly more potent as well as to exhibit significantly greater enzyme specificity.

During the 1970's and 80's SAHase was deemed as an attractive target for the design of potentially effective antiviral inhibitors.[95] These inhibitors were either irreversible; such as neplanocin A (NpcA) and aristeromycin (Ari) which are naturally occurring carbocyclic analogues, or competitive such; as 3-deazaadenosine, 3- deazaneplanocin A, and 3-deazaaristeromycin (Figure 24).[96,97]

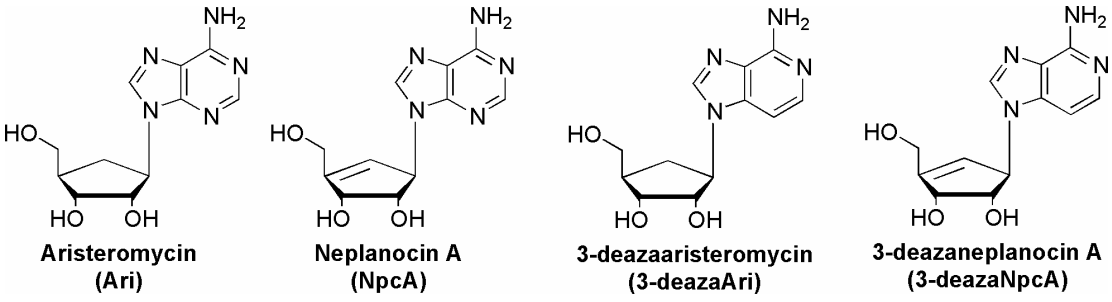

Figure 24. Some potent carbocyclic nucleosides that inhibit SAHase.

NpcA was a particularly interesting SAHase inhibitor since it has a unique mechanism of action. Upon binding NpcA to the active site of SAHase, NpcA is oxidized by enzyme-bound cofactor NAD^+ to form the 3'-keto-NpcA and subsequently NAD^+ is converted into its reduced form NADH. This induces a conformational change into the "closed" conformation of SAHase, therefore trapping the 3'-keto-NpcA resulting in cessation of enzymatic action. This phenomenon is known as a "cofactor depletion" mechanism, and any compound that inhibits SAHase via this particular mechanism is referred to as type I mechanism-based inhibitor.

NpcA, a first generation inhibitor, was indeed one of the most biologically active agents.[27,98,99] Since NpcA could be easily phosphorylated into its triphosphate form using a series of enzymes; adenosine kinase, adenylate kinase, and nucleoside diphosphate kinase, it closely resembled ATP which resulted in NpcA being extremely cytotoxic.[27,98,99] Based on the cellular toxicity of NpcA and several other first generation inhibitors of SAHase, the search continued for less toxic analogues.

In an effort to overcome the cellular toxicity of the first generation inhibitors, two different methodologies were applied in order to design more effective SAHase inhibitors. The first approach involved the modification of the cyclopentyl moiety, more specifically removal of the 4'-hydroxymethyl substituent of Ari and NpcA to provide the subsequent 4',5'-tetrahydro and 4',5'-unsaturated derivatives (Figure 25 on the next page).[100] Both of these analogues were shown to irreversibly inhibit SAHase via the type I mechanism.[101] More significantly, they were not substrates for adenosine kinase and adenosine deaminase.

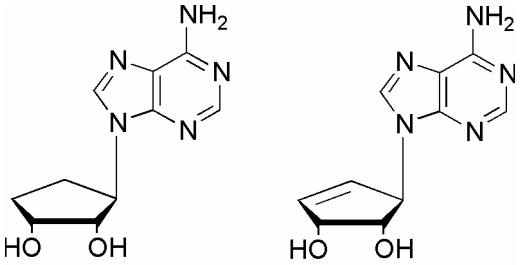

Figure 25. 4',5'-tetrahydro and 4',5'-unsaturated derivatives of Ari and NpcA.

The second approach involved the modification of the heterocyclic base, more specifically removal of the N-3 of adenine in both Ari and NpcA resulting in 3-deazaaristeromycin (3-deazaAri) and 3-deazaneplanocin A (3-deazaNpcA) respectively. This modification was made due to the potent inhibition of SAHase by 3-deazaadenosine which produced a simultaneous formation of *S*-3-deazaadenosylhomocysteine in addition to an increase in SAHase (Figure 26).[13] Hence, based on the effective inhibition of 3-deazaadenosine, the next logical step was to synthesize the 3-deaza carbocyclic analogues.

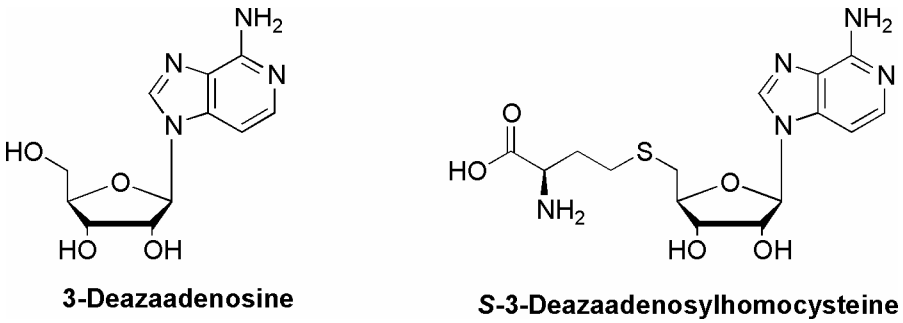

Figure 26. 3-Deazaadenosine (a potent inhibitor of SAHase) and *S*-3-Deazaadenosylhomocysteine.

It was thus shown, inhibition of SAHase by 3-deazaAri was reported to be significantly greater than that of Ari.[27,102] Similarly, inhibition of SAHase by 3-deazaNpcA was determined to be reversible and competitive.[27,102] Furthermore, the cytotoxicity of the 3-deazaAri and 3-deazaNpcA was significantly reduced due to the as yet unexplained ability for 3-deaza nucleoside analogues to avoid phosphorylation by adenosine kinase.[27,102]

More recently, several research groups attempted to design a series of type II mechanism based SAHase inhibitors. These inhibitors are catalytically activated by SAHase and subsequently become covalently bound the enzyme. In 1991, Jarvi *et al* synthesized (Z)-4',5'-didehydro-5'-deoxy-5'-fluoroadenosine which showed to possess inhibitory activity against SAHase.[103] Initially, the mechanism was thought to function via a type II mechanism pathway, where the enzyme was inhibited by reduction of NAD^+ to NADH and the subsequent elimination of the fluoride ion (Scheme 2 on the next page, pathways **b** and **b'**). However, it was later shown that the mechanism involved the rapid addition of water at the 5' position, and subsequent elimination of the fluoride ion followed by NAD^+ cofactor depletion (Scheme 2 on the next page, pathway **a**).[104] Surprisingly, the enzyme's hydrolytic activity functioned independently from its oxidative activity which implied that (*Z*)-4',5'-didehydro-5'-deoxy-5'-fluoroadenosine was actually a "pro inhibitor" for a type I mechanism based inhibitor for SAHase. Based on this unique mechanism of inactivation of SAHase by (*Z*)-4',5'-didehydro-5'-deoxy-5'-fluoroadenosine, many attempts have been made to exploit the enzyme's hydrolytic activity to convert a "pro

inhibitor" into either a type I mechanism based "inhibitor", or, an electrophilic substrate that could covalently modify the enzyme.

Scheme 2

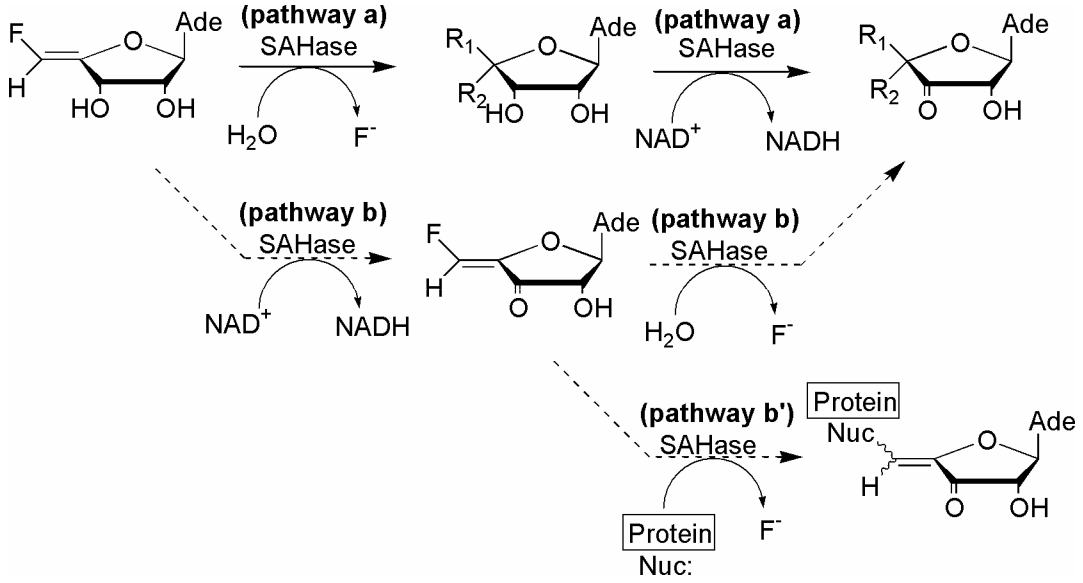

One such substrate for SAHase was (*E*)-5',6'-didehydro-6'-deoxy-6'-halohomoadenosines.[105] The mechanism of action was determined to be the addition of water across the 5',6'-π bond of the nucleoside analogue affiliated with the reduction of enzyme-bound NAD^+ to NADH.[105] Conversion of the possible "pro inhibitor" to its subsequent "inhibitor" form was proportional to the stability of the eliminating halogen. Although (*E*)-5',6'-didehydro-6'-deoxy-6'-halohomoadenosines were biologically inactive for SAHase,[105] it appeared that by taking advantage of their "5',6'-hydrolytic activity", potent inhibitors could possibly be designed.

In 1998, Borchardt *et al* synthesized and characterized the first type II mechanism-based inhibitor that relied solely on the enzyme's hydrolytic activity.[105] It was shown that the maximum inhibition of the enzyme was 83% and much to their delight, the original content of NAD^+ and NADH remained unchanged.[105] Based on ^3H-labeling studies, the mechanism of action by which 6'-bromo-5',6'-didehydro-6'-fluorohomoadenosine (Figure 27) inhibits SAHase, revealed that immediately following the "hydrolytic activity" and elimination of bromine, Arg196 nucleophilically attacked the electrophilic substrate resulting in the formation of an amide bond and concurrent loss of fluorine ion.[105]

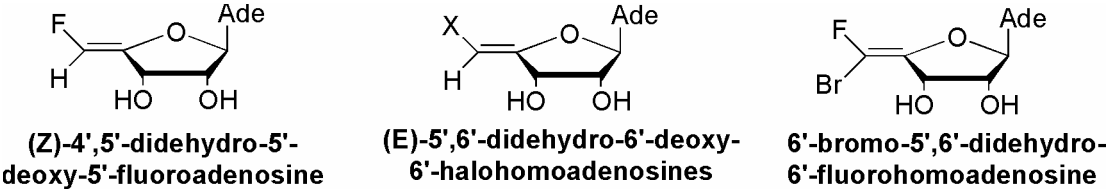

(Z)-4',5'-didehydro-5'-deoxy-5'-fluoroadenosine | **(E)-5',6'-didehydro-6'-deoxy-6'-halohomoadenosines** | **6'-bromo-5',6'-didehydro-6'-fluorohomoadenosine**

Figure 27. Some type II mechanism based inhibitors.

The knowledge that the binding site of SAHase was quite flexible and exhibited a large difference between the "open" and "closed" conformations,[90] combined with the recent findings that flexible inhibitors can over come drug resistance mutations in viral HIV,[50,51,53,75] led us to believe that inhibitors possessing variable degrees of flexibility could be a potential solution to overcome the flexibility of SAHase. Many nucleoside based inhibitors,[27,100,102,105-108] most of them structurally rigid, have been employed as enzyme inhibitors in antiviral drug design, however, we have strategically designed a novel series of split nucleosides referred to

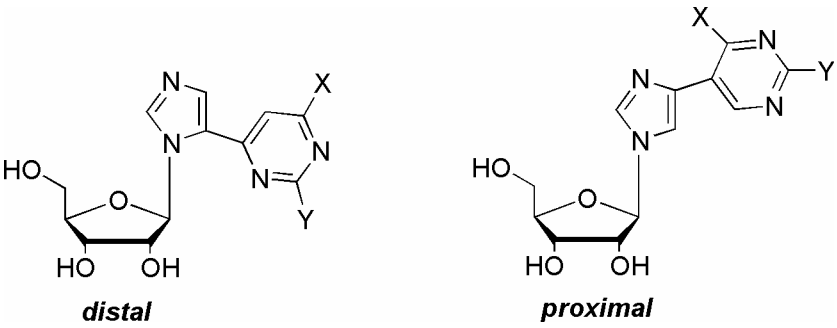

Figure 28. General structure of distal and proximal fleximers.

as "fleximers" (Figure 28). This new class of unique shape-modified nucleosides introduces flexibility to the heteroaromatic purine ring by "splitting" it into its two components (for example, an imidazole and pyrimidine ring), thereby conferring additional degrees of conformational freedom and torsional flexibility to the ligand while still retaining the molecular elements necessary for recognition. As a result, these molecular "chameleons" can adapt to the environment of the flexible binding site in order to maximize and complement structural interactions, without losing the integrity of the crucial contacts involved in an enzyme's mechanism of action. It is our hypothesis that endowing these structurally unique nucleosides with torsional flexibility will result in (i) increased inhibitory properties against biologically significant enzymes such as SAHase, (ii) increased ability to overcome viral resistance mechanisms, and (iii) will provide valuable insight toward increasing our understanding of enzyme/ligand structure and function, and as such they will serve as the foundation for the design of a new generation of chemotherapeutic agents.

While nucleosides have long been employed as enzyme inhibitors in chemotherapeutic drug design, there are surprisingly few examples of analogues structurally similar to the fleximers. The most striking example, initially reported by

Herdewijn *et al* in 1995, has exhibited potent biological activity against herpes simplex virus (HSV).[109,110] These analogues also possess a "split" scaffold, albeit "reversed" in their connectivity, with a pyrimidine ring connected to the sugar moiety, rather than the five membered ring system found in purines (Figure 29).

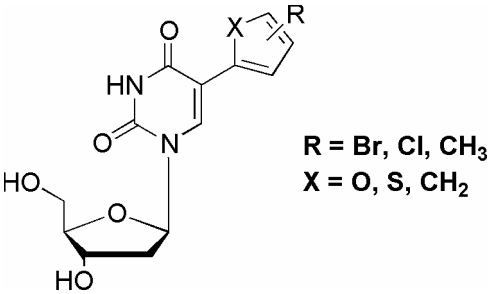

Figure 29. Herdewijn's "reversed" fleximers.

The C-5 position of the six-membered uracil ring is substituted by a series of five-membered heterocyclic ring systems that include thiophene, furan and cyclopentadiene rings. The results of a detailed structure activity study revealed that the key to their biological activity was their ability to adjust their conformational geometry in order to sample better hydrogen bonding interactions between the 3' and 5' hydroxyl groups of the 2'-deoxyribofuranose moiety in the binding site of HSV-thymidine kinase (TK). [109,110] Furthermore, the 5-substituted heterocyclic ring systems with small or no substituents showed that favorable hydrophobic interactions were occurring with the active site of HSV-TK. [109,110] After a series of rationally designed molecular modifications, it was shown that replacement of ring carbons with electronegative atoms resulted in improved interactions with the positive electrostatic potential within the enzyme's active site by compromising the favorable hydrophobic

interactions. [109,110] Hence, structural modifications of the 5-substituted heterocyclic ring systems to improve the hydrophobicity while maintaining the interaction energy has become a considerable challenge.

Soon after these "reversed fleximers" were introduced, a group in Sweden published[111] the synthesis of several related analogues, although little biological data were reported. The potent biological activity of Herdewijn's flexible analogues, while admittedly against a different enzymatic target, is highly promising and clearly lends support to our fleximers, however, given their reversed connectivity and their close structural similarity to thymidine as well as their inhibition of thymidine kinase, these analogues should be considered as examples of C-5 substituted pyrimidine nucleosides, rather than purine analogues.

To our knowledge, the only other example in the literature of a split nucleoside was recently introduced by Weisz *et al*,[112,113] whose connectivity more closely resembles our fleximers since the imidazole ring is connected to the sugar moiety, and the C-4 of the imidazole ring is substituted with either a pyridine or benzene ring (Figure 30).

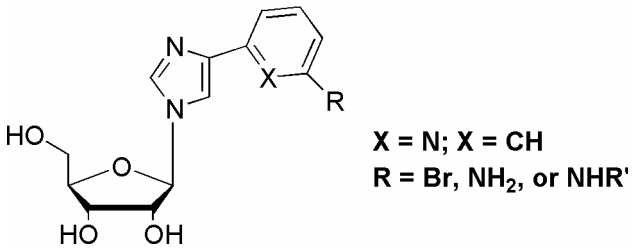

Figure 30. Weisz's imidazole-pyridine or imidazole-benzene fleximers.

In contrast to our fleximers, the connectivity of the six-membered ring is attached at the C-3 of the benzene ring (or the C-2 of the pyridine ring), rather than the C-5 or C-6 of the pyrimidine ring, thereby detracting from the standard purine motif. As a result, we believe our analogues are more true to a classic purine design. Weisz has not yet reported any biological investigations for his analogues, but rather, has employed his analogues to investigate triple helix formation in DNA, an interesting application for our analogues that could be pursued in the future.

Initially, Seley *et al* designed and synthesized a series of *distal*-fleximers,[114,115] more specifically the adenosine, guanosine and inosine analogues in efforts to resolve the aforementioned problems (Figure 31). Analogous to Leonard's *dist*-benzo analogues,[39] these fleximers are connected via a carbon-carbon single bond from the C-5 of the imidazole moiety to the C-6 of the pyrimidine ring. After performing a series of *ab initio* quantum mechanical structure optimization calculations on the fleximers, it was observed that these shape-modified nucleosides adopted an *anti*-conformation as well as a non-planar heterobase conformation in the gas phase.[116]

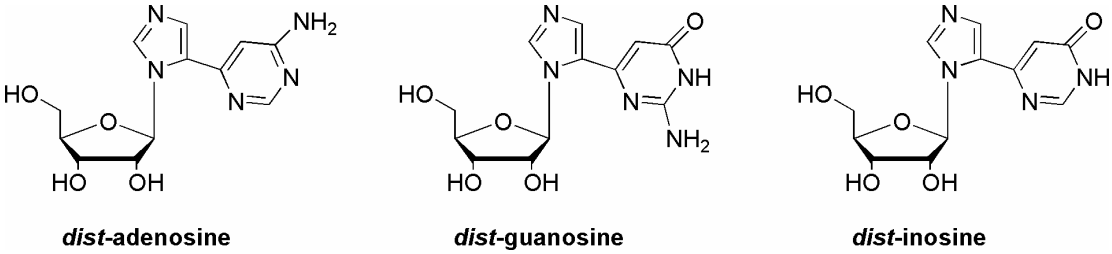

Figure 31. Previously synthesized *distal*-fleximers.

Furthermore, each of the fleximer analogues was modeled within SAHase to determine the degrees of conformational freedom and torsional flexibility. Using automated molecular docking (InsightII, Discover/Accelrys), Monte Carlo simulation, followed by simulated annealing revealed that the *dist*-fleximers, with exception of the guanosine fleximer, occupied a region in the SAHase active site in an orientation similar, but not identical to, the position of the known nucleoside inhibitor in the crystal structure published by Turner *et al*. The guanosine fleximer proved to be quite interesting; the lowest energy conformation revealed that the heterocyclic moieties had adopted a syn-like conformation, bending back over the sugar to form a curved structure.[116] More significantly, the pyrimidine moiety exhibited a degree of twist, essentially reversing the substituents to allow the fleximer to take advantage of intramolecular hydrogen bonding between the carbonyl of the pyrimidine and the 5'-hydroxyl of the sugar moiety.[116]

Following their synthesis, the fleximers and their corresponding parent nucleosides were assayed against SAHase. The adenosine fleximer was an alternative substrate for the enzyme, albeit worse than adenosine itself, while the inosine was a poor substrate, exhibiting weak enzymatic activity.[116] To our surprise, the guanosine fleximer inhibited the enzyme in the hydrolytic direction nearly twice as effectively as it did in the synthetic direction. This observation was unprecedented, since no other guanosine nucleoside has ever been reported to inhibit SAHase.[116] Our modeling efforts showed that the guanosine fleximer is twisting dramatically to place the C-2 amino group where the adenosine's amino group would normally reside.

Interestingly, this twist essentially mimics the inverted structural arrangement of isoguanosine (isoG) (Figure 32).

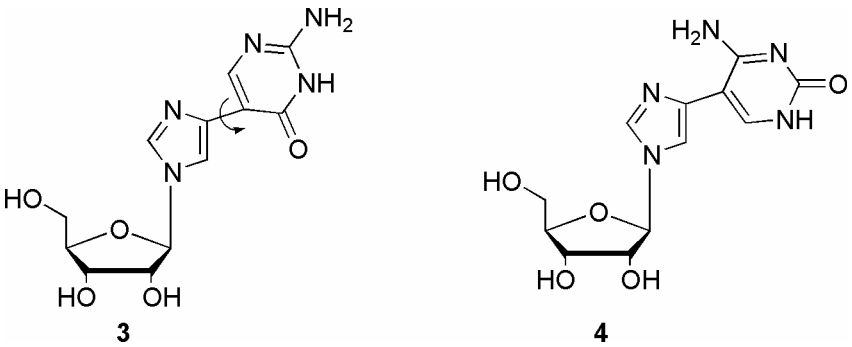

Figure 32. Twisted *prox*-guanosine 3 and *prox*-isoguanosine 4 fleximers.

Based on the design and synthesis of the *distal* fleximers,[114,115] we have turned our attention to a second series of flexible nucleosides collectively known as *proximal* fleximers (Figure 33). Since these second generation fleximers represented a new class of potential SAHase and antiviral inhibitors as yet uncharacterized, we felt it prudent to focus our initial synthetic efforts with rational stages.

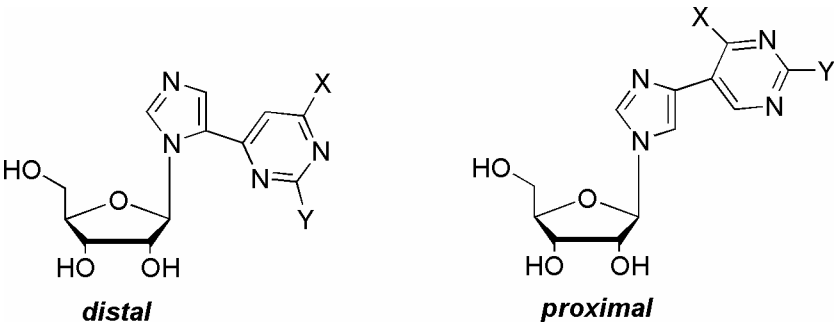

Figure 33. *Distal* and *Proximal* fleximers.

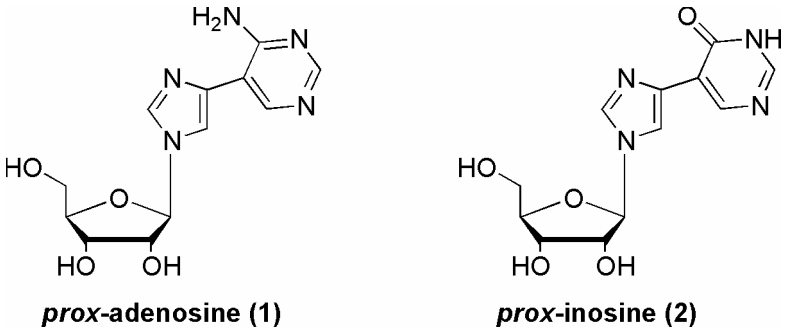

Figure 34. Synthetic targets proximal adenosine and inosine.

First, *proximal* adenosine and inosine were targeted (Figure 34 on the top of the page), in order to establish a basis (adenosine) for comparison with later analogues. *Proximal* inosine was a synthetic target that could be realized easily from adenosine. Next, based on surprising inhibitory information from the *distal* guanosine fleximer,[116] we sought out to synthesize the *proximal* guanosine along with its structural isomer, *proximal* isoguanosine such that we can "prearrange" the substituents in the conformation they appeared to prefer thereby resulting in a more favorable binding energy, since theoretically the pyrimidine moiety would not have to expend any energy to attain the desired conformation (Figure 32 on the top of previous page). Finally, two more synthetic targets arose out of the synthetic pathway of the *prox*-guanosine and –isoguanosine, which were the synthetic intermediates, proximal diamino and xanthine analogues (Figure 35 on the next page). The synthesis of these proximal analogues is presented herein.

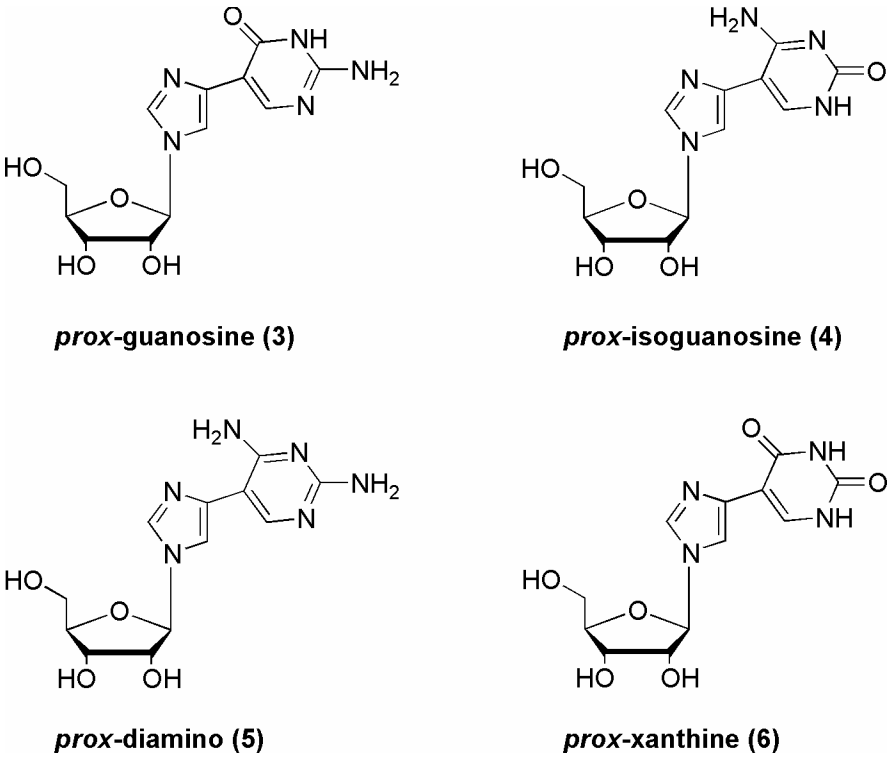

Figure 35. Synthetic targets of *proximal* fleximers.

CHAPTER II

MOLECULAR MODELING

We initially modeled a carbocylic fleximer, 4',5'-unsaturated-3-deazaNpcA fleximer, due to its close similarity with Borchardt's potent SAHase inhibitor, 4',5'-enyl-3-deazaNpcA (shown in Figure 36), using the InsightII modeling environment

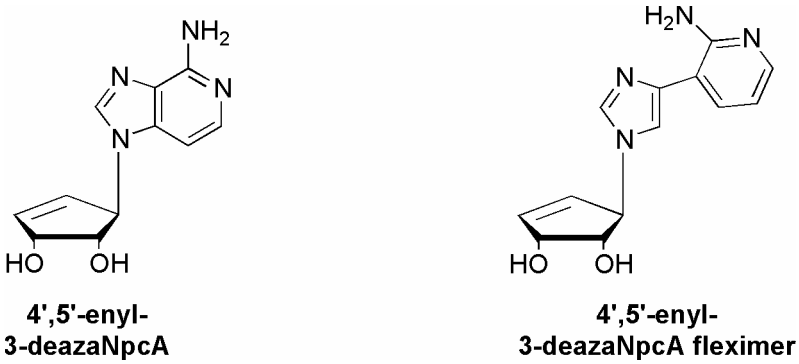

Figure 36. Borchardt's SAHase inhibitor and its analogous fleximer.

and the Affinity and Discover modules from Accelrys. PDB file 1A7A for SAHase was used, which had been crystallized with Borchardt's analogous 4',5'-unsaturated-3-deazaNpcA nucleoside in the binding domain.[88] Borchardt's substrate was removed and a fleximer inserted, and the new complex minimized. Using Infighter's Monte Carlo simulation, followed by simulated annealing, the binding conformation with the lowest intermolecular binding energy was predicted. This method utilized the constant valence force field (cvff) and allowed the ligand and binding site side

chains to be flexible. The fleximer was allowed to minimize using a conjugate gradient method. The difference in the planar biaryl ring system of the "rigid" nucleoside to the nearly 90 degree perpendicular twist of the "relaxed" biaryl ring system of the fleximer showed the ability of the fleximer showed the ability of the fleximers to draw on their inherent structural flexibility to attain the optimal conformation. Upon comparison, the 3-deazaNpcA fleximer exhibited several new hydrogen bonding interactions not observed with Borchardt's analogue as well as π-stacking between the imidazole and the imidazole ring of His353 (Figure 37).

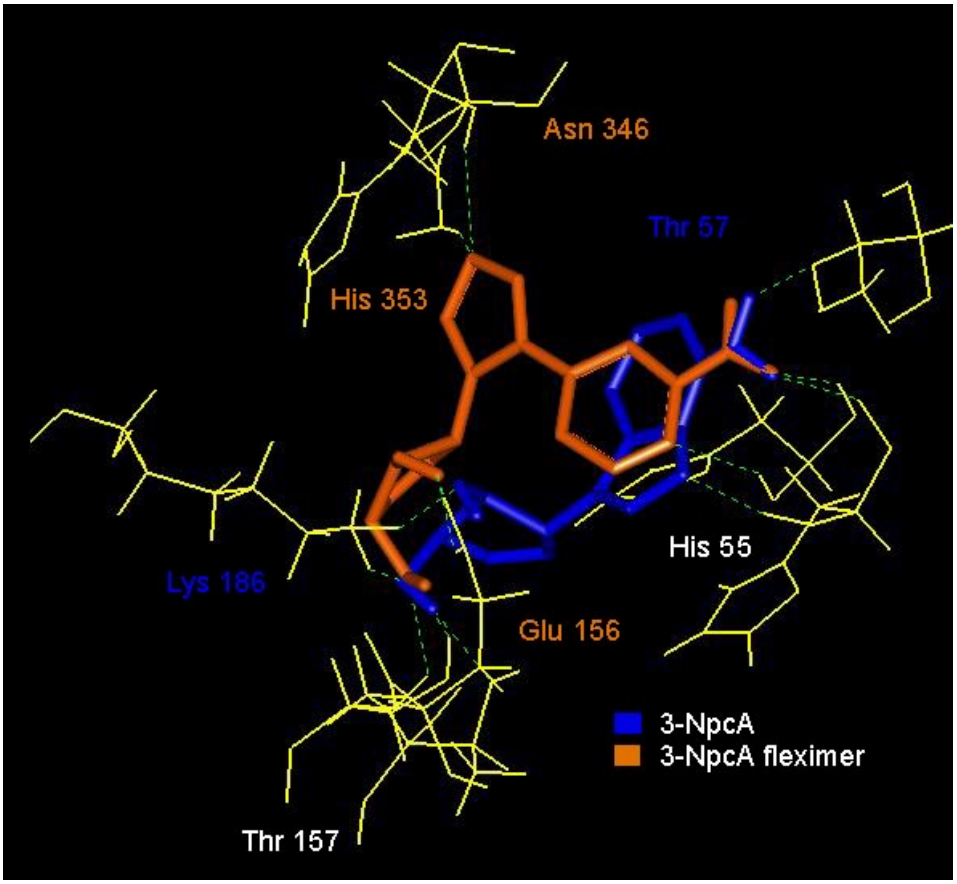

Figure 37. 4',5'-unsaturated-3-deazaNpcA fleximer and Borchardt's analogue.

Both analogues exhibited interactions between His55 and Thr157, but the fleximer exhibited additional interactions between Asn346, His353, and Glu156, while Borchardt's analogue showed interaction with only Lys186 and Thr57. The calculated binding energies differed by nearly 10 kcal/mol, with the more favorable energy (-26.83 kcal/mol) calculated for the enzyme/fleximer complex (Table 1). While this was highly encouraging, we realized that we needed to establish a more solid foundation for comparison, and hence we focused on the adenosine, inosine and guanosine fleximers.

Table 1. ***Ab initio*** **modeling results.**

COMPOUND	BINDING ENERGY (KCAL/MOL)
4',5'-enyl-3-deazaNpcA	–16.38
4',5'-enyl-3-deazaNpcA Fleximer	–26.83

Next, to gauge the level of conformational flexibility in the context of an enzyme active site, all three *distal* fleximers were modeled in SAHase. Using automated molecular docking (InsightII, Discover from Accelrys), Monte Carlo simulation, followed by simulated annealing revealed that the *distal* fleximers, with the exception of the guanosine fleximer, occupied a region in the SAHase active site in an orientation that is similar to, but not identical to, the position of the known nucleoside inhibitor in the crystal structure published by Turner *et al* (Figure 38 and 39 on pages 53 and 54 respecitively). The crystallographic water molecules in the

original structure for the active site were retained as they also interacted with the fleximers.

The *distal* guanosine fleximer, as shown in Figures 40 and 41 (on pages 54 and 55), proved to be quite interesting; the lowest energy conformation revealed that the heterocyclic moieties had adopted a syn-like conformation, bending back over the sugar to form a curved structure. More significantly, the pyrimidine moiety exhibited a high degree of twist, essentially reversing the substituents to allow the fleximer to take advantage of intramolecular hydrogen bonding between the carbonyl of the pyrimidine and the 5'-hydroxyl of the sugar moiety.

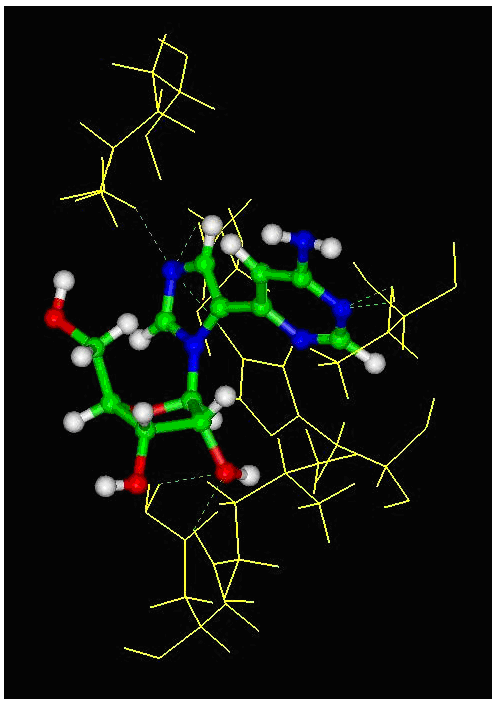

Figure 38. *Distal* adenosine in SAHase.

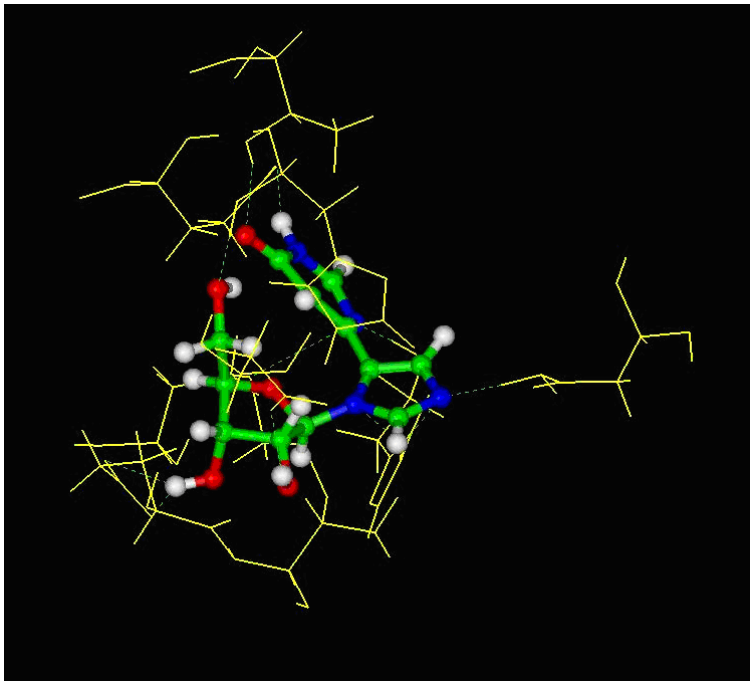

Figure 39. *Distal* inosine in SAHase.

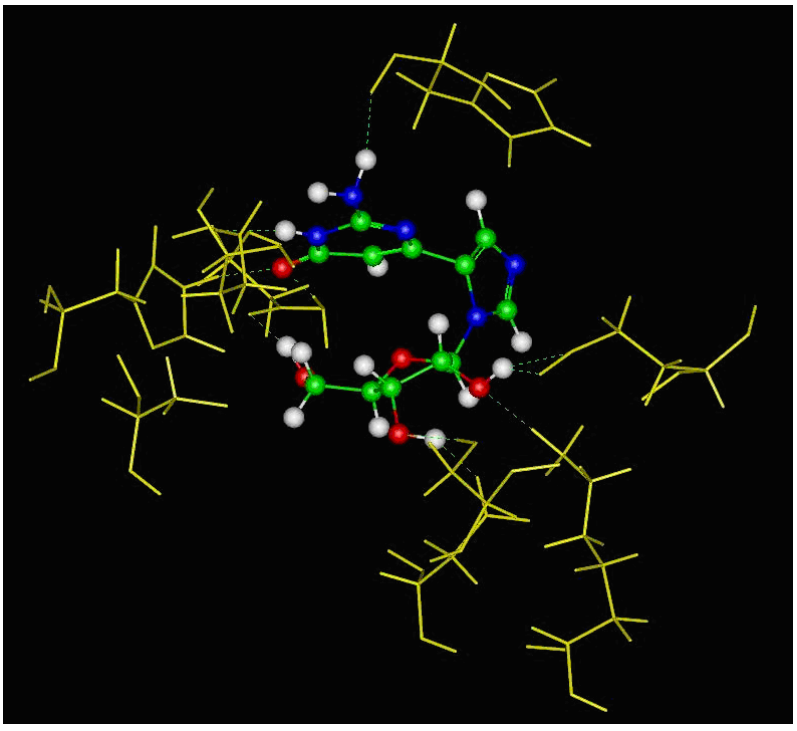

Figure 40. *Distal* guanosine in SAHase.

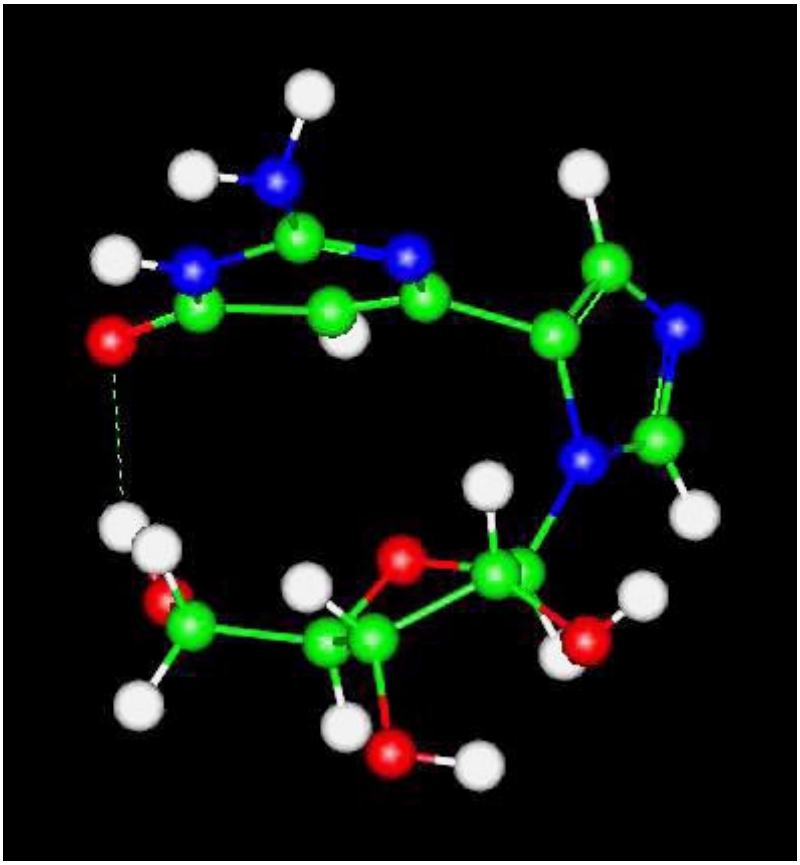

Figure 41. ***Distal*** **guanosine exhibiting intramolecular hydrogen bonding.**

Following their synthesis,[114,115] the distal fleximers and their corresponding parent nucleosides were assayed against SAHase. As shown in Table 2 on the next page, the adenosine fleximer was an alternative substrate for the enzyme, albeit worse than adenosine itself, while the inosine a worse substrate, but exhibiting weak enzymatic activity. To our surprise, the guanosine fleximer showed activity on both the synthetic and hydrolytic activity directions with K_i values of 217 and 128 μM, respectively. While these values are not spectacular since aristeromycin and neplanocin A have K_i values in the nanomolar range against SAHase, they are notable

since, to our knowledge, no guanosine nucleosides have ever been reported to exhibit activity against SAHase.

Table 2. Results of the enzyme essays with SAHase, parent nucleosides and the *distal* fleximers.

Compound	K_m (μM)	K_{cat} (m^{-1})	K_i (μM)
Synthesis Direction			
Adenosine	0.82 ± 0.004	91.2 ± 0.2	nd
Adenosine Fleximer	54.4 ± 1.1	0.56 ± 0.04	nd
Inosine	2.5 ± 0.03	44.2 ± 0.7	925 ± 21
Inosine Fleximer	421 ± 5.7	0.005 ± 0.003	422 ± 16
Guanosine	844 ± 6.6	0.06 ± 0.02	1472 ± 32
Guanosine Fleximer	ns	ns	217 ± 13
Hydrolysis Direction:			
SAHase and G-fleximer	6.6 ± 0.2	28.3 ± 1.2	128 ± 18

nd – not determined; ns – not a substrate

Based on the work on the *distal* fleximers, our initial calculations had shown that the binding energy for the *distal* guanosine fleximer was –24.88 kcal/mol, but these had been carried out on a lower level of theory, using a class one force field (CVFF), so in an effort to increase our accuracy, we moved to a Class II force field (CFF) and repeated the calculations.[117,118] Since the form of an energy surface is usually very complex, especially for large molecules or systems, with many energy minima and barriers and regions of greatly varying energy and curvature, the cff force field expands the analytical energy expression to include terms needed for an accurate model of the energy surface.[61] The new results all showed lower binding energies than for the previous force field with the new energy for the *distal* guanosine being

used as the reference in this study. The corresponding *proximal* guanosine fleximer was 5.36 kcal/mol lower in energy than the *distal* analogue, however, as we predicted, both the *distal* and *proximal* isoguanosine fleximers exhibited much more favorable binding energies. Relative to the *distal* guanosine fleximer, the *distal* and *proximal* isoguanosine fleximers were more favorable by –20.59 and –21.97 kcal/mol respectively. The structures shown in Figure 42 have been artificially overlaid, aligning each by their sugar moieties. From this one can see that the bases for each of the four analogues adopt different low energy conformations upon binding.

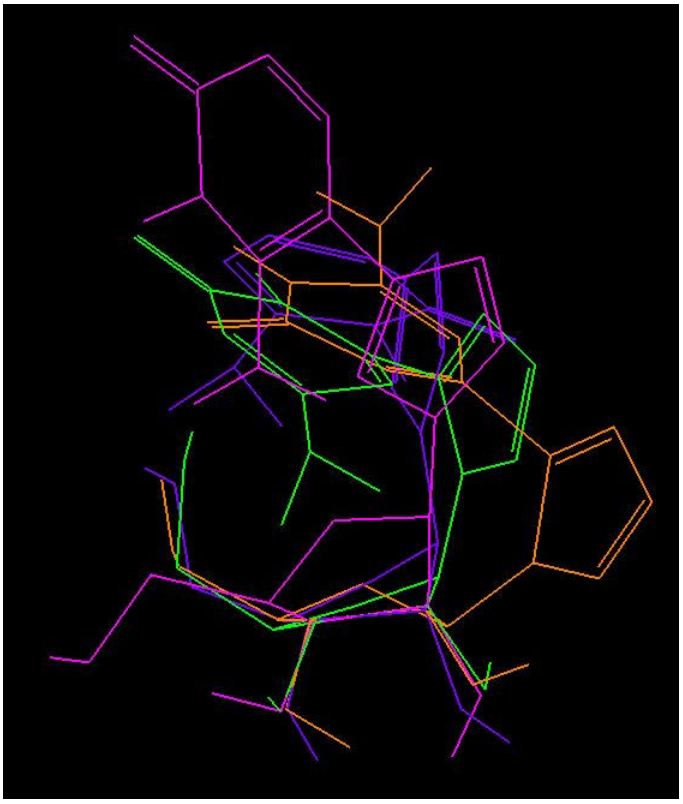

Figure 42. *Proximal* guanosine and isoguanosine fleximers aligned at C-3 and C-5 of the ribose moiety.

The isoguanosine fleximers, *distal* and *proximal*, have two tautomeric forms, and our calculations showed that the *distal* substituted isoguanosine fleximer preferred to exist as the N3(H) tautomer (shown in Figure 43), with a binding energy of –53.79 kcal/mol, rather than the N1(H) (–35.70 kcal/mol), while the *proximal* isoguanosine fleximer, preferred the N1(H) tautomeric form (shown in Figure 44 on the next page) with a binding energy of –55.17 kcal/mol, in contrast to the N3(H) tautomer at only –32.09 kcal/mol.

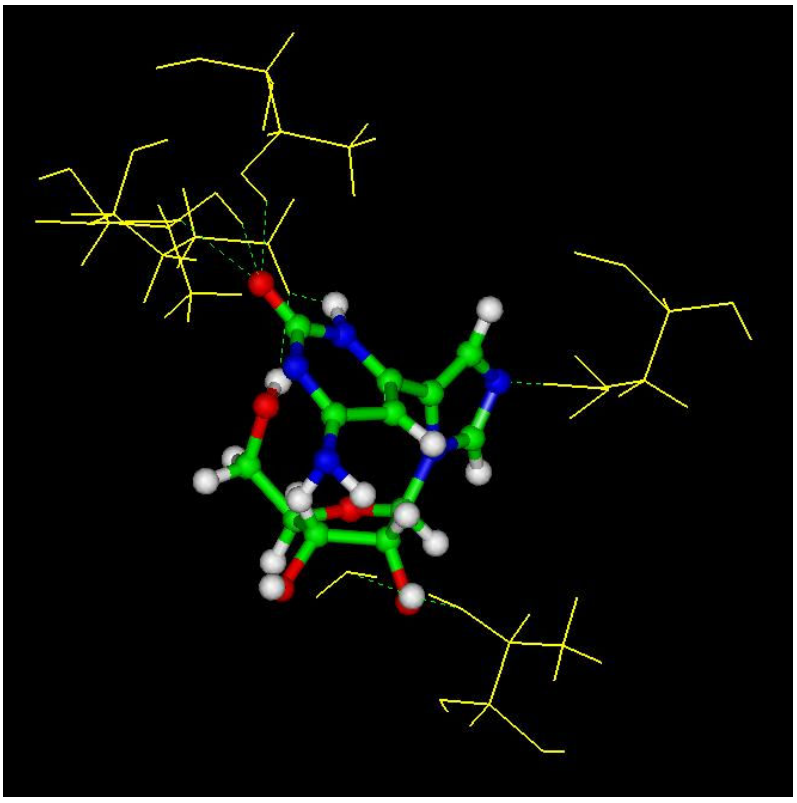

Figure 43. N3(H) tautomer for the *distal* isoguanosine fleximer in SAHase.

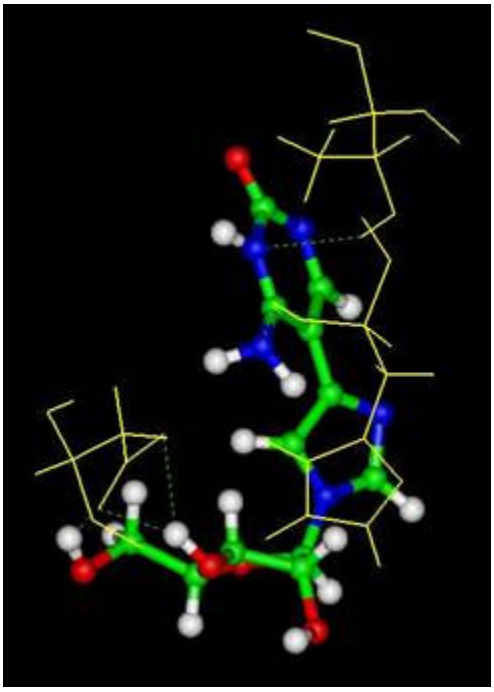

Figure 44. N1(H) tautomer for the *proximal* isoguanosine fleximer in SAHase.

Figure 45 (on the top of the next page) depicts the *proximal* and *distal* guanosine, as well as the isoguanosine aligned in the binding site of SAHase by the residues they interact with. As mentioned above, the *proximal* and *distal* isoguanosine fleximers exhibit the most favorable binding energy values (Table 3 on the next page), but it is clear that they are both capable of adopting a significantly different conformation from each other, while still maintaining critical contacts necessary for recognition.

Both the diamino and xanthosine *proximal* fleximers **5** and **6** were also modeled in SAHase to determine the level of conformational flexibility in the context of an enzyme active site (Figure 46 and 47 on page 61). Once again using automated

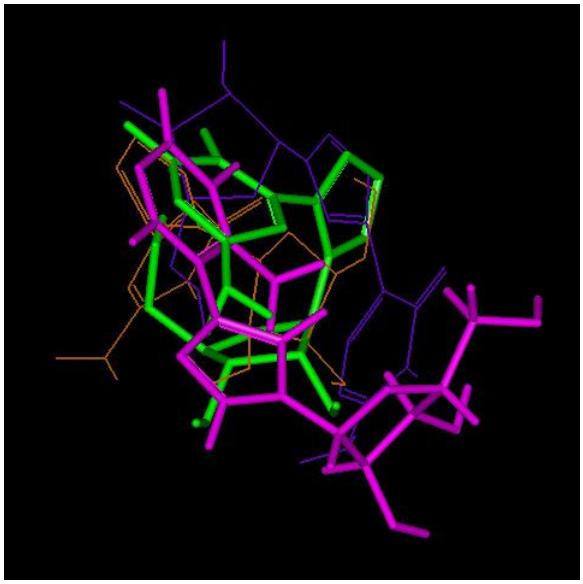

Figure 45. *Proximal* and *distal* guanosine and isoguanosine fleximers in SAHase.

molecular docking (InsightII, Discover from Accelrys), Monte Carlo simulation, followed by simulated annealing revealed that these *proximal* fleximers had a binding energies of –24.63 and –32.86 kcal/mol respectively. To our surprise, both fleximers

Table 3. Binding Energy values for *Proximal* and *distal* guanosine and isoguanosine fleximers.

FLEXIMER	COLOR	ΔG (KCAL/MOL)
Distal Guanosine	Orange	–33.20
Proximal Guanosine	Purple	–38.56
Distal Isoguanosine	Green	–53.79
Proximal Isoguanosine	Pink	–55.17

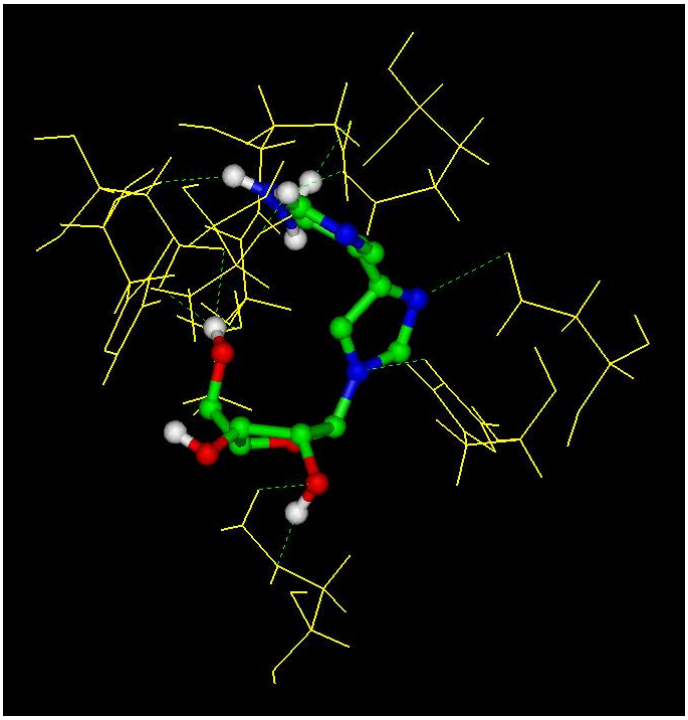

Figure 46. ***Proximal*** **diamino fleximer in SAHase.**

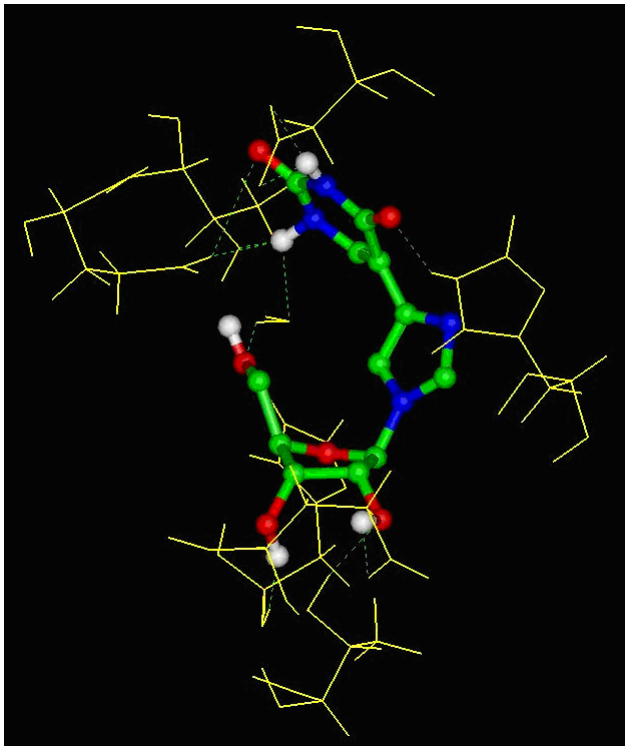

Figure 47. ***Proximal*** **xanthosine fleximer in SAHase.**

provided similar hydrogen bonding patterns with SAHase as was seen in Borchardt's inhibitor. Upon further analysis, both fleximers **5** and **6** did not maintain the necessary His353 to imidazole stacking interactions and the hydrogen bonding was slightly skewed – the sugar was binding to regions where the heterocyclic base, in Borchardt's inhibitor, was binding.

We also modeled both the *proximal* adenosine and inosine fleximers **1** and **2** in SAHase to determine the level of conformational flexibility within the active site. Using the same modeling parameters, it was shown that the binding energies for **1** and **2** were –30.59 and –36.67 kcal/mol respectively. The *proximal* adenosine fleximer (shown in Figure 48) had an analogous molecular recognition pattern as seen

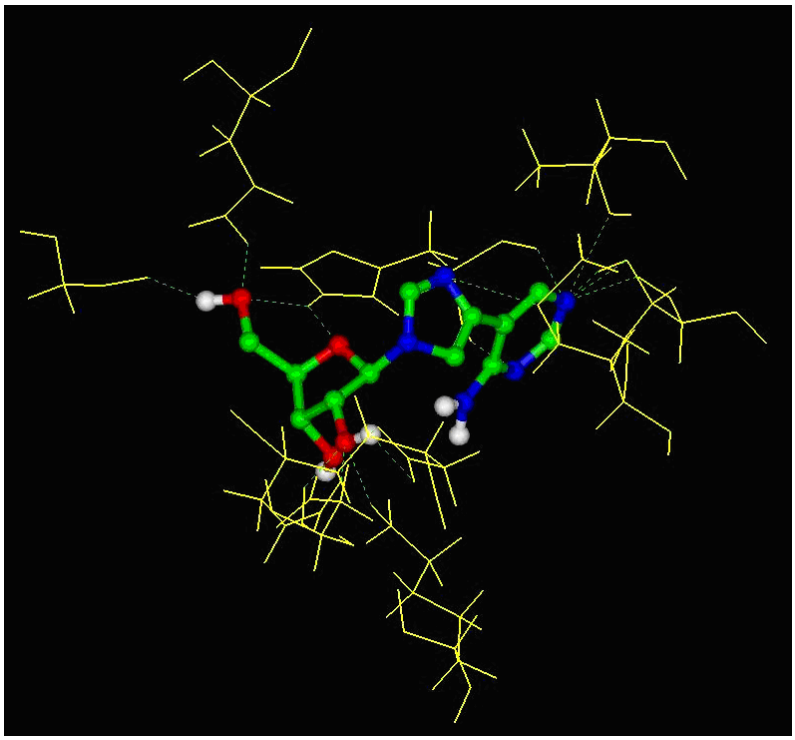

Figure 48. *Proximal* adenosine fleximer in SAHase.

with Borchardt's inhibitor. The heterocyclic base moiety, in both the fleximer and the inhibitor, showed hydrogen bonding patterns with His55 and Thr57. Furthermore, the sugar moiety showed similar pattern binding with Lys186, however, the *proximal* adenosine had many more interactions with SAHase. Even though the proximal inosine (as shown in Figure 49) had a "better" binding energy than both proximal adenosine and Borchardt's inhibitor, as expected, the hydrogen bonding pattern was significantly different since adenosine-based inhibitors should potentially inhibit SAHase.

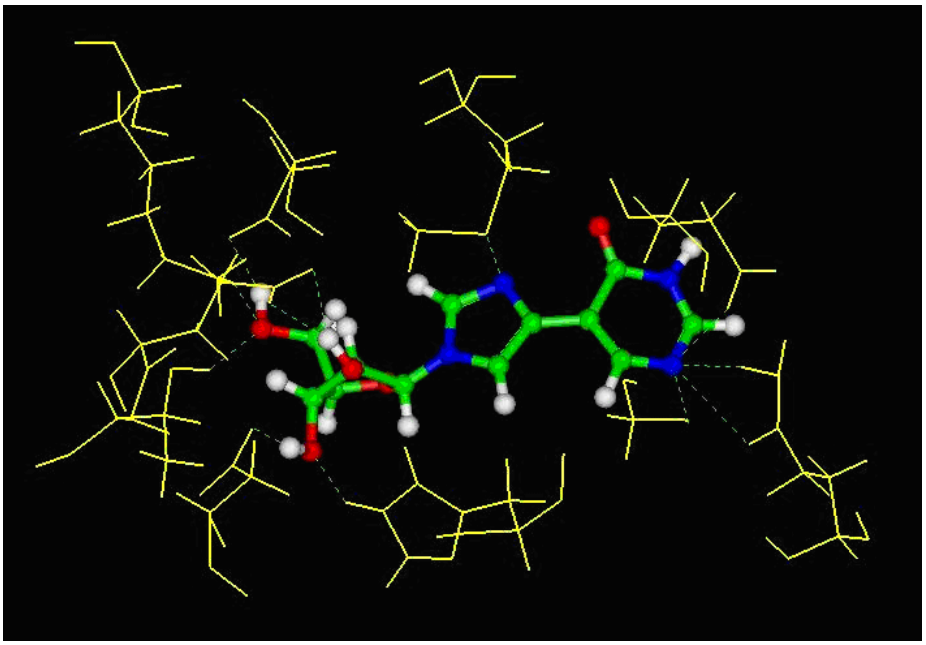

Figure 49. *Proximal* inosine fleximer in SAHase.

While we cannot be certain that the theoretical conformation adopted by all of these *distal* and *proximal* fleximers in the modeling studies will prove to be real once co-crystallized with SAHase, it still provides rationale for the synthesis of these

potential inhibitors of SAHase. If these fleximers indeed assemble within the active site of SAHase, as the modeling data suggests, it will provide valuable insight into the flexibility of the enzyme.

CHAPTER III

CHEMISTRY

Proximal Fleximers.

The nontrivial synthetic pathway that was required, since an organometallic cross-coupling approach would have mandated for a C-6 functionalized pyrimidine which is position to functionalize, for formation of the *distal* fleximers involved the formation of a tricyclic purine based nucleoside with a thiophene spacer ring followed by desulfurization to obtain the "split" purine nucleoside (Scheme 3).[115] As a result of the tedious nature of this approach, we turned our attention to a variety of transition metal catalyzed cross coupling reactions to synthesize the *proximal* fleximers.

Scheme 3. Retrosynthesis of *distal* adenosine.

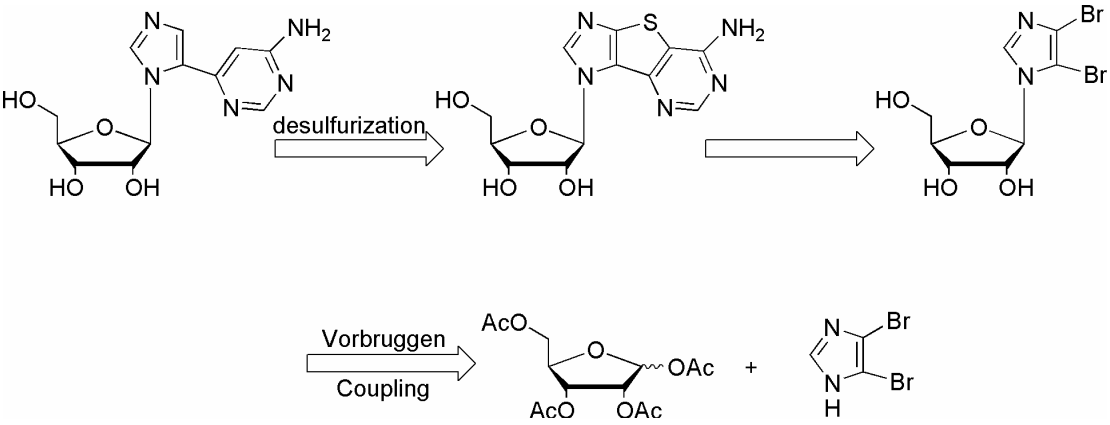

Our initial plan for the synthesis of the series of *proximal* fleximers involved conversion of benzyl protected 4-haloimidazole **(13a** or **13b)**, which was readily available from 4,5-dihaloimidazole **(9a** or **9b)** as shown in Scheme 4,[115,119] into its subsequent 4-*metallo*imidazole. This would allow its use as a component in a variety of palladium catalyzed cross coupling methods.[120] By utilizing a variety of substituted pyrimidine analogues, we postulated that strategic manipulation of the functional groups on the pyrimidine moiety would afford most of the desired *proximal* fleximers.

Scheme 4. Retrosynthetic Approach to the *proximal* fleximers.

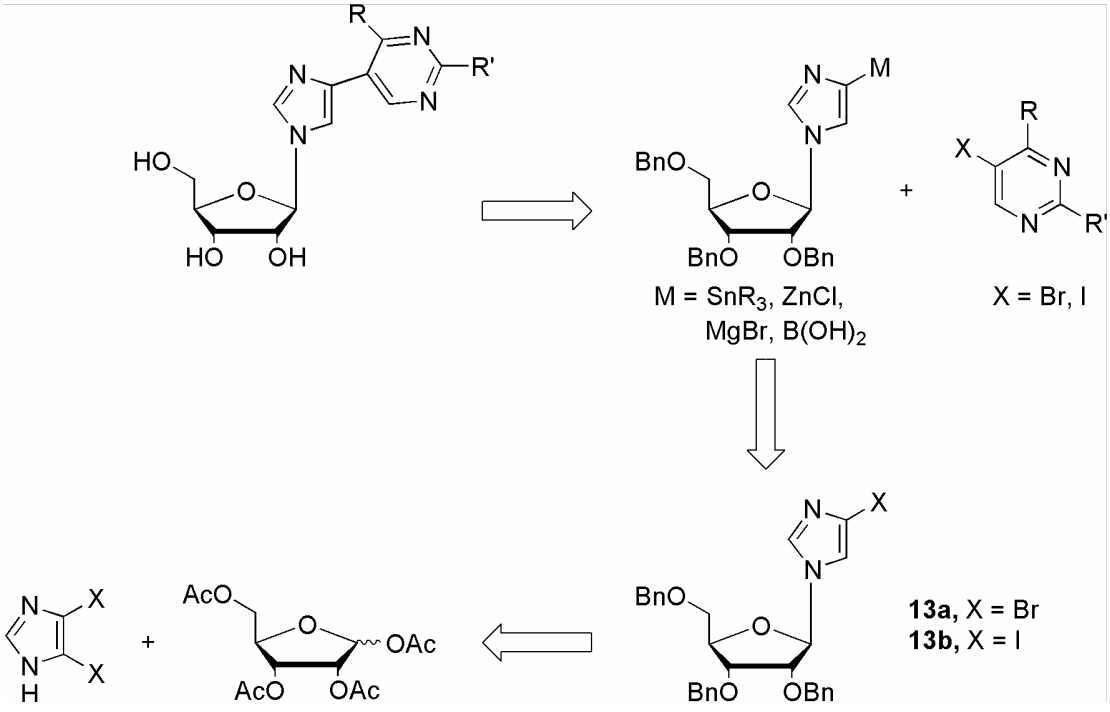

The synthesis of 2,3-dibenzyloxy-5-benzyloxymethyl-1-(4-bromoimidazol-3-yl)-1-β-D-ribofuranose **(13a)** was obtained in 6 steps by starting with inexpensive, commercially available imidazole **(7)**. As shown in Scheme 5, treatment of **8** with bromine, glacial acetic acid and sodium acetate produced 2,4,5-tribromoimidazole **(8)** in 75% yield.[121] Since the C-2 position is the most reactive towards nucleophilic substitution, treatment of 2,4,5-tribromoimidazole **(9)** with 2.5 equivalents of ethylmagnesium bromide in refluxing diethyl ether followed by NH_4Cl afforded 4,5-dibromoimidazole **(9a)** in 86% yield.[115,122]

Scheme 5

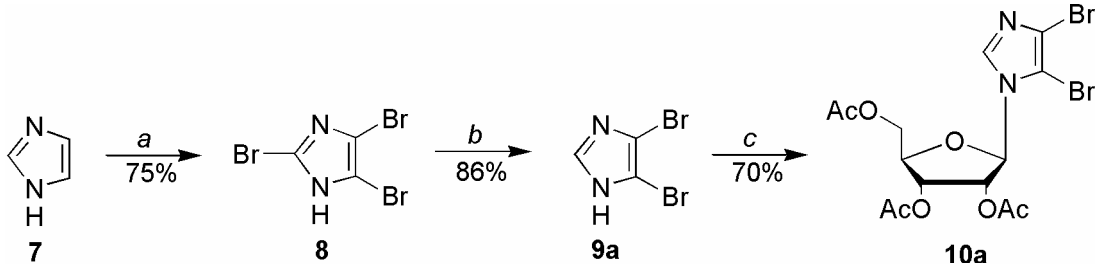

Reaction conditions: a) Br_2, AcOH, NaOAc; b) *i*) EtMgBr, Et_2O, *ii*) NH_4Cl; c) *i*) BSA, 1,2,3,5-*O*-tetraacetate-β-D-ribofuranose, CH_3CN, *ii*) TMSOTf, 60 ºC, 18 h.

Since 4,5-dibromoimidazole is a symmetric molecule, Vorbruggen coupling of **9a**, at either N-1 or N-3, with 1,2,3,5-*O*-tetraacetate-β-D-ribofuranose resulted in only the nucleoside **10a**.[123] Vorbruggen coupling involved the reaction of persilylated heterocyclic moiety with peracylated sugars in the presence of a Lewis acid catalyst such as $SnCl_4$ or trimethylsilyl triflate (TMSOTf).[124] Silylation of 4,5-dibromoimidazole was achieved with N,*O*-bis(trimethylsilyl) acetamide (BSA) rather

than the more traditional hexamethyldisilazane due to difficulties in removing the excess HMDS, which, if still present in the reaction mixture, can inactivate the catalyst (Scheme 6). The mechanism of the Vorbruggen coupling method first involves the conversion of the peracylated sugar into the stable 1,2-acyloxonium salt by both (i) anchimeric assistance of the 2'-acetate group and (ii) a Lewis acid, TMSOTf. The resulting triflate anion reacts with the persilylated dibromoimidazole base, to regenerate TMSOTf, along with the simultaneous attack of the β face of the electrophilic "ribofuranose cation" to afford only the β-nucleoside **10a** (Scheme 7 on the next page).

Scheme 6. Persilylation of dibromoimidazole with BSA.

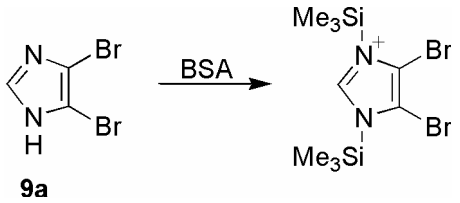

Since the acetate groups would be susceptible to attack by future reaction conditions, specifically Grignard reagents, the acetate groups were removed with saturated methanolic ammonia at 100 ºC for 18 hours to afford triol **11a** in 75% yield. However, the workup was tedious, so this, combined with the less than satisfactory yield prompted us to look for another procedure. Employing another literature procedure, which used NH_4OH in 95% ethanol at room temperature overnight, produced **11a** quantitatively (Scheme 8 on the next page).[115]

Scheme 7. Mechanism of Vorbruggen coupling.

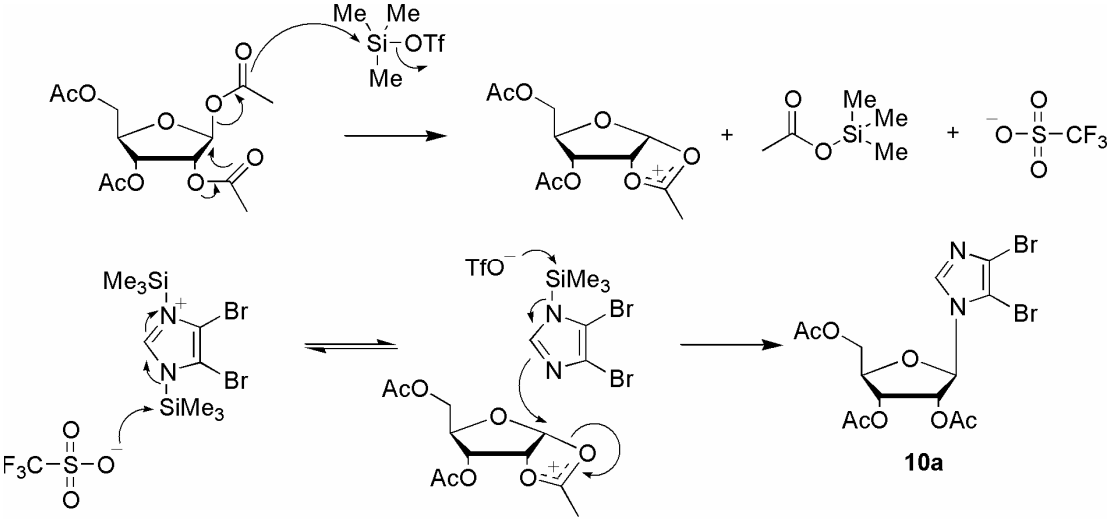

Scheme 8

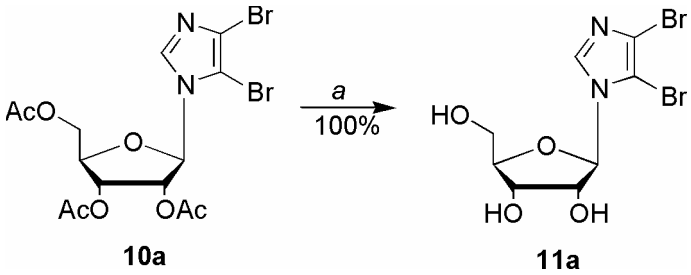

Reaction conditions: a) NH_4OH, EtOH.

The hydroxyl groups were then reprotected as benzyl ethers since they should be stable to all the reaction conditions in the synthetic pathway. Standard benzylation conditions of NaH followed by BnBr, however, resulted in incomplete benzylation of the three hydroxyls of **11a**. Various combinations of mono- and di- benzylated products were formed, which could not be separated effectively. As a result, we

turned our attention to use an *in situ* formation of benzyl iodide, from benzyl bromide and tetrabutylammonium iodide (TBAI), which proved to be superior to the more traditional route. The resulting modification produced **12a** in excellent yield (85%) (Scheme 9).[125] Because the order of reactivity towards nucleophilic substitution for N1 protected imidazole rings is C2 > C5 >> C4, **12a** was treated with ethylmagnesium bromide in diethyl ether to afford the 4-bromoimidazole protected nucleoside **13a**.[119]

Scheme 9

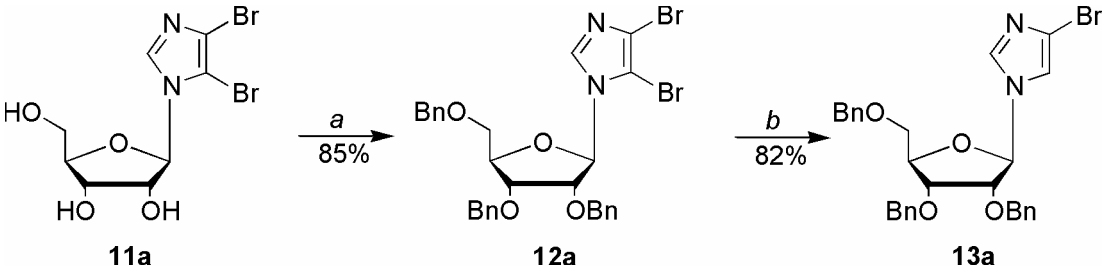

Reaction conditions: a) *i*) NaH, THF, 0 ºC, 3 h *ii*) TBAI, BnBr; b) *i*) EtMgBr, Et_2O, 3h, *ii*) NH_4Cl.

We then turned our attention to conversion of the 4-bromoimidazole protected nucleoside **13a** into the requisite 4-*metallo*imidazole so that it could act as a coupling partner for the various Pd catalyzed cross-coupling methods which include the Stille, Negishi, Kumada and Suzuki reactions.[120]

We initially chose to try the Stille reaction,[126,127] as there were examples in the literature with imidazolylstannanes that had been obtained in reasonable yields.[120,126,127] In some respects, Stille coupling offered forth several advantages that

made it an attractive choice; organostannanes are i) stable towards moisture and air, ii) readily prepared and purified, and iii) tolerate an assortment of functional groups including amines, hydroxyls, and amides.[120,126,127] The only drawback for medicinal chemistry purposes however, is the unfortunate toxicity that is inherent with the use of tin. Despite this, we decided the advantages outweighed the disadvantages, and we went ahead.

The Stille reaction is a versatile palladium-catalyzed cross coupling reaction of organostannanes with organic halides, acetates or perfluorinated sulfonates lacking a sp^3 hybridized β-hydrogen.[120,128,129] Mechanistically, the carbon-carbon bond forming reaction begins with the formation of the organopalladium complex by oxidative addition of the Pd(0) species to the aryl halide or triflate. Although a Pd(II) complex can be used, it is reduced to its active Pd(0) form by either ligand dissociation or nucleophilic organostannane (Scheme 10).[130] During the formation of the organopalladium intermediate, the Pd(0) is oxidized to Pd(II) and the carbon-halide bond is cleaved and two new σ-bonds to palladium are formed. The palladium complex must be coordinatively unsaturated for the oxidative addition to take place.[131] The mechanism proposed for this reaction step is an S_N2 mechanism, or a concerted insertion of the $Pd(0)L_2$ into the carbon-halide bond. Next, transmetalation, the rate limiting step in Stille couplings,[120,127] occurs to form a biarylated palladium moiety. This step involves transfer of an aryl group from an organostannane adduct to palladium complex. Prior to reductive elimination, the trans spatial arrangement of the ligands, L, are rearranged into a cis geometry by assistance of either the solvent or a palladium halide species. Finally, a reductive

elimination produces the cross coupling product and the Pd(0) complex is regenerated (Scheme 10). The mechanism of reductive elimination has been proposed to proceed from a "T shaped" unsaturated palladium complex.

Scheme 10

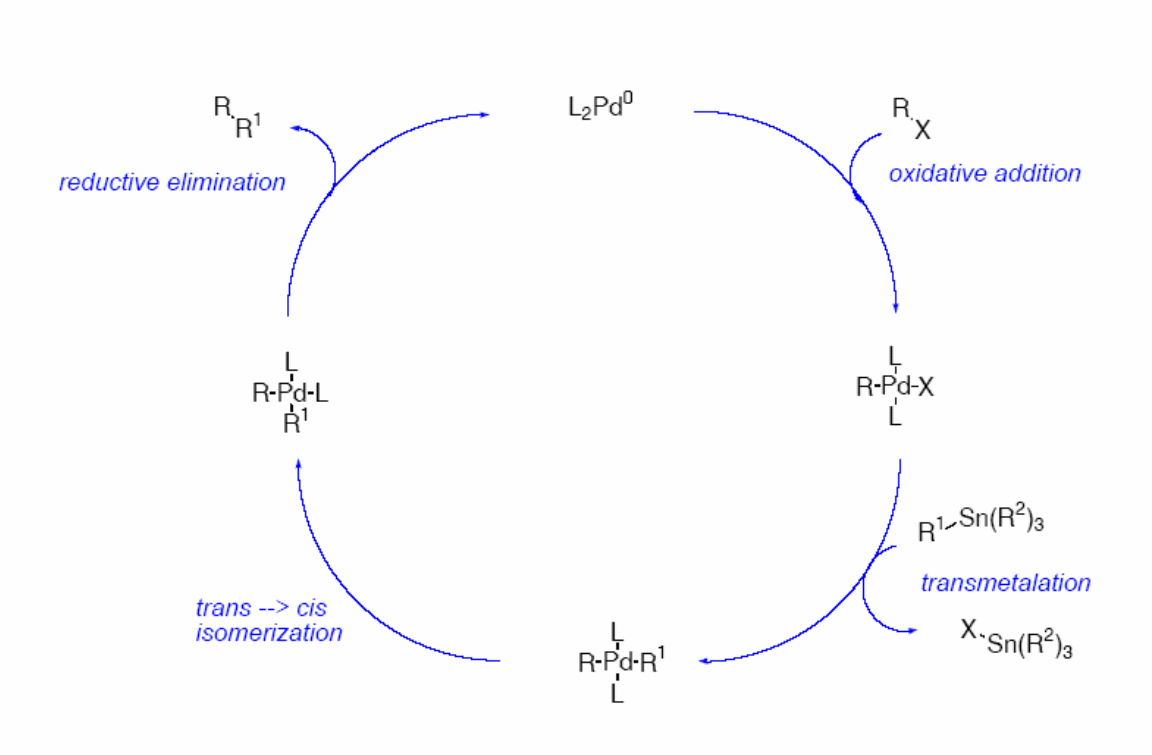

Based on the mechanism of the Stille cross coupling reaction, we initially sought to convert the 4-bromoimidazole protected nucleoside **13a** into its subsequent imidazolylstannane **14** by using either trimethyl- or tributyltin chloride along with a combination of organic bases such as n-butyllithium or ethylmagnesium bromide.[132-135] To our disappointment, the product isolated was the dehalogenated imidazole nucleoside **15**, which, interestingly was obtained in excellent yield (Scheme 11 on the next page). [132-135] This was most likely due to the unfortunate, but unavoidable, humidity in our laboratories at the time, since the building was undergoing renovation

and was open to the environment during much of the day. As a result, it was impossible to maintain a truly "dry" atmosphere, given our lack of access to an appropriate dry box. Based on the failure of the aforementioned reaction, several attempts by altering the solvent from Et_2O to THF to CH_2Cl_2 were attempted but proved to be unsuccessful. [132-135]

Scheme 11

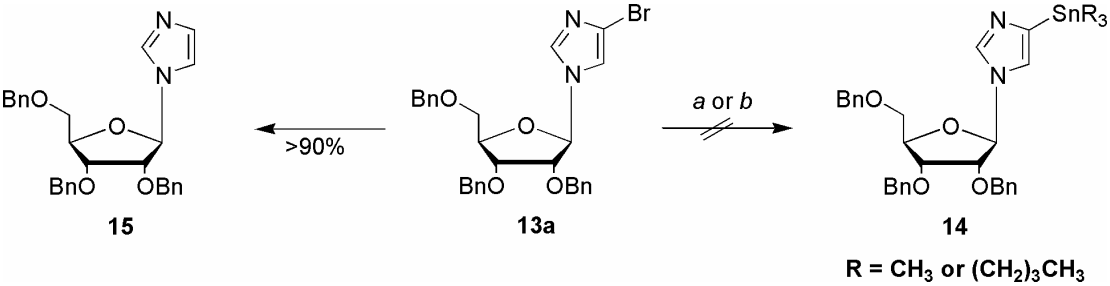

Reactions Conditions: R_3SnCl, in Et_2O or THF or CH_2Cl_2 with a) *n*-BuLi *or* b) EtMgBr, >90%.

Based upon the low reactivity of 4-bromoimidazole protected nucleoside **13a**, we postulated that replacing the bromine at the C-4 position of the imidazole ring with a better leaving group such as iodine might allow for effective oxidative addition, thereby leading to the cross-coupling products.[120] Hence, we synthesized the analogous 4-iodoimidazole protected nucleoside **13b** using similar synthetic methodology (Figure 50 on the next page). This proved to be advantageous, since the workup and purification steps for the diiodoimidazole analogue were much less tedious than for the dibromoimidazole analogue.

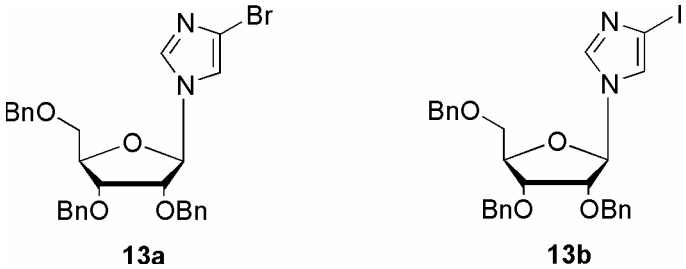

Figure 50. 4-Haloimidazole protected nucleosides.

Synthesis began with replacement of the C-4 and C-5 hydrogens with iodine using a facile literature procedure to give **9b** in 93% yield (Scheme 12).[122,136] Next, coupling diiodoimidazole **9b** as before with the commercially available tetraacetate-protected ribofuranose using N,*O*-bis(trimethylsilyl)acetamide and trimethylsilyltriflate gave **10b**.

Scheme 12

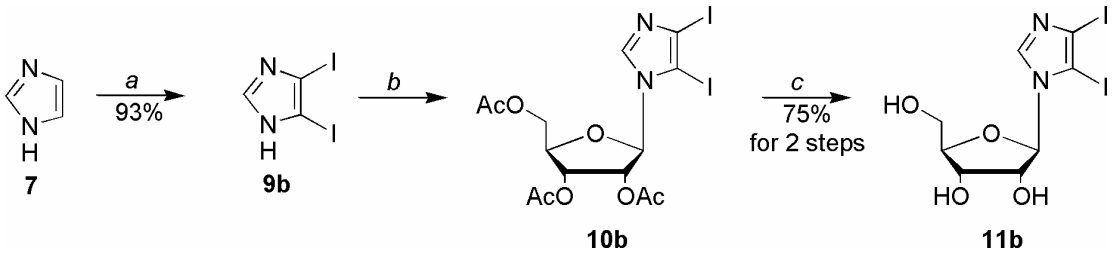

Reaction conditions: a) ICl, KCl; b) *i*) BSA, CH_3CN, *ii*) TMSOTf, 60 ºC, 18 h; c) NH_4OH, EtOH.

As previously mentioned, replacement of the acetate blocking groups with a more robust protecting group was necessary, due to the various reaction conditions that would be encountered in subsequent steps that would not be tolerated by either an alcohol or ester functionality. Standard base-promoted removal of the acetates afforded **11b** as a white crystalline solid in a 75% overall yield for the two steps.

Reprotection of the three hydroxyls with the *in situ*[125] formation of benzyliodide, was then accomplished to give **12b** in an 80% yield. Displacement of the C-5 iodine using Grignard conditions, yielded **13b** also in an 80% yield (Scheme 13).[119]

Scheme 13

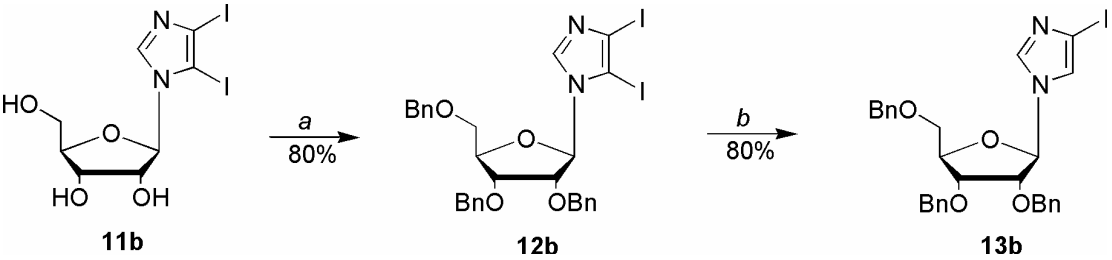

Reaction conditions: a) *i*) NaH, THF, 0 ºC, 3 h *ii*) TBAI, BnBr; b) *i*) EtMgBr, Et_2O, 3 h, *ii*) NH_4Cl.

As shown in Scheme 14, we used similar reaction conditions, as were used in Scheme 11, [132-135] in an effort to convert the protected 4-iodoimidazole **13b** into its subsequent imidazolylstannane **14**. Unfortunately the dehalogenated imidazole nucleoside **15** was once again the only product, albeit in exceptional yields.

Scheme 14

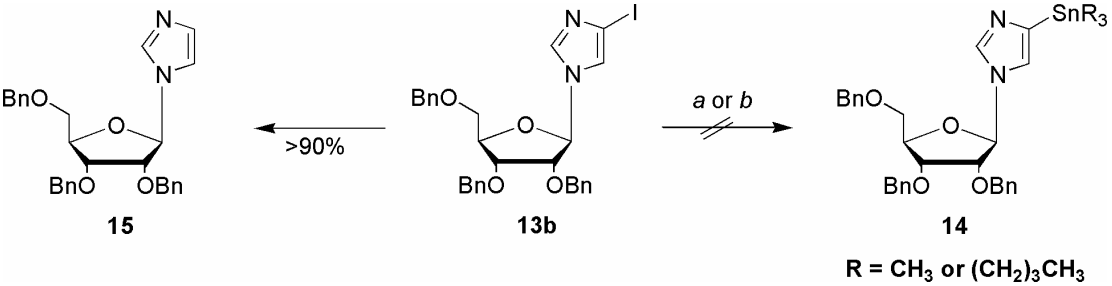

Reactions Conditions: R_3SnCl, in Et_2O or THF with a) *n*-BuLi *or* b) EtMgBr, >90%.

Based on the low yielding reactions encountered in the efforts to produce **14**, we attempted to form the imidazolylstannane *in situ* using hexabutylditin and then subsequently coupling it to 5-iodopyrimidin-4-one (**17**) (Scheme 15) using a variety of palladium catalyst such as $PdCl_2(PPh_3)_2$, $PdCl_2(dppf)$, $Pd(PPh_3)_4$ and $Pd_2(dba)_3$ in DMF or toluene (Scheme 16 on the next page).[133,137,138]

Scheme 15

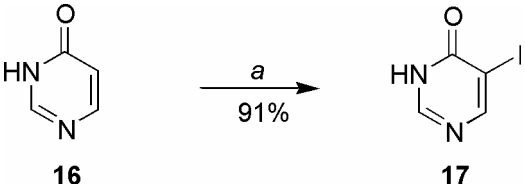

16 **17**

Reaction Conditions: a) I_2, NaOH, H_2O.

Unfortunately, no formation of the desired cross-coupling product **18**, the requisite intermediate needed for the synthesis of *proximal* fleximers, inosine **2** and adenosine **1** (Scheme 16 on the next page), could be detected. We then turned our attention to the Kumada and Negishi cross-coupling methodology.[139,140] Kumada coupling involves cross-coupling Grignard reagents with alkyl, vinyl or aryl halides or triflates under nickel or palladium catalysis.[120] The advantage of this reaction is the direct coupling of the Grignard reagent, which avoids the need for additional reaction steps such as the conversion of the Grignard reagent to organotin or organozinc compounds.[120] Furthermore, the reaction does not need to be heated at high or even moderate temperatures. The reaction, however, is limited to halide partners that do not react with organomagnesium compounds.

Scheme 16

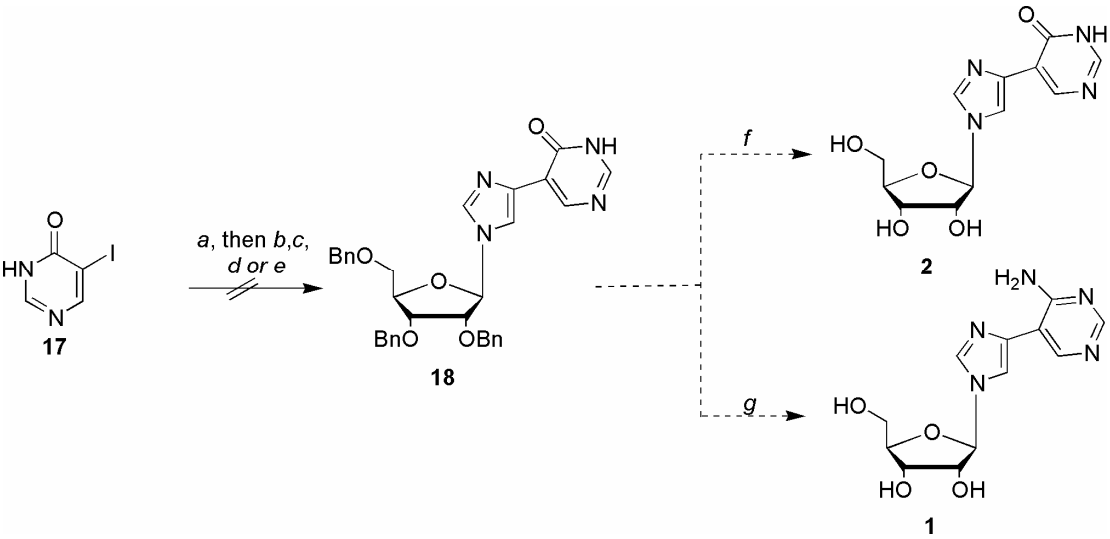

Reaction Conditions: a) *i*) **13b** with *n*-BuLi in Et_2O and $(Bu_3Sn)_2$ then *ii*) **17** with: b) $PdCl_2(PPh_3)_2$; c) $PdCl_2(dppf)$; d) $Pd(PPh_3)_4$; or e) $Pd_2(dba)_3$; to form **2** f) Pd/C, HCO_2NH_4, EtOH, reflux or to form **1** g) *i*) P_2S_5, pyridine, reflux; *ii*) MeI, K_2CO_3; *iii*) NH_3, butanol, 160°C; *iv*) Pd, HCO_2NH_4, EtOH, reflux.

Negishi coupling is a very versatile palladium catalyzed cross-coupling reaction involving an organozinc species and an electrophile such as an organohalide or triflate.[120,140,141] Negishi coupling has several advantages that made it an attractive choice; organozinc reagents are highly selective towards a variety of electrophiles, they are prepared relatively easily and are compatible with a variety of functional groups such as amines, nitriles, and amides.[141] Organozinc compounds are prepared *in situ* via organic bases such as organolithium or Grignard based reagents. As shown in Scheme 17 on the next page, the mechanism of the Negishi coupling is similar to that of the Stille coupling.

Scheme 17

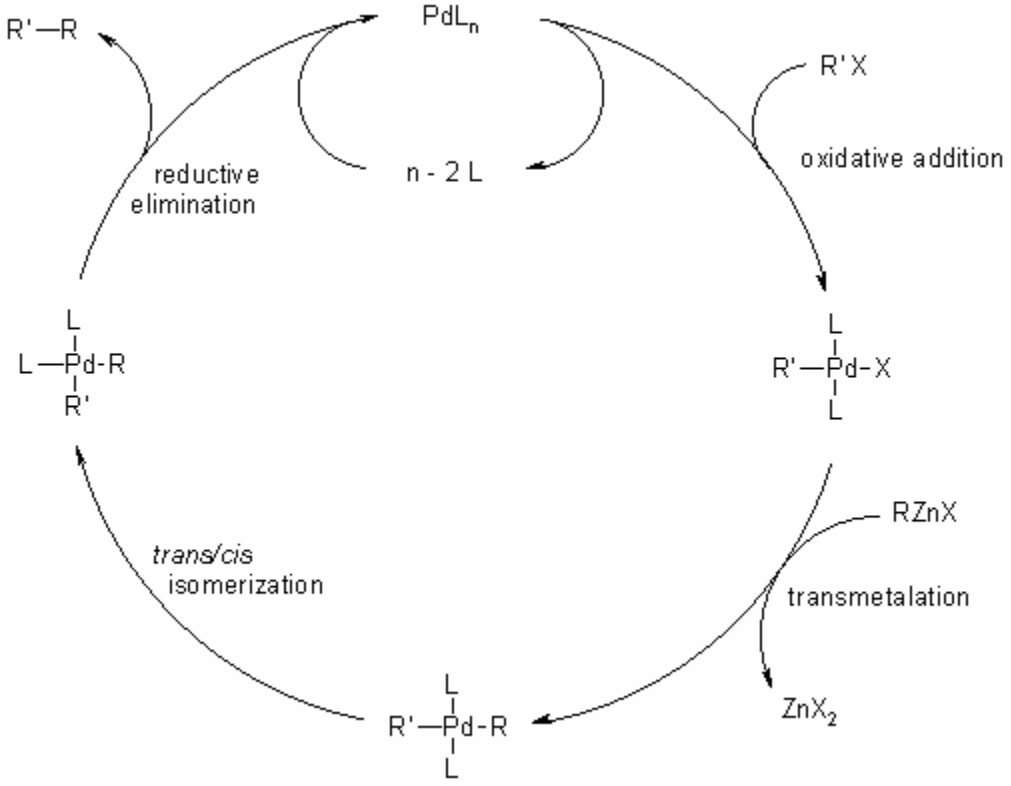

As summarized in Scheme 18 on the next page, the Kumada and Negishi were some of the other cross-coupling methods tried.[139,141,142] We attempted to couple a halouracil analogue with the C- 4 substituted metalloimidazole, formed *in situ*, to form the cross-coupling adduct **21**. Unfortunately, all efforts to construct the C-4 substituted scaffold proved fruitless. We altered the nature of the halouracil derivative by synthesizing both 5-bromo-1,3-dimethyluracil (**20a**) and 5-iodo-1,3-dimethyluracil (**20b**) from 5-bromouracil (**19a**) and 5-iodouracil (**19b**) respectively (Scheme 18 on the next page).[143]

Scheme 18

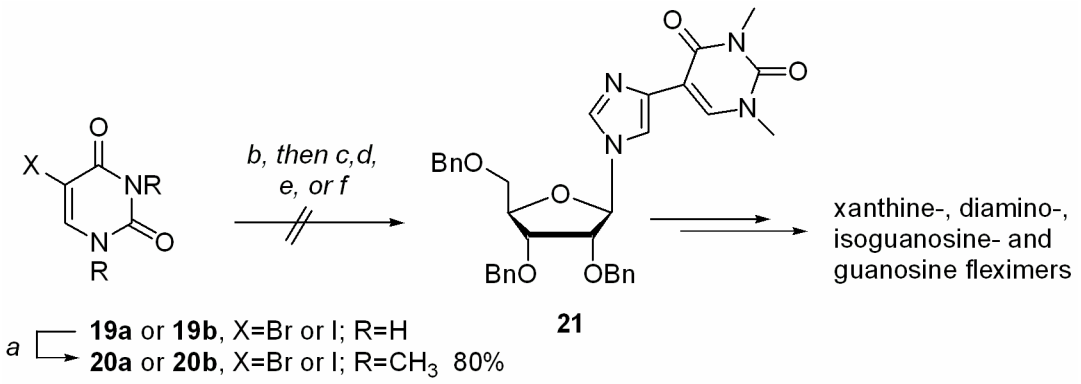

Reaction conditions: a) Me_2SO_4, NaOH, H_2O; b) *i*) **13b** with EtMgBr or $ZnCl_2$ in Et_2O, then *ii*) **20a** or **20b** with: c) $PdCl_2(PPh_3)_2$; d) $PdCl_2(dppf)$; e) $Pd(PPh_3)_4$ or f) $Pd_2(dba)_3$.

Also, altering the choice of solvent (Et_2O or THF), the reaction temperature, or the palladium catalyst such as $PdCl_2(PPh_3)_2$, $PdCl_2(dppf)$, $Pd(PPh_3)_4$, or $Pd_2(dba)_3$ failed to yield the desired intermediate **21**,[133,144] from which several of the target fleximers could be realized. The failure of the Negishi conditions were surprising, since Negishi coupling had been reported to work well with C-4 iodo-substituted imidazoles, and was more tolerant of sensitive functional groups than traditional Grignard and organolithium approaches. We speculated that it could have been due to the π-electron deficient nature of the dimethyluracil since literature precedence indicated that the formation of the nucleophilic imidazole moiety, both *in situ* and as an isolated intermediate. As a result, it appeared that the pyrimidine system was simply insufficiently activated to participate in the cross coupling.

As shown in Scheme 19 on the next page, we then proposed an alternate synthetic route to obtain the *proximal* fleximers by a Negishi cross-coupling reaction between an organozinc analogue of **13b**, formed *in situ*, and 5-bromo-2,4-

dimethylthiopyrimidine (**27**) (synthesized from uracil (**22**) in Scheme 20 on page 81) to form the cross coupling intermediate **28**.[145]

Scheme 19

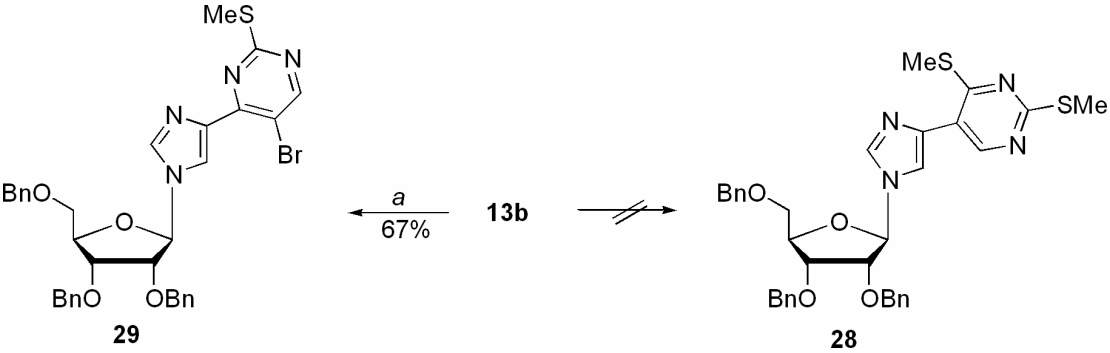

Reaction conditions: a) EtMgBr, Et_2O, then $ZnCl_2$, then **27**, $Pd(PPh_3)_4$, CH_2Cl_2.

Since, oxidative addition step involving organic halides, for example, Pd (0) is oxidized by two electrons to Pd (II), while organic halides are reduced by two electrons. So, electron withdrawing substituents on the organic halide moiety may be expected to accelerate the oxidative addition reaction.[120] The same reasoning also predicts that electron donating substituents in the ligands on Pd would accelerate oxidative addition. Speculation that the inherent electron deficient nature of the pyrimidine ring system was the cause for the significant lack of reactivity noted to date was a strong possibility. If this was indeed true, it was clear that to be successful, the electronics of the pyrimidine ring system had to be enhanced, therefore electron donating substituents such as ethers or thioethers might prove to be a possible solution. We chose to focus on the thioethers first, as their conversion to the requisite substituents appeared to be facile.

Scheme 20

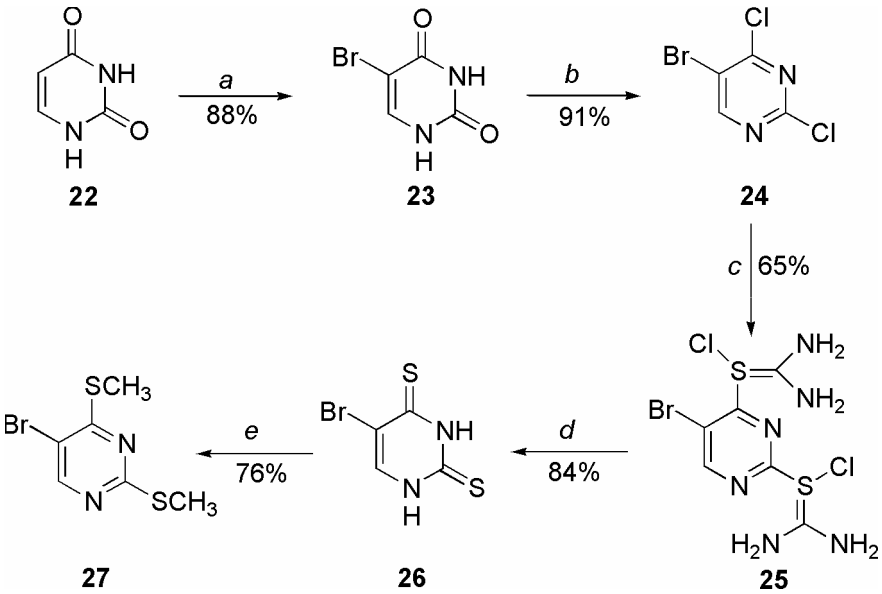

Reaction conditions: a) Br_2, H_2O; b) $POCl_3$, DEA; c) $S=C(NH_2)_2$, anhydrous EtOH; d) NaOH; e) Me_2SO_4, NaOH.

In order to synthesize **27** (Scheme 20), cheap, commercially available uracil (**22**) was readily converted to 5-bromouracil (**23**) using bromine and H_2O.[146] Subsequent chlorination of **23** with standard conditions provided 5-bromo-2,4-dichloropyrimidine (**24**) in 91% yield.[147] Next, treatment with thiourea gave **25** in 65% yield, which was then hydrolyzed to the dithiocarbonyl analogue **26** in 84% yield using sodium hydroxide.[148,149] Finally, methylation with standard conditions gave **27** in a 76% yield.

We postulated that by using standard ammonolysis conditions, subsequent desulfurization, and deprotection of the hydroxyls on cross-coupled intermediate **28** would have formed proximal adenosine **1** (Scheme 21 on the next page). Unfortunately, upon Negishi coupling of **13b** and **27** the only product that was formed was shown by NMR to be **29** (Scheme 19 on top of page 81), where coupling

to the imidazole had occurred at the C-4 of the pyrimidine, displacing the C-4 thiomethyl group, rather than the C-5 bromine.

Scheme 21

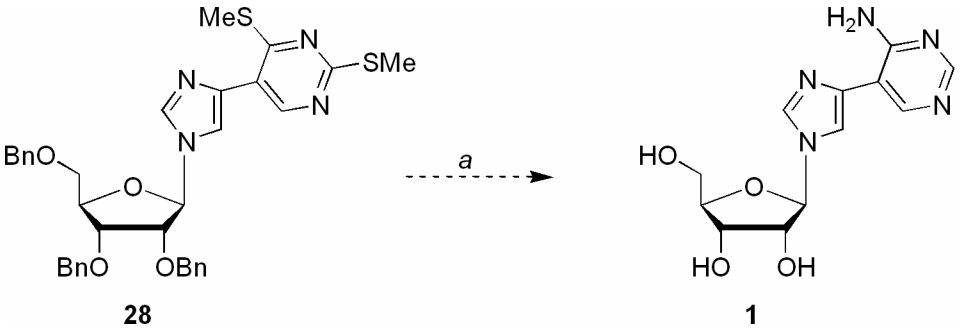

28 **1**

Reaction Conditions: a) *i*) NH_3, butanol, 160°C; *ii*) Raney Ni, MeOH, reflux; *iii*) Pd, HCO_2NH_4, EtOH, reflux.

After exhausting options with the Stille, Kumada and Negishi cross coupling reactions, we turned our attention to Suzuki-Murayama cross couplings.[120,129,150] The Suzuki coupling involves palladium-catalyzed cross coupling between organoboronic acid reagents and organohalides (or triflates).[120] Suzuki coupling reactions have three major advantages; one, they tolerate the presence of various functional groups in the coupling moieties, two, they are air and moisture stable making them relatively simple to handle, and three, they are non-toxic unlike the organotin compounds used in Stille cross coupling.[120] Although there were some challenges associated with the synthesis of aryl boronic acid; since they require very low temperatures, as well as their tendency to cross couple with each other, we still pursued this synthetic pathway hoping to overcome these disadvantages.

Initially, we attempted to convert protected 4-iodoimidazole **13b** into its analagous protected imidazolyl-4-boronic acid **30**.[150,151] Iodinated imidazole based nucleoside **13b** was treated with either *n*-BuLi or EtMgBr in anhydrous THF or CH_2Cl_2 at –78 °C followed by the addition of a trialkyl borate, $B(O^iPr)_3$ while maintaining the temperature at -78 °C.[150,151] As shown in Scheme 22, these efforts proved futile as well, since all attempts once again resulted in formation of the dehalogenated imidazole nucleoside **15**, rather than the desired imidazole boronic acid **30**.

Scheme 22

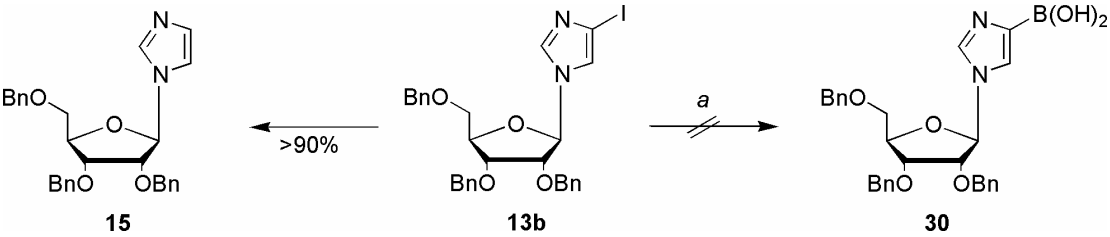

Reaction Conditions: a) *i*) *n*-BuLi or EtMgBr, THF or CH_2Cl_2, -78 °C; *ii*) $B(O^iPr)_3$; *iii*) aq. HCl.

Continuing the pursuit for the proximal fleximers via Suzuki coupling, we decided to form an aryl borate complex (which was not isolated) *in situ* by the addition of *bis*(pinacolato)diboron, KOAc, $PdCl_2$(dppf) in DMF.[152,153] Upon formation of **31**, 5-iodopyrimidin-4-one (**17**), $PdCl_2$(dppf), and K_2CO_3 were added such that the proximal fleximer intermediate **18** would be realized and subsequently isolated. Unfortunately, formation of **18** did not occur and only starting material **13b** was recovered (Scheme 23 on the next page).

Scheme 23

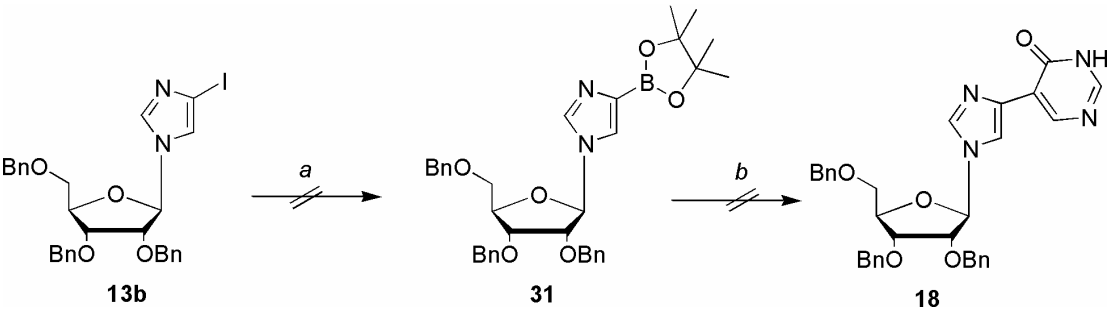

Reaction Conditions: a) *bis*(pinacolato)diboron, KOAc, $PdCl_2$(dppf), DMF, 80 ºC, 2 h; b) **17**, $PdCl_2$(dppf), K_2CO_3.

At this point we reversed our strategy to employ the pyrimidine as the nucleophilic component. Based on retrosynthetic analysis, we once again utilized palladium catalyzed cross-couplings such as Stille, Kumada, Negishi and Suzuki reactions (Scheme 24). We attempted to couple **13b** to a variety of organometallic pyrimidine species, including the pyrimidinylstannane **32** which was synthesized by first treating 5-iodouracil (**19b**) with sodium hydroxide in refluxing dimethyl sulfate to afford 5-iodo-1,3-dimethyluracil (**20b**).[154] This was followed by heating **20b** with hexabutylditin in toluene with $PdCl_2(PPh_3)_2$ under Ar to yield 5-tri-n-butylstannyl-1,3-dimethyluracil (**32**) in a 66% yield (Scheme 25 on the next page).[143]

Scheme 24

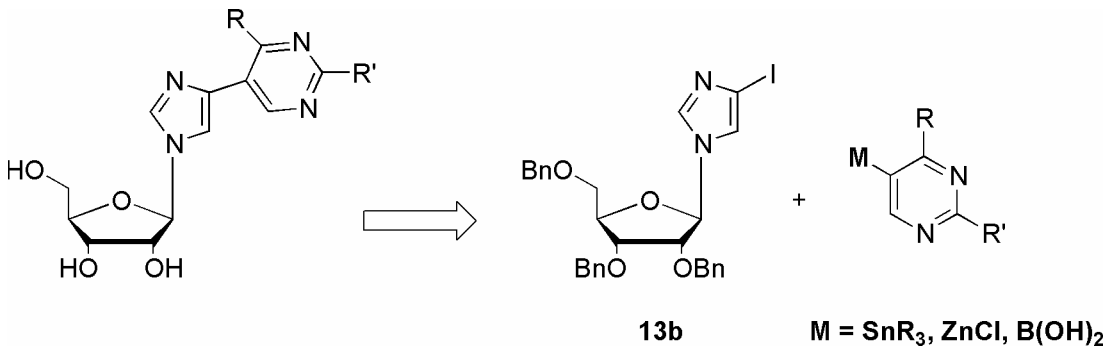

Scheme 25

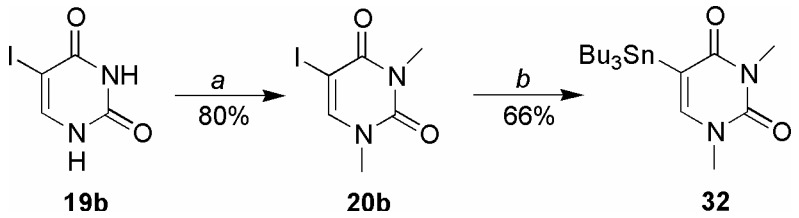

19b 20b 32

Reaction Conditions: a) Me_2SO_4, NaOH, H_2O; b) $(Bu_3Sn)_2$, $PdCl_2(PPh_3)_2$, $PhCH_3$.

Upon formation of the pyrimidinylstannane, we attempted to couple **32** to **13b** using a variety of palladium reagents including; $Pd(PPh_3)_4$ and $PdCl_2(PPh_3)_2$ in either DMF or 1,2-dimethoxyethane (DME) at 80 ºC (Scheme 26).[143,155] Unfortunately, pyrimidinylstannane **32** failed to undergo coupling with **13b** under standard Stille reaction conditions.

Although Stille cross-coupling reactions have higher chemoselectivity than their analogous Negishi cross-coupling reactions, organostannanes have been shown to be less reactive than organozinc compounds.[120] Therefore, we sought out to synthesize organozinc based pyrimidine **33** analogous to the organostannane **32**.

Scheme 26

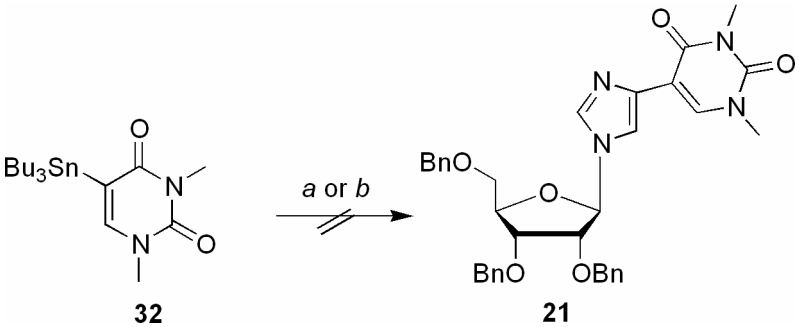

32 21

Reaction conditions: a) **13b**, $Pd(PPh_3)_4$, CuI, DMF or DME; b) **13b**, $PdCl_2(PPh_3)_2$, DMF or DME, 80 °C.

Using our previously synthesized 5-iodo-1,3-dimethyluracil (**20b**), we attempted to form **33** through the addition of EtMgBr or *n*-BuLi in ether or THF, followed by the addition of zinc (II) chloride (Scheme 27). Attempts to couple the organozinc moiety **33** synthesized *in situ* with **13b** using a variety of palladium reagents including; $Pd(PPh_3)_4$ and $PdCl_2(PPh_3)_2$ in either DMF or DME at 80 ºC (Scheme 27) remained unsuccessful.

Scheme 27

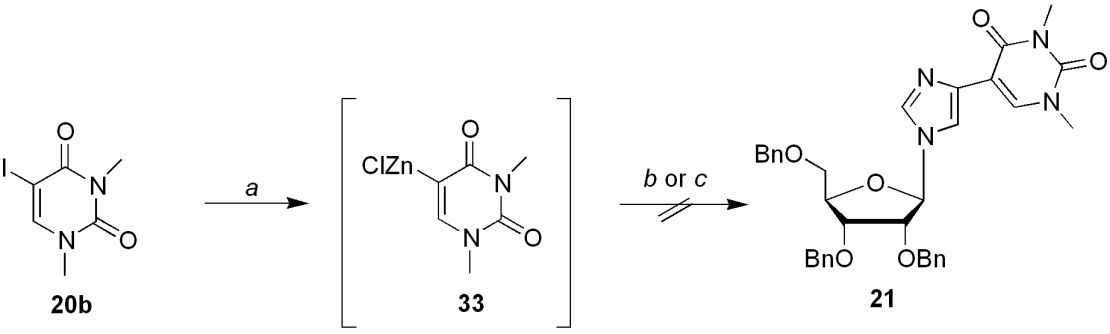

Reaction Conditions: a) *i*) EtMgBr or *n*-BuLi, Et_2O or THF; *ii*) $ZnCl_2$; b) **13b**, $Pd(PPh_3)_4$, CuI, DMF or DME; c) **13b**, $PdCl_2(PPh_3)_2$, DMF or DME, 80 °C.

We postulated that the organozinc chloride complex **33** did not form effectively, therefore we attempted to insert Zn between the C-I bond, by heating 5-iodo-1,3-dimethyluracil (**20b**) with activated zinc powder, to form the organozinc iodide adduct **34** *in situ*.[140,156] Once again as shown in Scheme 28 on the next page, attempts to couple the **13b** to **34** synthesized using a variety of palladium reagents including; $Pd(PPh_3)_4$ and $PdCl_2(PPh_3)_2$ in either DMF or DME at 80 ºC were ineffective.[140,141]

Scheme 28

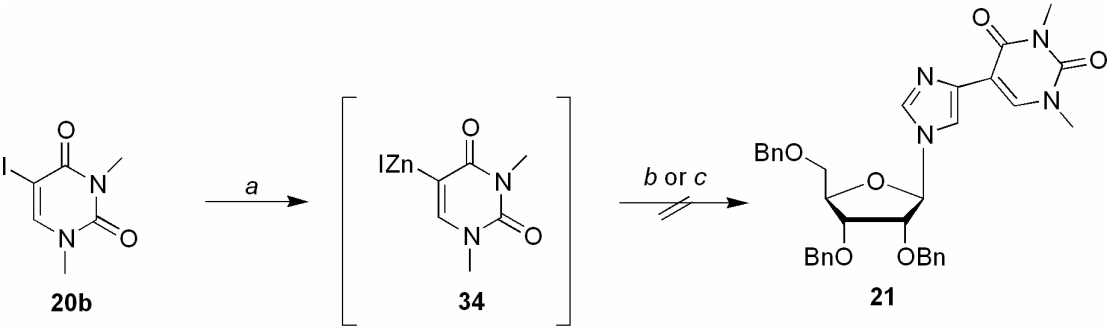

Reaction Conditions: a) Zn powder, *N*,*N*-dimethylacetamide, heat; b) **13b**, $Pd(PPh_3)_4$, CuI, DMF or DME; c) **13b**, $PdCl_2(PPh_3)_2$, DMF or DME, 80 °C.

Moving next to the Suzuki coupling, we sought to synthesize our boronic acid coupling partner **36**. Using an *in situ* formation of sodium benzoate, from NaH and benzyl alcohol, we converted 5-bromo-2,4-dichloropyrimidine (**24**) into its analogous dibenzyloxy ether pyrimidine system **35** in 91% yield.[157] Sequential treatment of 5-bromo-2,4-dibenzyloxypyrimidine (**35**) with *n*-BuLi, triisopropyl borate, followed by aqueous HCl afforded the aryl boronic acid **36**, albeit in low yield (22%) (Scheme 29).[151] Attempts to increase the yield of **36**, either by (i) lowering temperatures to aid in formation of the boronic acid or (ii) adding molecular sieves to remove any trace amounts of moisture proved futile.

Scheme 29

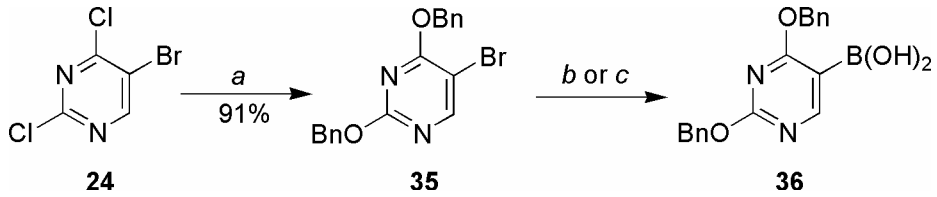

Reaction Conditions: a) NaH, BnOH, $PhCH_3$; b) *i*) *n*-BuLi, THF, -78 °C, *ii*) $B(O^iPr)_3$; *iii*) aq. HCl or c) *i*)$B(O^iPr)_3$, THF, $PhCH_3$, -78 °C, *ii*) *n*-BuLi, *iii*) aq. HCl.

Eventually, a procedure outlined by Schinazi and Prusoff showed that slow, dropwise addition of *n*-BuLi to an aryl halide and alkyl borate provided excellent yields.[157] We implemented this protocol to a solution containing 5-bromo-2,4-dibenzyloxy-pyrimidine (**35**) and triisopropyl borate in THF:toluene (1:4 volume ratio) at –78 °C and slowly added *n*-BuLi dropwise. Upon quenching the reaction with aqueous HCl, we obtained 5-(dihydroxyboryl)-2,4-bis(benzyloxy)pyrimidine (**36**) in exceptional yield (95%).[157]

Coupling was then successfully carried out with tetrakis (triphenylphosphine) palladium (0) in refluxing DME and saturated aqueous $NaHCO_3$ to give **37** (67%) (Scheme 30).[158] Removal of all five of the benzyl groups with palladium on carbon, ammonium formate in EtOH was accomplished in 88% yield to give the *proximal* xanthosine fleximer **6** directly (Scheme 31 on the next page).[159]

Scheme 30

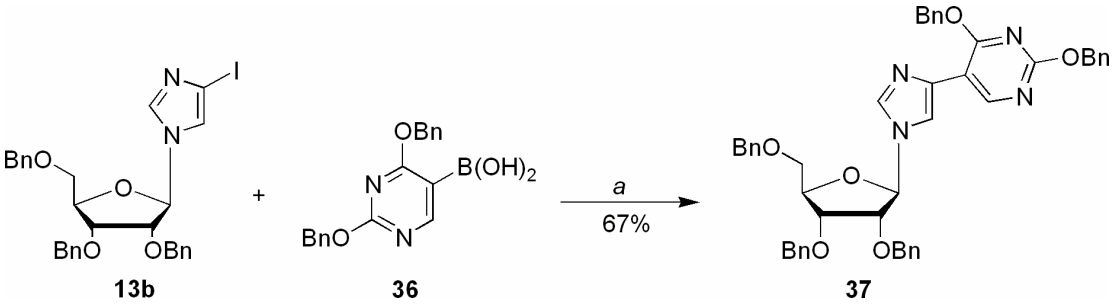

Reaction Conditions: a) $Pd(PPh_3)_4$, DME, NaHCO3, reflux, 4h.

Using the *proximal* xanthosine fleximer **6**, we postulated that both the guanosine and isoguanosine fleximers **3** and **4** could be readily obtained. In order to form the *proximal* isoguanosine **4**, we attempted to directly convert the C-4 oxo

moiety into the free amino group via a literature procedure by Selway *et al*[160] which showed that a uridine analogue was readily converted into its cytidine analogue in excellent yields.

Scheme 31

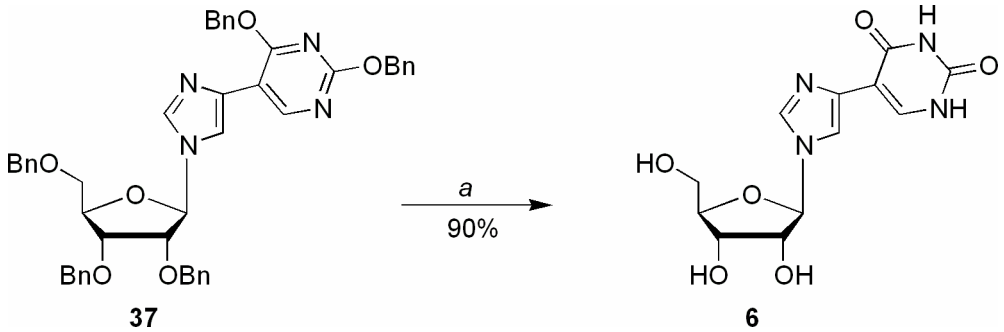

Reaction Conditions: a) Pd/C, HCO_2NH_4, EtOH, reflux.

Therefore, treatment of the xanthosine fleximer **6** with hexamethyldisilazane, formamidine and ammonium sulfate was heated in a Parr bomb for 72 hours (Scheme 32).[160] Unfortunately, our analogous reaction did not provide us with the *proximal* isoguanosine **4**.

Scheme 32

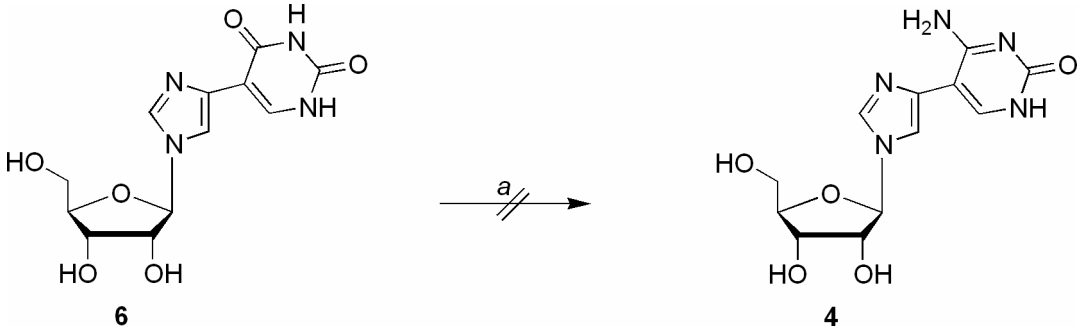

Reaction Conditions: a) HMDS, formamidine, $(NH_4)_2SO_4$, 120 °C, 72 h.

We turned our attention to the synthesis of the *proximal* guanosine fleximer **3** (from xanthosine fleximer **6**) using a procedure outlined by Watanabe *et al* which presented the analogous conversion of Ψ-uridine into Ψ-isocytidine (Scheme 33).[161] Treatment of Ψ-uridine with dimethylformamide dimethylacetal provided the methylated Ψ-uridine which was then subsequently treated with guanidine to afford Ψ-isocytidine in excellent yield. Therefore, we used our analogous Ψ-uridine system, *proximal* xanthosine fleximer **6** and alkylated the pyrimidine moiety to yield **38**.[161] Attempting to convert the "urea" moiety in the pyrimidine ring, with guanidine, into the *proximal* guanosine fleximer **3** was unsuccessful (Scheme 34 on the next page).

Scheme 33

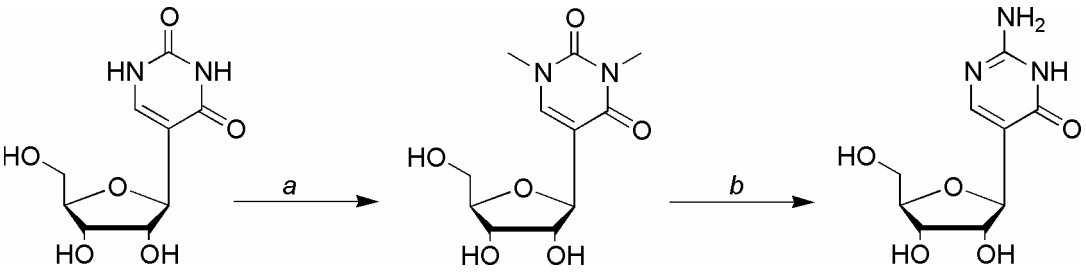

Ψ-uridine **Ψ-isocytidine**

Reaction Conditions: a) $(CH_3)_2NCH(OCH_3)_2$; b) guanidine.

Alternatively, we attempted to obtain the *proximal* guanosine and isoguanosine fleximers (**3** and **4**) by selectively treatment of *proximal* diamino fleximer **5**. Based on literature precedence[162] for the conversion of a 2,4-diaminopurine based nucleoside into either a 2-amino-4-oxopurine or 4-amino-2-oxopurine nucleoside, we needed to synthesize the *proximal* diamino fleximer **5**.

Scheme 34

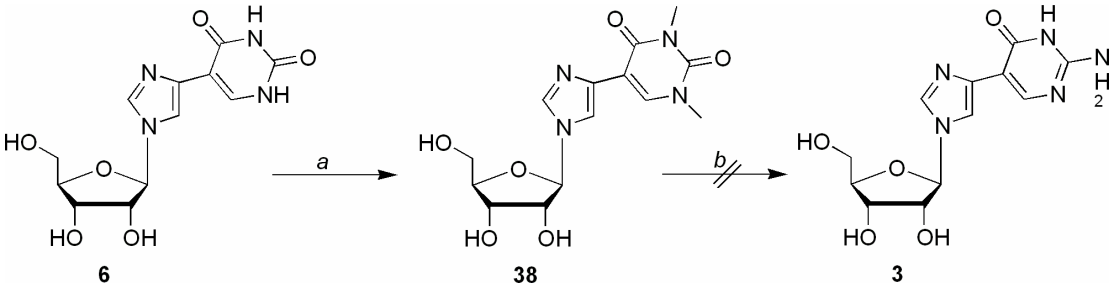

Reaction Conditions: a) $(CH_3)_2NCH(OCH_3)_2$; b) NaOEt, guanidine.

Therefore, treatment of **37** with ammonia in ethanol at 160 °C for 96 hours in a steel Parr bomb afforded **39** in albeit moderate yield (40%),[162] which, following by standard deprotection, gave the desired *proximal* diamino fleximer **5** (90%) (Scheme 35).[159]

Scheme 35

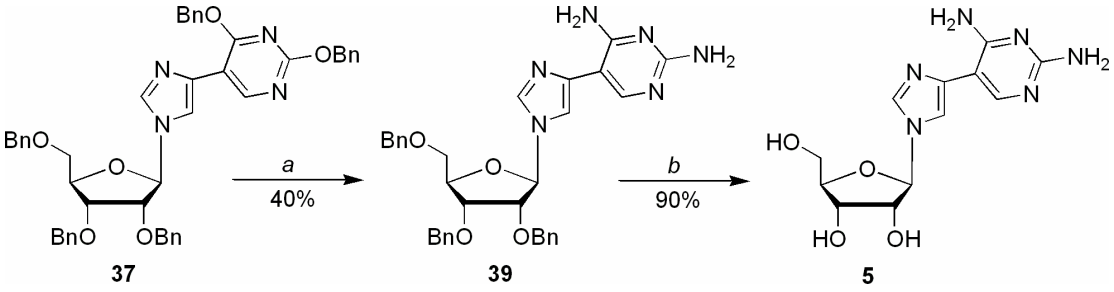

Reaction Conditions: a) NH_3, EtOH, 160 °C, 96 h; b) Pd/C, HCO_2NH_4, EtOH, reflux.

With the first two proximal fleximers finally in hand, the remaining goal was to manipulate the diamino fleximer **5** to give us the guanosine and isoguanosine fleximers (**3** and **4** respectively) we had initially set our sights on. The *proximal*

isoguanosine fleximer **4** was realized following selective conversion of the C-2 amino group of the protected diamino fleximer **39** to the desired carbonyl using typical diazotization conditions, and subsequent deblocking of the benzyl protecting groups with Pd/C and ammonium formate in refluxing ethanol (41% yield, two steps from **39**) (Scheme 36).[162] Finally, the diamino fleximer **5** was converted directly to **3** using aqueous sodium bisulfite and heat in an 88% yield (Scheme 37 on the next page).[163]

Scheme 36

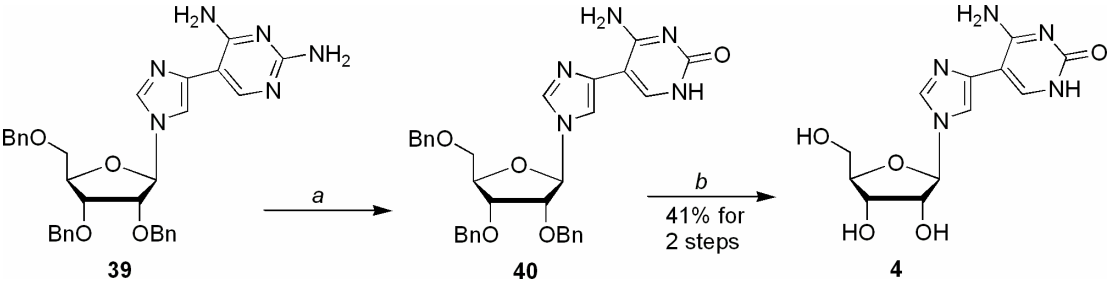

Reaction Conditions: a) $NaNO_2$, AcOH, THF:H_2O (1:1); b) Pd/C, HCO_2NH_4, EtOH, reflux.

After accomplishing the formation of the proximal fleximers; guanosine, isoguanosine, diamino-, and xanthosine **3-6** respectively, we revisited the synthesis of the proximal adenosine and inosine fleximers **1** and **2**. Based on our previous success of the Suzuki coupling, we wanted to implement similar reaction conditions on an analogous imidazole and pyrimidine moiety. With this in mind, we coupled commercially available 5-(dihydroxyboryl)pyrimidine (**41**) to the previously synthesized C-4 iodoimidazole nucleoside **13b** using $PdCl_2$(dppf) (Scheme 38).[152]

Scheme 37

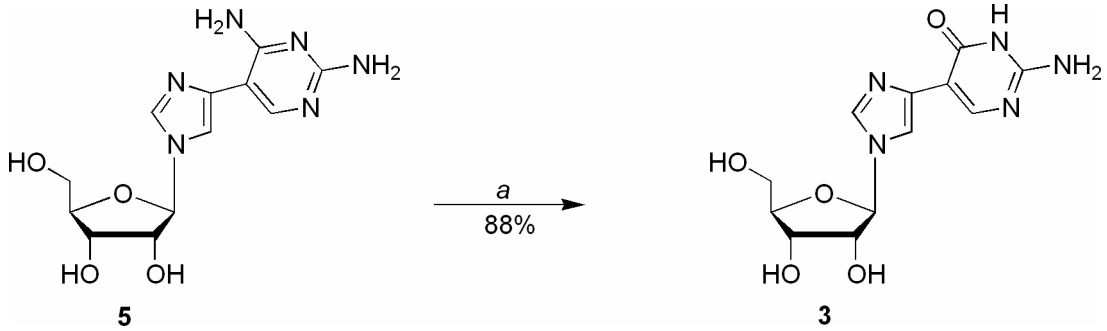

Reaction Conditions: a) Saturated aqueous $NaHSO_3$, 60 °C.

Scheme 38

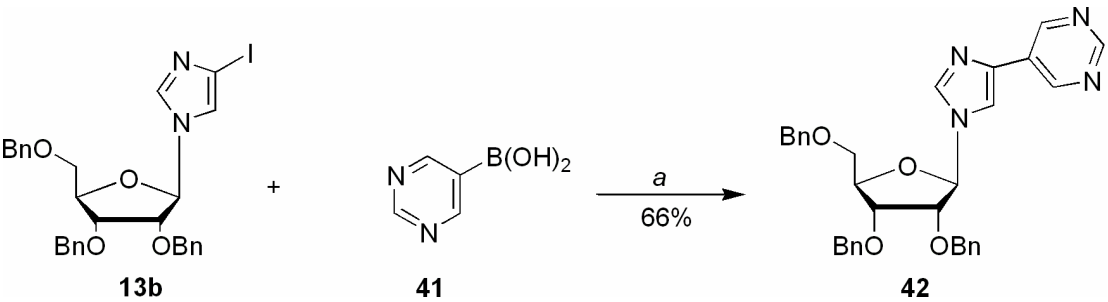

Reaction Conditions: a) $PdCl_2(dppf)$, K_2CO_3, THF, 60 °C, 18 h.

While this initially appeared successful, since the coupling produced **42** in a 66% yield, attempts to form **43** using dissolving metal chemistry, specifically KNH_2 and NH_3, followed by strong oxidizing conditions using $KMnO_4$ resulted in decomposition of the starting materials (Scheme 39 on the next page).[164]

At this point we turned to construction of the heterocyclic moieties by means of linear approach. Starting with commercially available histidine hydrochloride (**44**), treatment with commercially available sodium hypochlorite (household bleach)[165] afforded **45** in a 70% yield (Scheme 40). This particular reaction proved to be erratic

in nature, as all attempts with a variety of generic brands of bleach resulted in low to poor yields, while the best results were obtained with Clorox® brand bleach.

Scheme 39

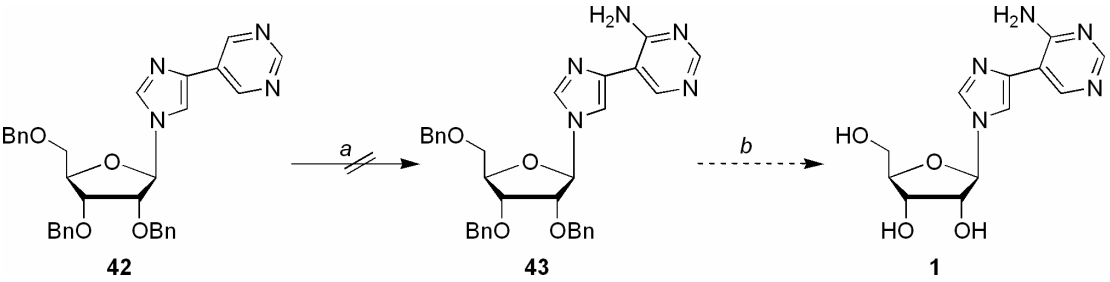

Reaction Conditions: a) *i*) KNH_2, NH_3, *ii*) $KMnO_4$ b) Pd/C, HCO_2NH_4, EtOH, reflux.

Scheme 40

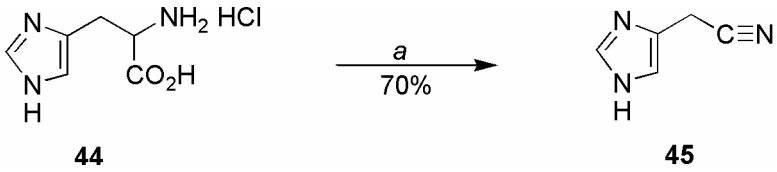

Reaction Conditions: a) NaOCl, H_2O.

Upon closer inspection, reasons for this irregular behavior became obvious; the Clorox® bleach had a higher percentage of sodium hypochlorite per bottle than the generic brands. More importantly, the Clorox® bleach contains none of the common stabilizers found in the generic brands. These stabilizers likely interfere with product formation, since this reaction appears to proceed by a radical mechanism (Scheme 41).

Scheme 41

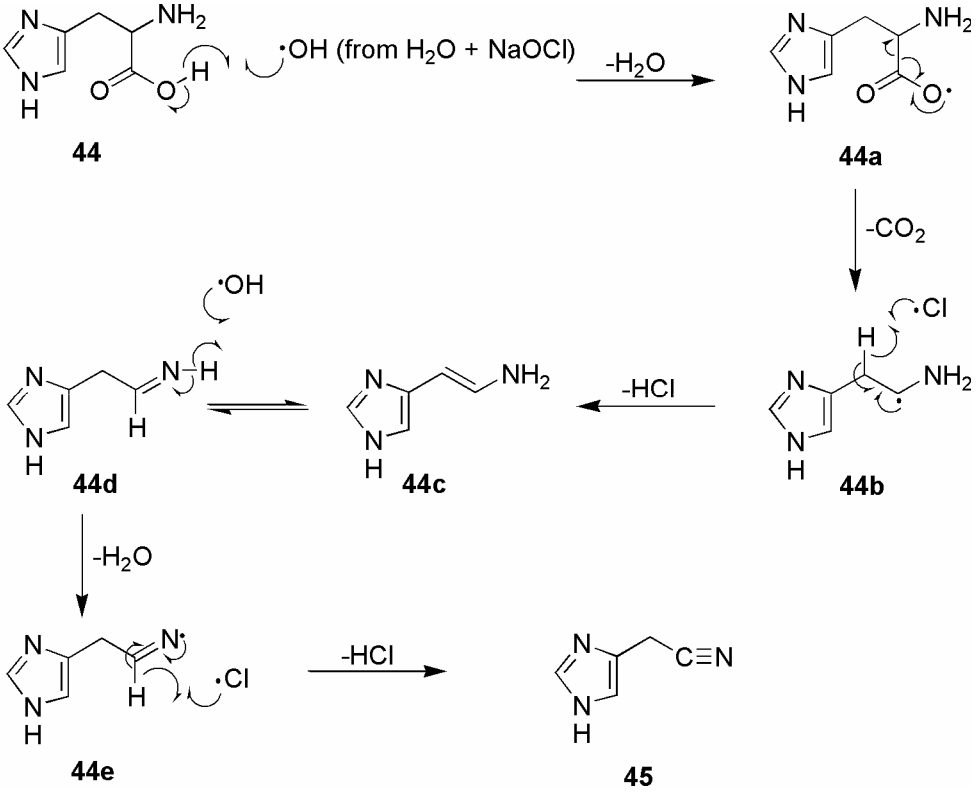

Once **45** was in hand, standard nucleoside coupling to commercially available 1,2,3,5-*O*-tetraacetate-β-D-ribofuranose with N,*O*-bis(trimethylsilyl)acetamide and trimethylsilyltriflate was accomplished, albeit in less than desirable yields (36%),[166] to give **46a**. This low yield was due to the formation of both possible coupling products, the 1,4- and 1,5-disubstituted imidazoles (**46a** and **46b**), which were readily separated by column chromatography (Scheme 42 on the next page). Literature has shown that by ^{1}H NMR analysis it is possible to distinguish between the two products. The characteristic downfield shift of the H-5 proton as compared to the shift

for H-2 is indicative of the 1,4-disubsituted imidazole, whereas for the 1,5-disubstituted imidazole, one would see a shift upfield for H-4 as compared to H-2.[167]

Scheme 42

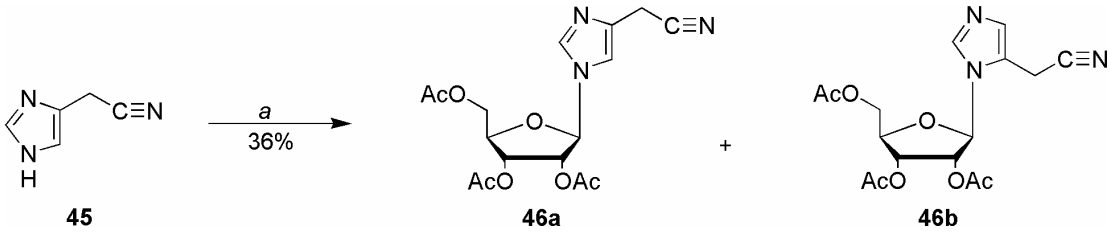

Reaction Conditions: a) *i*) 1,2,3,5-*O*-tetraacetate-*β*-D-ribofuranose, BSA, CH_3CN, 4 h, *ii*) TMSOTf, 60 °C, 18 h.

Subsequent inverse electron demand Diels-Alder reaction of nucleoside **46a** with commercially available 1,3,5-triazine (**47**) provided the amino substituted pyrimidine ring with concurrent deblocking of the acetate protecting group albeit in less than desirable yields (15%) (Scheme 43 on the next page).[168-170] The reaction proceeds via an *in situ* nitrile to a substituted ene-imine tautomerization [4 + 2] cycloaddition with 1,3,5-triazine to afford the bicyclic adduct **48**. Nucleophilic addition of sodium methoxide to the endocyclic imine as well as concurrent deblocking of the acetate protecting group provided **49**. Finally, the bicyclic intermediate **49** underwent a retro Diels-Alder reaction, resulting in a loss of methyl formimidate, and subsequent formation of the proximal adenosine **1** (Scheme 44 on page 99). Although these reactions which produced *proximal* adenosine **1** were relatively low yielding, the final target was obtained in a 3.8% overall yield in only 3 steps from histidine hydrochloride (**44**).

Scheme 43

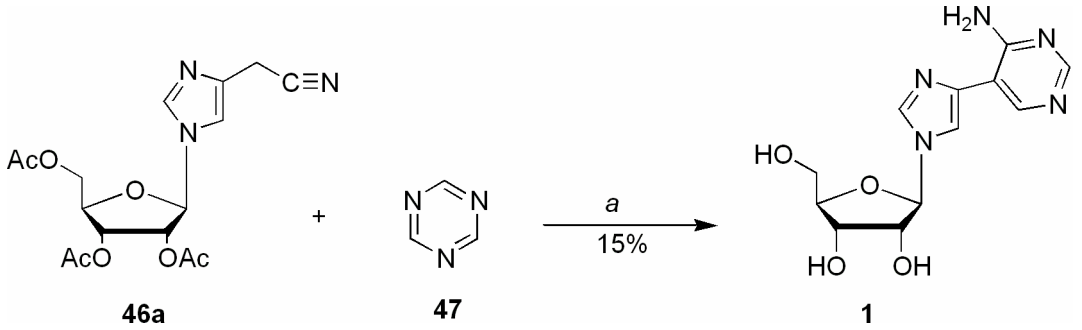

Reaction Conditions: a) NaOMe, MeOH, reflux.

Inosine fleximer **2** was then realized from **1** using standard diazotization conditions, to give **2** in 68% yield (Scheme 45 on the next page).[162] While admittedly the yields for these steps are not optimal, it is notable that the overall yield is comparable to the typical yields obtained for other modified nucleosides, since **1** (and subsequently, **2**) are possible in only three (or four) steps using cheap, commercially available materials. As a result, while we will continue to optimize these yields, we feel this is not a hindrance to using this route.

With the *proximal* fleximers **1-6** now in hand, we can proceed with our investigations into exploring the confines of biologically significant enzymes. By comparing the results already obtained with the distal fleximers, it will be possible to see if altering the position of the fleximer bond has a significant effect on recognition with SAHase and the other biologically relevant enzymes we are investigating.

Scheme 44

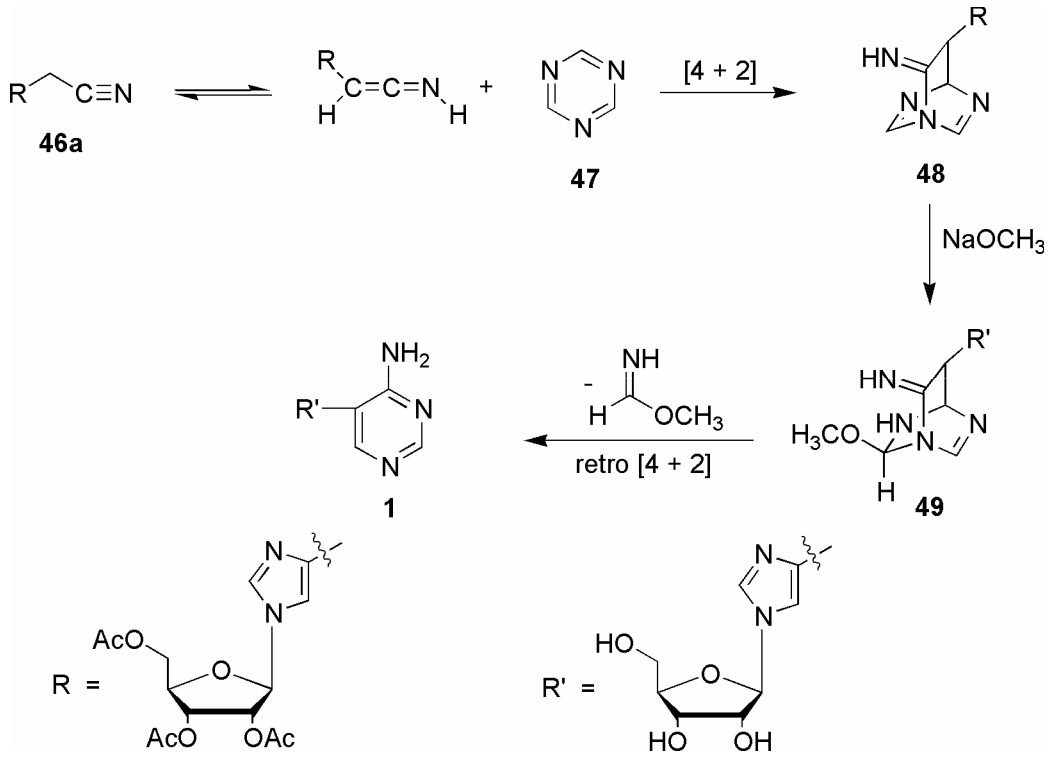

Scheme 45

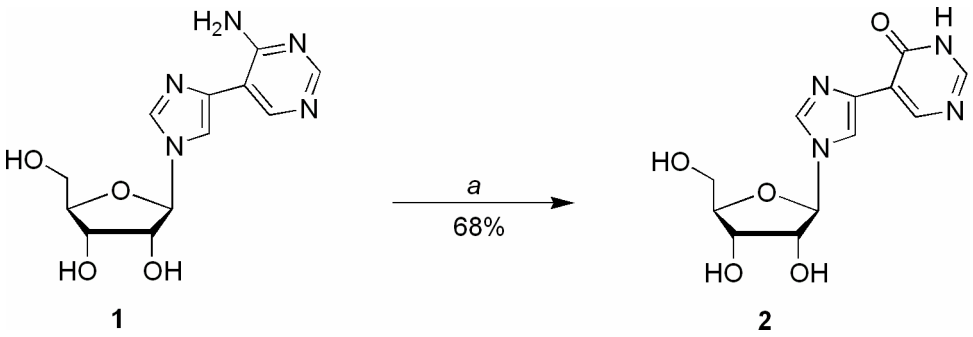

Reaction Conditions: a) $NaNO_2$, AcOH, H_2O.

In summary, a series of traditional cross coupling methods using a variety of catalysts and conditions were explored to realize the synthesis of the second series of fleximers. It is clear from the efforts outlined herein that the imidazole and

pyrimidine ring systems are recalcitrant at best and that work remains to fully understand the ideal conditions to manipulate these heterocycles more efficiently. We are, however, encouraged by the reasonably good results finally obtained with the Suzuki system, and we will continue to optimize this promising route.

CHAPTER IV

FUTURE DIRECTIONS

SAHase Assays

It will be necessary to investigate the consequences of flexibility for enzyme recognition and inhibition. First, inhibition assays for SAHase will need to be done by Dr. Sunny Zhou at Washington State University. As previously mentioned, SAHase catalyzes the reversible transformation from SAH to homocysteine (Hcy) and adenosine (Ado). The equilibrium constant (K_{eq}) is about 1 μM, favoring, the synthetic direction. For instance, if 100 μM SAH is incubated with SAHase, only about 10% of product conversion is expected when equilibrium is reached (final concentration of Hcy and Ado is 9.5 μM). Under physiological conditions, however, the net reaction proceeds in the hydrolysis direction, as the hydrolysis products are rapidly depleted via several metabolic pathways. Ado is metabolized by adenosine deaminase (ADA) and adenosine kinase, and Hcy is used for cysteine and methionine biosynthesis.

ADA is used to shift the overall equilibrium to the hydrolysis direction in a continuous photometric SAHase assay (as shown in Scheme 46 on the next page). ADA irreversibly converts the adenosine product into inosine which is associated with a decrease of absorption at 265 nm with a change of the extinction coefficient of 8,100 M^{-1} cm^{-1}.[85,171] This method will be used for the initial inhibitor screening. Another commonly used assay is based on the quantification of Hcy, the other hydrolysis product. As shown in Scheme 47 on the next page, the Hcy product is

then reacted with 5,5'-dithiobis-2-nitrobenzoic acid (DTNB, Ellman's reagent) to form Hcy and 2-nitro-5-thiobenzoic acid (TNB). Concentrations of Hcy are

Scheme 46

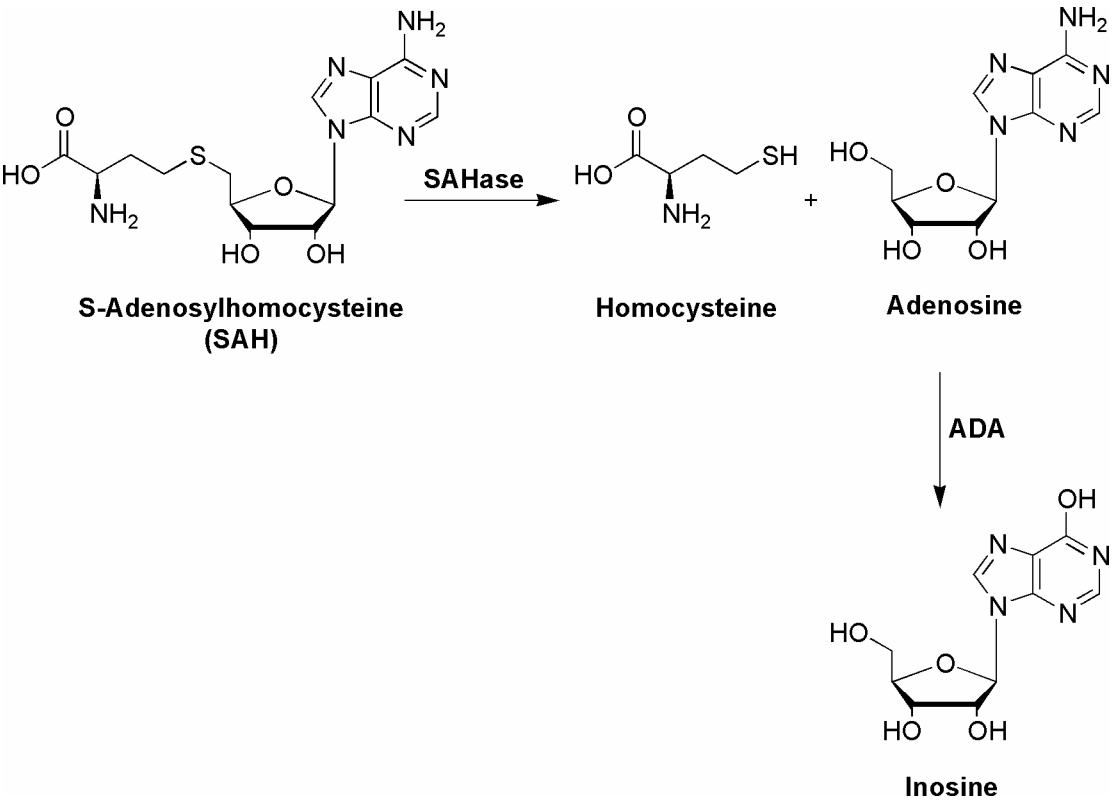

Scheme 47

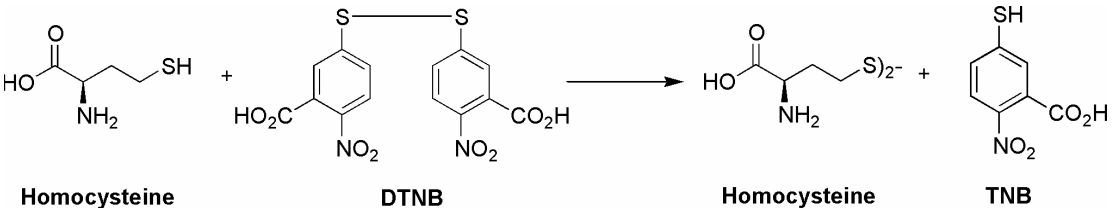

determined from the absorption changes at 412 nm due to TNB, using an extinction coefficient of 13,700 M^{-1} cm^{-1}.[172] Since the fleximers **1-6** do not absorb around 410 nm, the sensitivity of the assay will not be affected by inhibitor concentrations.

Because reactions catalyzed by SAHase are reversible and involve multiple steps, it might be desirable to characterize enzyme inhibition in the synthetic direction. There is, however, no reported continuous activity assay for SAHase in the synthetic direction. There are however, assays based on HPLC analysis of the SAH product and the Hcy and Ado substrates. However, the process is tedious and time consuming. More importantly, since the reaction is reversible, accumulation of SAH complicates kinetic analysis. Our collaborators have developed an enzyme-coupled continuous photometric assay for SAHase in the synthetic direction (Scheme 48).

Scheme 48

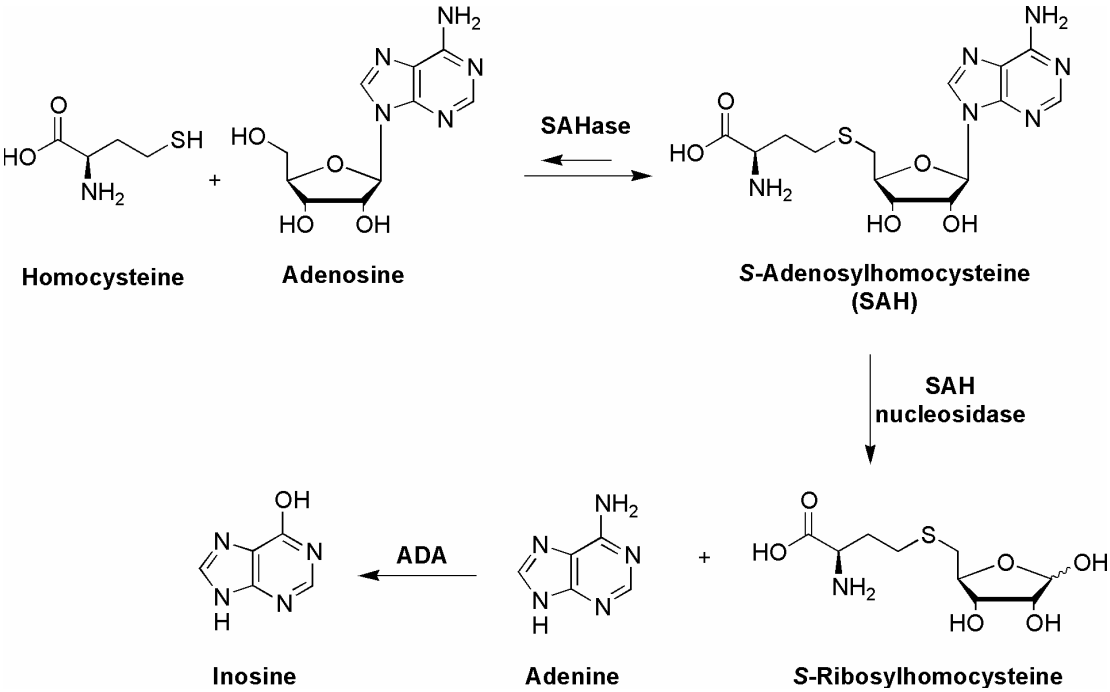

In this assay, SAH formed in the synthetic direction is cleaved into adenine and *S*-ribosyl-homocysteine by SAH nucleosidase and the adenine intermediate is subsequently converted into hypoxanthine in the presence of ADA.[173,174] The latter transformation is associated with an absorption decrease at 265 nm with a change of extinction coefficient of ~8,000 M^{-1} cm^{-1}, similar to the reaction catalyzed by ADA currently used for the hydrolysis assay. Again, absorption changes at 265 nm can be conveniently monitored in a microplate format on a UV-visible microplate reader. Furthermore, since SAH nucleosidase irreversibly cleaves SAH, no SAH product is built up using this enzyme-coupled assay, thereby simplifying the kinetic analysis.

X-Ray Crystallography

Using recombinant human SAHase for the crystallization experiments will be eventually purified from cell-free extracts of *E. coli* transformed with the plasmid pPROKcd20. It will be necessary to obtain a pure NAD^+ form of the enzyme, such that incubation with the fleximers **1-6** (Figure 51 on the next page) can readily occur. Followings the structure determination and refinement of the various fleximer complexes, an analysis of the structures will be performed to identify any conformational changes that may result from the presence of the specific inhibitor. It is hoped that these structurally unique nucleosides will provide critical information regarding the dynamic structure and function of biological significant enzymes.

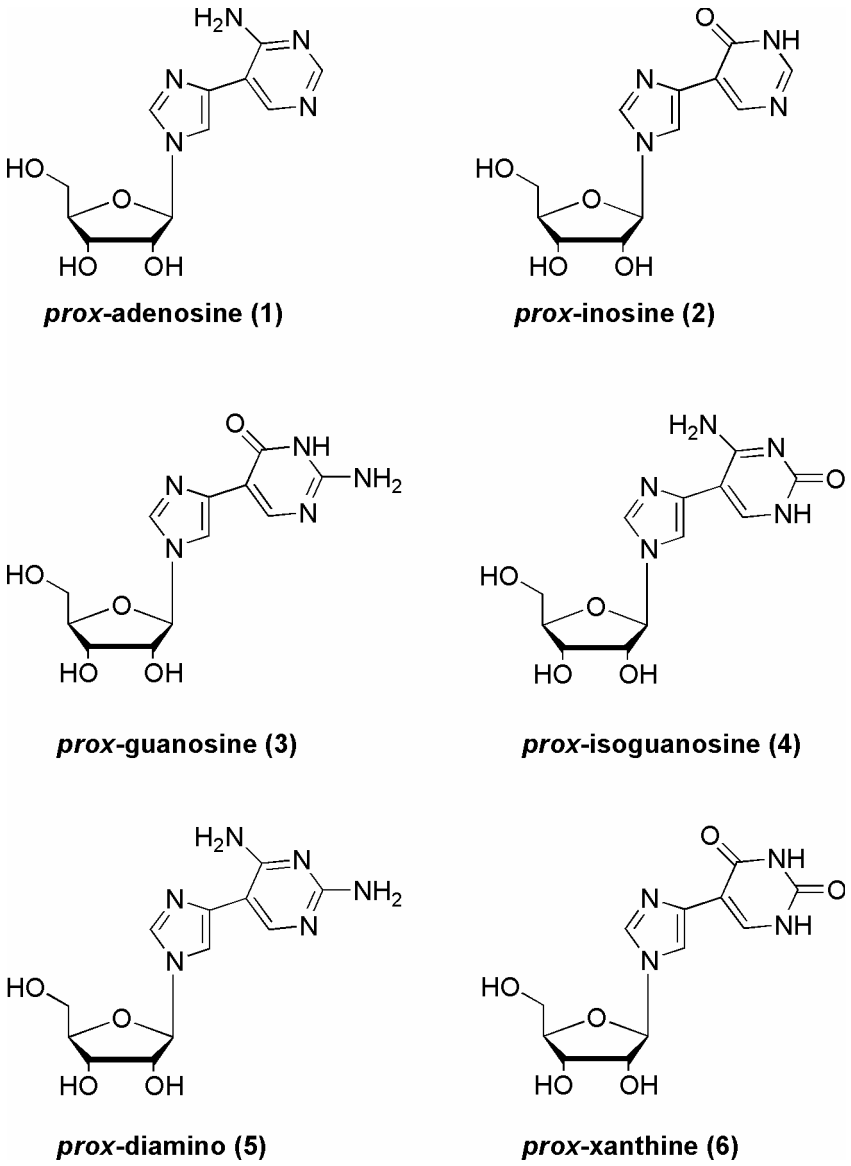

Figure 51. Six *proximal* fleximer targets

Carbocyclic Fleximers

Since the fleximers represent an entirely new class of potential SAHase and antiviral inhibitors as yet uncharacterized, fleximers **1**-**6** (Figure 51 on the previous page) have provided us a strong basis set for comparison with later analogues. Given the potent biological activity exhibited by 3-deazaadenosine analogues,[13] the next rational step is the synthesis of *proximal* 3-deazaadenosine fleximer (Figure 52).

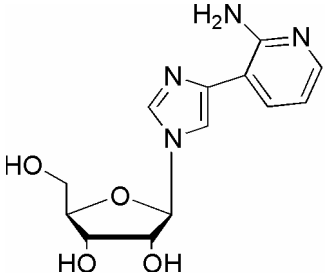

Figure 52. *Proximal* 3-deazaadenosine fleximer.

Due to the extremely potent biological activity exhibited by the carbocyclic aristeromycin and Neplanocin A analogues,[96,97] the carbocyclic fleximers, also present logical targets. Furthermore, due to the cytotoxicity of the Ari and NpcA analogues (since they can easily be phosphorylated and thus resemble ATP),[96,97] it would be interesting to synthesize the subsequent 4',5'-tetrahydro and 4',5'-unsaturated derivatives (Figure 53 on the next page). As previously mentioned, both of these analogues were shown to irreversibly inhibit SAHase and more significantly, they were not substrates for adenosine kinase and adenosine deaminase.[101]

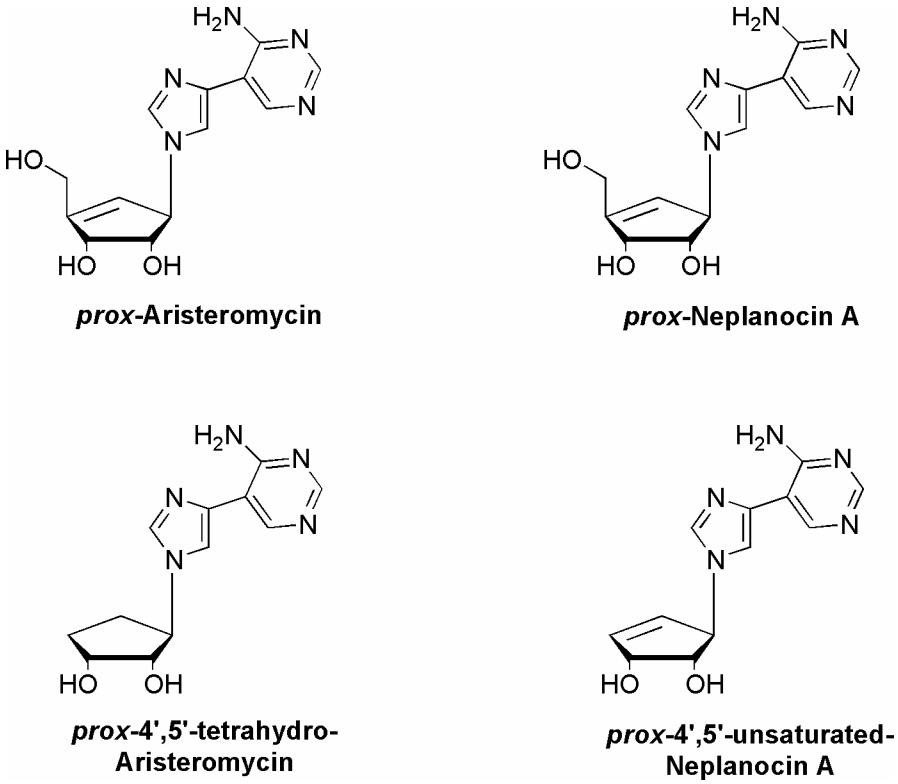

Figure 53. Carbocylic *proximal* adenosine fleximers.

Hence, given the antiviral and SAHase activity of carbocyclic nucleosides along with the potential for overcoming resistance mechanisms by incorporations of flexibility that is inherent in the fleximers, it is hoped that these two leads may eventually result in a synergistic inhibition of SAHas

CHAPTER V

EXPERIMENTAL

Modeling. All potential inhibitors were docked into the SAHase crystal structure (PDB 1A7A) and calculations performed on a SGI Octane2 using Accelrys® InsightII/Discover with a CFF forcefield, which is derived from *ab initio* calculations on the Hartree-Fock level of theory using the 6-311G* basis set. The inhibitors were optimized using steepest descent calculations. Then using Monte Carlo techniques, up to twenty spatial conformers were generated for each inhibitor. The ten lowest energy conformations were then minimized using simulated annealing techniques. The final structures were analyzed for the best ligand structure with the lowest energy value. The nonessential hydrogens have been removed for clarity.

General. Melting points were recorded on a Meltemp II melting point apparatus and are uncorrected. Combustion analyses were performed by Atlantic Microlabs, Inc., Atlanta, GA. ^{1}H and ^{13}C NMR spectra were recorded on a Bruker 300 spectrometer (operated at 400 and 100 MHz, respectively) all referenced to internal tetramethylsilane (TMS) at 0.0 ppm. The spin multiplicities are indicated by the symbols s (singlet), d (doublet), t (triplet), m (multiplet) and b (broad). UV-vis activity was measured on a Shimadzu 1601 UV/Vis spectrophotometer. Reactions were monitored by thin-layer chromatography (TLC) using 0.25-mm Whatman

Diamond silica gel 60-F254 precoated plates with visualization by irradiation with a Mineralight UVGL-25 lamp. Column chromatography was performed on Whatman silica, 200-400 mesh, 60 Å, and elution with the indicated solvent system. HPLC purification was carried out on a Hewlet- Packard 1090 liquid chromatograph. Yields refer to chromatographically and spectroscopically (^{1}H and ^{13}C NMR) homogeneous materials.

2,4,5-Tribromoimidazole (8).[121] Bromine (100 g, 0.625 mol) in glacial acetic acid (200 mL) was added during 1 h to a stirred suspension of imidazole **7** (13.6 g, 0.200 mol) and anhydrous sodium acetate (200 g) in acetic acid (1.0 L). When approximately one-third of bromine/acetic acid mixture had been consumed, additional sodium acetate (50 g) was added to the suspension. Stirring continued for 18 h and the solvent was removed under reduced pressure. H_2O (4 L) was added to the residue and the mixture was filtered. The precipitate was washed with excess amount of H_2O (2.0 L) to give a white powder (45.7 g, 75%), mp: 220-222 °C (from Aldrich: 217-220 °C).

4,5-dibromoimidazole (9a).[115,122] EtMgBr (3.0 M in ethyl ether, 83.3 mL, 0.250 mol) was added dropwise to a suspension of 2,4,5-tribromoimidazole (**8**) (30.5 g, 0.100 mol) in anhydrous ethyl ether (1 L) at 0 °C. Then the mixture was heated under gentle reflux for 18 h. The solvent was removed under reduced pressure and subsequently saturated aqueous NH_4Cl (500 mL) was slowly added to the residue. The mixture was extracted with ethyl acetate (3 x 300 mL). The organic extracts were combined,

washed with brine (600 mL), dried over $MgSO_4$, and the solvent was removed under reduced pressure to give a light brown powder. Recrystallization in hot ethyl acetate gave the titled compound as a white crystalline solid (19.4 g, 86%), mp: 223-226 °C. (Lit.[122], 225-226 °C).

4,5-Diiodoimidazole (9b).[136] An aqueous solution (500 mL) of imidazole (30.0 g, 0.441 mol) was added dropwise to a solution of $KICl_2$ (2.0 M, 550 mL, 1.1 mol, prepared from dissolving ICl (79.9 g, 1.03 mol) in an aqueous solution of KCl (131.5 g, 1.77 mol in 550 mL of H_2O) at rt. The mixture was stirred for an additional 10 h, followed by slow addition of 2M NaOH solution until the suspension was completely dissolved. The clear solution was then acidified to pH 9.50 by dropwise addition of concentrated HCl. The resulting product was filtered to afford an off-white powder, which, following recrystallization in EtOH, gave **9b** as a white crystalline solid (131.2 g, 93%), mp 188-191 °C. ^{1}H NMR (DMSO-d_6) δ 7.76 (s, 1 H); ^{13}C NMR (DMSO-d_6) δ 141.4.

2,3-Diacetoxy-5-acetoxymethyl-1-(4,5-dibromoimidazol-3-yl)-*β*-D-ribofuranose (10a).[115,123] To a stirred solution of 1,2,3,5-*O*-tetraacetate-β-D-ribofuranose (16.0 g, 50 mmol) and 4,5-dibromoimidazole (**9a**) (11.3 g, 50 mmol) in anhydrous acetonitrile (500 mL) was added N,*O*-bis(trimethylsilyl)acetamide (BSA) (48.7 mL, 0.20 mol). The reaction mixture was stirred for 3 h at room temperature and cooled to 0 °C, at which point, trimethylsilyl trifluoromethylsulfonate (TMSOTf) (10.7 mL, 56 mmol) was slowly added. The mixture was further stirred at 60 °C for 18 h. The solution

was cooled to room temperature and the solvent was removed to produce a brown syrup. The residue was then chilled to 0 °C, and saturated aqueous $NaHCO_3$ solution (400 mL) was slowly added. The mixture was extracted with CH_2Cl_2 (3 x 250 mL). The organic extracts were combined, washed with brine (250 mL), dried over $MgSO_4$. Then the solvent was removed under reduced pressure to give a brown syrup. Column chromatography eluting with petroleum ether:EtOAc (1:1) gave **10a** as a pale yellow syrup (17.4 g, 70%), which was used directly in the next step: ^{1}H NMR ($CDCl_3$) δ 2.06 (s, 9 H), 4.25-4.30 (m, 2 H), 4.33-4.38 (m, 1 H), 5.31 (dt, 2.7 Hz, 5.2 Hz, 1 H), 5.46 (dd, 2.2 Hz, 5.2 Hz, 1 H), 5.77 (dd, 2.6 Hz, 4.6 Hz, 1 H), 7.76 (s, 1 H); ^{13}C NMR ($CDCl_3$) δ 20.2, 20.3, 20.5, 62.3, 69.6, 73.5, 80.0, 88.0, 102.4, 118.2, 135.2, 168.8, 169.3, 170.0.

2,3-Diacetoxy-5-acetoxymethyl-1-(4,5-diiodoimidazol-3-yl)-*β*-D-ribofuranose (10b).[115,123] *N*,*O*-bis(trimethylsilyl)acetamide (BSA) (73.9 mL, 0.30 mol) was added to a stirred solution of **9b** (50.0 g, 156 mmol) and 1,2,3,5-tetra-*O*-acetate-β-D-ribofuranose (50.0 g, 157 mmol) in anhydrous acetonitrile (500 mL). The mixture was stirred for an additional 4 h at rt under Ar. The solution was then cooled to 0°C, at which point trimethylsilyl trifluromethylsulfonate (TMSOTf) (31 mL, 172 mmol) was added dropwise. The mixture was heated at 60°C under Ar for 18 h. The solvent was removed under reduced pressure and the resulting residue was cooled to 0°C, followed by portionwise addition of aqueous $NaHCO_3$ until production of gas ceased. The mixture was extracted with CH_2Cl_2 (3 x 400 mL), the organic extracts combined, washed with brine (2 x 300 mL), dried over $MgSO_4$, and the solvent removed under

reduced pressure to give **10b** as a light brown syrup (67.6 g), which was used without further purification.

(4,5-Dibromoimidazol-3-yl)-1-*β*-D-ribofuranose (11a).[115] A solution of 2,3-diacetoxy-5-acetoxymethyl-1-(4,5-dibromoimidazol-3-yl)-β-D-ribofuranose (**10a**) (13.7 g, 28.3 mmol) and concentrated aqueous ammonium hydroxide (28%, 300 mL) in ethanol (250 mL) was stirred at room temperature for 18 h. Then the solvent removed under reduced pressure to afford a light brown foam. Column chromatography eluting with $CHCl_3$:MeOH (9:1) gave **11a** as a colorless syrup (10.1 g, quantitative): ^{1}H NMR (CD_3OD) δ 3.72 (dd, 3.2 Hz, 12.2 Hz, 1 H), 3.84 (dd, 3.0 Hz, 12.2 Hz, 1 H), 4.03-4.07 (m, 1 H), 4.22 (t, 5.1 Hz, 1 H), 4.32 (t, 4.8 Hz, 1 H), 5.69 (d, 4.5 Hz, 1 H), 8.24 (s, 1 H); ^{13}C NMR (CD_3OD) δ 61.9, 71.0, 76.8, 86.6, 92.4, 104.3, 117.5, 138.1. Anal. Calcd for $C_8H_{10}Br_2N_2O_4$·0.25MeOH: C, 27.05; H, 3.02; N, 7.64; Br, 43.68. Found: C, 26.99; H, 2.83; N, 7.62; Br, 43.57.

(4,5-Diiodoimidazol-3-yl)-1-*β*-D-ribofuranose (11b).[115] A mixture of crude **10b** (67.6 g, 0.117 mol) and concentrated ammonium hydroxide (28%, 500 mL) in EtOH (300 mL) was stirred at rt for 18 h. The resulting precipitate was filtered and washed with cold H_2O to afford **11b** as a white crystalline solid (52.8 g, 75% for 2 steps). ^{1}H NMR (DMSO-d_6) δ 3.49 (dd, 3.9 Hz, 12.0 Hz, 1 H), 3.57 (dd, 3.9 Hz, 12.0 Hz, 1 H), 3.88 (q, 3.6 Hz, 1 H), 4.01 (t, 3.6 Hz, 1 H), 4.24 (t, 5.0 Hz, 1 H), 5.19 (t, 5.1 Hz, 1 H), 5.33 (d, 4.8 Hz, 1 H), 5.46 (d, 5.1 Hz, 1 H), 5.60 (d, 6.3 Hz, 1 H), 8.15 (s, 1 H). ^{13}C NMR (DMSO-d_6) δ 61.1, 70.2, 75.0, 85.6, 92.4, 97.3, 130.5, 140.8.

2,3-Dibenzyloxy-5-benzyloxymethyl-1-(4,5-dibromoimidazol-3-yl)-β-D-ribofuranose (12a).[125] Sodium hydride (95%, 2.9 g, 0.115 mol) was added to a stirred solution of **11a** (13.7 g, 38.3 mmol) in anhydrous THF (100 mL) at 0 °C under Ar. The mixture was then stirred at room temperature for 3 h. Next, tetrabutylammonium iodide (0.5 g, 1.35 mmol) was added followed by benzyl bromide (19.7 g, 0.115 mol). The mixture was stirred at room temperature for 3 h, followed by quenching with ethanol (50 mL). The solvent was removed under reduced pressure; saturated NH_4Cl solution (200 mL) was added and the mixture extracted with CH_2Cl_2 (3 x 200 mL). The organic extracts were combined, washed with brine (200 mL), and dried over $MgSO_4$. The solvent was removed under reduced pressure to provide a pale brown syrup. Column chromatography eluting with hexane:ethyl acetate (3:1) gave **12a** as a colorless crystalline solid (20.4 g, 85% yield), mp 86-88 °C: ^{1}H NMR ($CDCl_3$) δ 3.54 (dd, 2.4 Hz, 10.8 Hz, 1 H), 3.75 (dd, 2.7 Hz, 10.8 Hz, 1 H), 4.10-4.16 (m, 2 H), 4.31-4.34 (m, 1 H), 4.43-4.66 (m, 6 H), 5.83 (d, 3.3 Hz, 1 H), 7.22-7.38 (m, 15 H), 7.88 (s, 1 H); ^{13}C NMR ($CDCl_3$) δ 68.3, 72.5, 72.6, 73.5, 75.5, 80.5, 81.9, 89.5, 101.8, 117.6, 127.8, 127.9, 128.0, 128.2, 128.5, 128.6, 136.2, 136.7, 137.1. Anal. Calcd for $C_{29}H_{28}Br_2N_2O_4$: C, 55.43; H, 4.49; N, 4.46; Br, 25.43. Found: C, 55.33; H, 4.60; N, 4.29; Br, 25.15.

2,3-Dibenzyloxy-5-benzyloxymethyl-1-(4,5-diiodoimidazol-3-yl)-1-β-D-ribofuranose (12b).[125] To a stirred solution of **11b** (21.0 g, 45.9 mmol) in anhydrous THF (300 mL) at 0°C was added NaH (95% dry, 4.06 g, 161 mmol) in small portions over a period of 10 minutes. The resulting mixture was stirred at rt for 3 h, at which

point, tetrabutylammonium iodide (3.4 g, 9.20 mmol) was added, followed by dropwise addition of benzyl bromide (19.1 mL, 161 mmol). The new mixture was stirred at rt for 18 h. The solvent was then removed under reduced pressure, and saturated aqueous NH_4Cl solution (200 mL) added to the residue. The mixture was extracted with CH_2Cl_2 (3 x 250 mL), the organic extracts combined, washed with brine (2 x 300 mL), dried over $MgSO_4$, and the solvent removed under reduced pressure to give a yellow syrup. Column chromatography eluting with hexane:EtOAc (3:1) gave **12b** as a white crystalline solid (26.5 g, 80% yield), mp 86-88 °C. ^{1}H NMR ($CDCl_3$) δ 3.53 (dd, 2.5 Hz, 10.8 Hz, 1 H), 3.75 (dd, 2.4 Hz, 10.8 Hz, 1 H), 4.08-4.18 (m, 2 H), 4.31-4.34 (m, 1 H), 4.44-4.70 (m, 6 H), 5.82 (d, 3.6 Hz, 1 H), 7.21-7.37 (m, 15 H), 7.99 (s, 1 H). ^{13}C NMR ($CDCl_3$) δ 66.3, 72.6, 72.9, 73.5, 75.7, 79.8, 80.9, 81.9, 92.0, 127.8, 127.9, 128.2, 128.5, 128.6, 136.9, 137.2, 140.3. Anal. Calcd for $C_{29}H_{28}I_2N_2O_4$: C, 48.22; H, 3.91; N, 3.88; I, 35.14. Found: C, 48.48; H, 3.91; N, 3.86; I, 35.41.

2,3-Dibenzyloxy-5-benzyloxymethyl-1-(4-bromoimidazol-3-yl)-1-*β*-D-ribofuranose (13a).[119] EtMgBr (3.0 M, 19 mL, 57 mmol) was added dropwise to a solution of **12a** (34.7 g, 48.0 mmol) in anhydrous ether (500 mL) at room temperature. The mixture was further stirred at room temperature for 3 h. Anhydrous ethanol (50 mL) was added to quench the reaction mixture. The solvent was then removed under reduced pressure and the residue was cooled to 0 °C. Saturated aqueous NH_4Cl solution (300 mL) was added and the mixture was extracted with CH_2Cl_2 (3 x 200 mL). The organic extracts were combined, washed with brine (400

mL), dried over $MgSO_4$, and the solvent was removed under reduced pressure to give a colorless syrup. Column chromatography eluting with hexane:ethyl acetate (2:1) gave **13a** as a colorless syrup (23.6 g, 82%). ^{1}H NMR ($CDCl_3$) δ 3.51 (dd, 2.4 Hz, 10.8 Hz, 1 H), 3.67 (dd, 3.0 Hz, 10.8 Hz, 1 H), 4.04-4.16 (m, 3 H), 4.30-4.66 (m, 6 H), 5.69 (d, 6.0 Hz, 1 H), 7.03 (d, 1.2 Hz, 1 H), 7.11 (dd, 2.0 Hz, 7.8 Hz, 2 H), 7.21-7.42 (m, 13 H), 7.46 (d, 1.2 Hz, 1 H). ^{13}C NMR ($CDCl_3$) δ 60.3, 69.7, 72.3, 72.6, 73.7, 76.5, 81.6, 82.6, 88.8, 121.9, 127.8, 127.9, 128.0, 128.2, 128.5, 128.6, 136.6, 137.1, 137.2, 137.5.

2,3-Dibenzyloxy-5-benzyloxymethyl-1-(4-iodoimidazol-3-yl)-1-β-D-ribofuranose (13b).[119] To a solution of **12b** (34.7 g, 48.0 mmol) in anhydrous ether (500 mL) at rt was added EtMgBr (3.0 M, 19 mL, 57 mmol) in a dropwise manner. The mixture was stirred at rt for 3 h, then quenched with anhydrous EtOH (50 mL). The solvent was removed under reduced pressure, saturated aqueous NH_4Cl solution (300 mL) added, and the mixture extracted with CH_2Cl_2 (3 x 200 mL). The organic layers were combined, washed with brine (2 x 400 mL), dried over $MgSO_4$, and the solvent removed under reduced pressure. Column chromatography of the residue, eluting with hexane:EtOAc (3:1) gave **11** as a colorless syrup (23 g, 80%). ^{1}H NMR ($CDCl_3$) δ 3.51 (dd, 2.4 Hz, 10.8 Hz, 1 H), 3.67 (dd, 3.0 Hz, 10.8 Hz, 1 H), 4.04-4.16 (m, 3 H), 4.30-4.66 (m, 6 H), 5.69 (d, 6.0 Hz, 1 H), 7.03 (d, 1.2 Hz, 1 H), 7.11 (dd, 2.0 Hz, 7.8 Hz, 2 H), 7.21-7.42 (m, 13 H), 7.46 (d, 1.2 Hz, 1 H). ^{13}C NMR ($CDCl_3$) δ 60.3, 69.7, 72.3, 72.6, 73.7, 76.5, 81.6, 82.6, 88.8, 121.9, 127.8, 127.9, 128.0, 128.2, 128.5,128.6,

136.6, 137.1, 137.2, 137.5. Anal. Calcd for $C_{29}H_{29}IN_2O_4$: C, 58.40; H, 4.90; N, 4.70; I, 21.28. Found: C, 58.29; H, 4.93; N, 4.61; I, 21.06.

2,3-Dibenzyloxy-5-benzyloxymethyl-1-(imidazol-3-yl)-1-β-D-ribofuranose (15). [132-135] EtMgBr (3.0 M in ethyl ether, 0.62 mL, 1.84 mmol) was added dropwise to a solution of **13a** (1.0 g, 1.67 mmol) in anhydrous CH_2Cl_2 (15 mL) at rt under Ar. The resulting solution was stirred at rt for 2 h, followed by dropwise addition of trimethyltin chloride (1.0 M in CH_2Cl_2, 2.0 mL, 2.0 mmol) at rt. The mixture was allowed to stir at rt for 18 h, then quenched with water. The organic layer was separated and the aqueous layer washed with CH_2Cl_2 (2 x 20 mL). The organic extracts were combined, washed sequentially with saturated KF solution (30 mL) to form insoluble organotin fluoride, and then with brine (50 mL). The organic layer was dried over $MgSO_4$, and the solvent removed to afford **15** as a colorless syrup (714 mg, 91%). ^{1}H NMR ($CDCl_3$) δ 3.48 (dd, 2.4 Hz, 10.8 Hz, 1 H), 3.62 (dd, 3.0 Hz, 10.8 Hz, 1 H), 4.03 (dd, 2.8 Hz, 4.8 Hz, 1 H), 4.10 (br t, 5.4 Hz, 1 H), 4.29 (dd, 2.8 Hz, 5.4 Hz, 1 H), 4.36-4.61 (m, 6 H), 5.74 (d, 6.4 Hz, 1 H), 6.98 (d, 6.8 Hz, 2 H), 7.10-7.32 (m, 15 H), 7.59 (s, 1 H). ^{13}C NMR ($CDCl_3$) δ 69.5, 72.0, 72.3, 73.3, 76.4, 81.4, 82.1, 88.5, 116.1, 127.3, 127.4,127.5, 127.6, 127.7, 128.1, 129.3, 135.7, 136.5, 137.0, 137.1.

5-Iodo-4(3*H*)-pyrimidinone (17). A mixture of 4(3*H*)-pyrimidinone **16** (1.14 g, 11.8 mmol), I_2 (3.02 g, 11.8 mmol) and H_2O (12 mL) was stirred at 80°C for 18 h. The solution was neutralized with glacial acetic acid to give a light yellow solid. The solid

was recrystallized in hot ethanol to give a white powder (2.37 g, 91%). ^{1}H NMR ($CDCl_3$) δ 8.16 (s, 1 H), 8.42 (s, 1 H). ^{13}C NMR ($CDCl_3$) δ 150.0, 160.3.

Attempted synthesis of 2,3-dibenzyloxy-5-benzyloxymethyl-1-[4-(1,3-dimethyl-5-pyrimidinyl-2,4-one)imidazol-1-yl]-1-β-D-ribofuranose (18). To a solution of **13b** (500 mg, 0.85 mmol) in Et_2O was added *n*-BuLi (1.3 M in hexane, 0.42 mL, 1.02 mmol) at -78 °C under Ar and the mixture was stirred for 2 h. Next, hexabutyldistannane (0.52 mL, 1,02 mmol) was added, followed by the addition of either one of these catalysts; $PdCl_2(PPh_3)_2$, $PdCl_2$(dppf), $Pd(PPh_3)_4$ or $Pd_2(dba)_3$ (5 mol%). After refluxing for 12 h, the mixture was cooled and saturated aqueous KF (50 mL) was added. Upon TLC analysis, it was indicative that all of the reactions did not any product formation and the starting materials were only present.

5-Bromo-1,3-dimethyluracil (20a).[143] Dimethyl sulfate (11.0 mL, 116 mmol) was added dropwise to a stirring slurry of 5-bromouracil **19a** (10.0 g, 52.4 mmol), NaOH (5.24 g, 131 mmol) in H_2O (80 mL) at 0 °C. The mixture was heated under reflux for 2 h, cooled to rt and extracted with CH_2Cl_2 (3 x 200 mL). The organic layers were combined, washed with brine (300 mL), and dried over $MgSO_4$. The solvent was removed under reduced pressure to give a white solid, which, following recrystallization in hot EtOH, gave **20a** as a white crystalline solid (9.17 g, 80%), mp: 224 °C (Aldrich, 225 °C). ^{1}H NMR ($CDCl_3$) δ 3.40 (s, 3 H), 3.41 (s, 3 H), 7.62 (s, 1 H) ^{13}C NMR ($CDCl_3$) 29.5, 37.3, 67.1, 147.2, 151.2, 160.2.

5-Iodo-1,3-dimethyluracil (20b).[143] Dimethyl sulfate (13.0 mL, 137 mmol) was added dropwise to a stirring slurry of 5-iodouracil **19b** (14.9 g, 62.6 mmol), NaOH (7.4 g, 156 mmol) in H_2O (100 mL) at 0 °C. The mixture was heated under reflux for 2 h, cooled to rt and extracted with CH_2Cl_2 (3 x 200 mL). The organic layers were combined, washed with brine (300 mL), and dried over $MgSO_4$. The solvent was removed under reduced pressure to give a white solid, which, following recrystallization in hot EtOH, gave **20b** as a white crystalline solid (13.5 g, 63%), mp: 224 °C (Aldrich, 225 °C). ^{1}H NMR ($CDCl_3$) δ 3.40 (s, 3 H), 3.41 (s, 3 H), 7.62 (s, 1 H) ^{13}C NMR ($CDCl_3$) 29.5, 37.3, 67.1, 147.2, 151.2, 160.2.

Attempted synthesis of 2,3-dibenzyloxy-5-benzyloxymethyl-1-[4-(1,3-dimethyl-5-pyrimidinyl-2,4-dione)imidazol-1-yl]-1-β-D-ribofuranose (21). EtMgBr (3.0 M in Et_2O, 140 μL, 0.420 mmol) was added dropwise to a stirred solution of **13b** (220 mg, 0.368 mmol) in anhydrous Et_2O (40 mL) at room temperature under Ar. The mixture was allowed to stir for 1 h. Next, $ZnCl_2$ (1.0 M in Et_2O, 400 μL, 0.40 mmol) was added dropwise to the mixture and allowed to stir for 1 h under Ar at rt. In a separate flask charged with Ar, a mixture of 5-iodo-1,3-dimethyluracil (**20b**) (107 mg, 0.405 mmol) and $Pd(PPh_3)_4$, $PdCl_2(PPh_3)_2$, $PdCl_2$(dppf) or $Pd_2(dba)_3$ (5 mol %)in CH_2Cl_2 was stirred at rt for 15 min. To this mixture was added the Grignard reagent (prepared in the first flask) was slowly added and the resulting mixture as stirred for 6 h at rt. Upon TLC analysis, it was indicative that all of the reactions did not show formation of **21**.

Attempted synthesis of 2,3-dibenzyloxy-5-benzyloxymethyl-1-[4-(1,3-dimethyl-5-pyrimidinyl-2,4-dione)imidazol-1-yl]-1-β-D-ribofuranose (21). EtMgBr (3.0 M in THF, 150 μL, 0.450 mmol) was added dropwise to a stirred solution of **13b** (235 mg, 0.394 mmol) in anhydrous Et_2O (35 mL) at room temperature under Ar. The mixture was allowed to stir for 1 h. Next, $ZnCl_2$ (1.0 M in Et_2O, 450 μL, 0.45 mmol) was added dropwise to the mixture and allowed to stir for 1 h under Ar at rt. In a separate flask charged with Ar, a mixture of 5-bromo-1,3-dimethyluracil (**20a**) (95 mg, 0.433 mmol) and $Pd(PPh_3)_4$, $PdCl_2(PPh_3)_2$, $PdCl_2$(dppf) or $Pd_2(dba)_3$ (5 mol %) in CH_2Cl_2 was stirred at rt for 15 min. To this mixture was added the Grignard reagent (prepared in the first flask) was slowly added and the resulting mixture as stirred for 6 h at rt. Upon TLC analysis, it was indicative that all of the reactions did not show formation of **21**.

Attempted synthesis of 2,3-dibenzyloxy-5-benzyloxymethyl-1-[4-(1,3-dimethyl-5-pyrimidinyl-2,4-dione)imidazol-1-yl]-1-β-D-ribofuranose (21). EtMgBr (3.0 M in THF, 285 μL, 0.854 mmol) was added dropwise to a stirred solution of **13b** (463 mg, 0.776 mmol) in CH_2Cl_2 (50 mL) at room temperature under Ar. The mixture was allowed to stir for 30 min. Next, $ZnCl_2$ (1.0 M in Et_2O, 0.78 mL, 0.78 mmol) was added dropwise to the mixture and allowed to stir for 1 h under Ar at rt. To the mixture was added a solution of 5-iodo-1,3-dimethyluracil (**20b**) (206 mg, 0.776 mmol) and $PdCl_2$(dppf) (50 mg, 0.061 mmol) in anhydrous DMF (5 mL). The solution was stirred under Ar at rt for 18 h. The solvent was removed under reduced

pressure. Upon TLC analysis (3% EtOH in CH_2Cl_2), it was indicative that all of the reactions did not show formation of **21**.

5-Bromouracil (23).[146] Bromine (100 mL, 1.95 mol) was added dropwise to a suspension of uracil (100 g, 0.89 mol) in H_2O (400 mL) while stirring. The reaction was allowed to stir overnight. Next, the solvent and excess reagents were evaporated at 100 °C. The residue was decolorized with activated carbon and recrystallized in hot H_2O to produce **23** as a colorless crystalline solid (150 g, 88% yield). mp > 300°C (from Aldrich > 300 °C). ^{1}H NMR (DMSO-d_6) δ 2.71 (s, 3 H), 2.74 (s, 3 H), 8.26 (s, 1 H) ^{13}C NMR (DMSO-d_6) δ 28.4, 35.0, 91.6, 141.7, 154.0, 162.1.

5-Bromo-2,4-dichloropyrimidine (24).[147] A mixture of **23** (50.0 g, 0.262 mol), $POCl_3$ (250 mL, 2.68 mol), and diethylaniline (60 mL, 0.377 mol) was heated under reflux for 100 min. Then **24** was subsequently isolated via distillation under reduced pressure (110-120 ºC/10 mmHg) (Ref. 112-113 ºC/12 mmHg) to afford a colorless liquid (54.3 g, 91%). ^{1}H NMR (DMSO-d_6) δ 8.94 (s, 1 H) ^{13}C NMR (DMSO-d_6) δ 118.3, 160.1, 162.4, 164.9.

2,2'-(5-Bromo-2,4-pyrimidinediyl)-bis(thiourium chloride) (25).[148] A mixture of **24** (5.5 g, 24.1 mmol), thiourea (4.1 g, 53.9 mmol) in anhydrous EtOH (50 mL) was heated under reflux for 30 minutes.[148] After cooling at 0°C, the precipitate was filtered, washed with cold EtOH and then diethyl ether to yield **24** as yellow crystalline solid (6.0 g, 65% yield); mp: 186-188°C (Lit. 186-190 ºC dec).

5-Bromo-2,4(1*H*, 3*H*)-pyrimidinedithione (26).[148] An aqueous solution of **25** (5.6 g, 10.8 mmol) in NaOH (10%, 45 mL) was heated at 110°C for 1 h. The hot solution was slowly acidified with acetic acid to afford a yellow precipitate. The precipitate was filtered, washed with H_2O and EtOH, and then re-precipitated from a hot dilute NaOH solution by addition of acetic acid to give **25** as a yellow powder (2.8 g, 84% yield). Mp > 250°C (dec), (Lit. 253-255 ºC).

5-Bromo-2,4-bis(methylthio)pyrimidine (27).[148] A mixture of **26** (2.8 g, 12.5 mmol) and NaOH (4.5 g) in H_2O (40 mL) was stirred to form a yellow solution. Dimethylsulfate (3.6 mL, 38 mmol) was added dropwise, and the mixture stirred for 30 min at rt.[148] The mixture was extracted with diethyl ether (3 x 50 mL). The extracts were combined, washed with brine (50 mL), dried over $MgSO_4$ and the solvent removed under reduced pressure to give a yellow-orange solid. The solid was recrystallized in EtOH, followed by a second recrystallization in hexanes to afford **26** as a yellow crystalline solid (2.4 g, 76% yield), mp: 63-65°C. ^{1}H NMR ($CDCl_3$) δ 2.54 (s, 6 H), 8.20 (s, 1 H). ^{13}C NMR ($CDCl_3$) δ 13.5, 14.5, 113.0, 155.0, 169.3, 170.0.

2,3-Dibenzyloxy-5-benzyloxymethyl-1-[4-(5-bromo-2-thiomethylpyrimidine)-imidazol-1-yl]-1-*β*-D-ribofuranose (29).[145] EtMgBr (3.0 M in Et_2O, 140 µL, 0.420 mmol) was added dropwise to a stirred solution of **13b** (220 mg, 0.368 mmol) in anhydrous CH_2Cl_2 (10 mL) at rt under Ar and was stirred for 1 h. $ZnCl_2$ (1.0 M in Et_2O, 400 µL, 0.40 mmol) was added dropwise. The mixture was then stirred at rt for

an additional 1 h under Ar. The suspension formed was added to a solution of **27** (70.8 mg, 0.405 mmol) and $Pd(PPh_3)_4$ in anhydrous CH_2Cl_2 (15 mL), and the mixture stirred overnight. The solvent was removed under reduced pressure, saturated aqueous NH_4Cl solution (10 mL) was added, and the mixture was extracted with CH_2Cl_2 (3 x 25 mL). The organic extracts were combined, washed with brine (25 mL), dried over $MgSO_4$ and the solvent removed under reduced pressure to produce a yellow syrup. Column chromatography eluting with 2% EtOH in CH_2Cl_2 yielded **29** as a colorless syrup (132 mg, 67% yield). ^{1}H NMR ($CDCl_3$) δ ^{1}H NMR ($CDCl_3$) δ 2.54 (s, 3 H), 3.52 (dd, 2.4 Hz, 10.8 Hz, 1 H), 3.66 (dd, 2.4 Hz, 10.8 Hz, 1 H), 4.06 (br s, 3 H), 4.09-4.15 (m, 1 H), 4.22 (br s, 1 H), 4.32-4.64 (m, 6 H), 5.75 (d, 5.6 Hz, 1 H), 7.01-7.53 (m, 15 H), 7.79 (br s,1 H), 7.92 (br s, 1 H), 8.44 (s, 1 H). ^{13}C NMR ($CDCl_3$) δ 30.1, 69.9, 72.7, 73.2, 73.8, 76.8, 82.1, 82.4, 82.9, 88.6, 115.6, 117.2, 120.2, 127.8, 128.0, 128.1, 128.2, 128.3, 128.4,128.5, 128.6, 128.7, 128.8, 132.1, 136.9, 137.5, 155.5, 158.4, 169.3.

Attempted synthesis of 2,3-dibenzyloxy-5-benzyloxymethyl-1-[4-(dihydroxyboryl)-imidazol-3-yl]-1-β-D-ribofuranose (30). *N*-Butyllithium (1.3 M in hexane, 0.14 mL, 0.34 mmol) was dropwise added over a 1 h period to a solution of **13b** (170 mg, 0.29 mmol) and $B(O^iPr)_3$ (0.09 mL, 0.29 mmol) in anhydrous THF (50 mL total) at –78 ºC under Ar. The mixture was stirred for an additional 8 h at rt, followed by addition of dilute HCl (1 M). The residue was then treated with H_2O (50 mL) and extracted with CH_2Cl_2 (3 x 30 mL). The organic extracts were combined, washed with brine (50 mL), dried over $MgSO_4$ and the solvent removed under

reduced pressure to give the dehalogenatged nucleoside **15** as a white powder. ^{1}H NMR ($CDCl_3$) δ 3.48 (dd, 2.4 Hz, 10.8 Hz, 1 H), 3.62 (dd, 3.0 Hz, 10.8 Hz, 1 H), 4.03 (dd, 2.8 Hz, 4.8 Hz, 1 H), 4.10 (br t, 5.4 Hz, 1 H), 4.29 (dd, 2.8 Hz, 5.4 Hz, 1 H), 4.36-4.61 (m, 6 H), 5.74 (d, 6.4 Hz, 1 H), 6.98 (d, 6.8 Hz, 2 H), 7.10-7.32 (m, 15 H), 7.59 (s, 1 H). ^{13}C NMR ($CDCl_3$) δ 69.5, 72.0, 72.3, 73.3, 76.4, 81.4, 82.1, 88.5, 116.1, 127.3, 127.4,127.5, 127.6, 127.7, 128.1, 129.3, 135.7, 136.5, 137.0, 137.1.

Attempted synthesis of 2,3-dibenzyloxy-5-benzyloxymethyl-1-[4-(pinacolatoboryl)-imidazol-3-yl]-1-β-D-ribofuranose (31). A mixture of **13b** (775 mg, 1.3 mmol), *bis*(pinacolato)diboron (363 mg, 1.43 mmol), anhydrous potassium acetate (383 mg, 3.9 mmol) and $PdCl_2$(dppf) (32 mg, 0.039 mmol) in DMF (10 mL) was heated under Ar at 80 ºC for 2 h. An additional amount of $PdCl_2$(dppf) (32 mg, 0.039 mmol) was added to the reaction mixture and was stirred overnight. Upon TLC observation, the reaction failed to afford **31** and only starting material **30** was recovered.

5-Tri-*n*-butylstannyl-1,3-dimethyluracil (32). A mixture of 5-iodo-1,3-dimethyluracil (**20b**) (2.66 g, 10.0 mmol), *bis*(tributyltin) (10.1 mL, 20.0 mmol) and $PdCl_2(PPh_3)_4$ (280 mg, 0.40 mmol) in anhydrous toluene (300 mL) was heated under Ar at 90 °C for 4 h. The mixture was filtered through a plug of alumina. The solvent was removed under reduced pressure and the product was purified by column chromatography (silica was pretreated with 5% triethylamine in hexane; eluted with 2% triethylamine in hexane) to afford a colorless oil (2.87 g, 66%). ^{1}H NMR ($CDCl_3$)

δ 0.88 (t, 7.2 Hz, 9 H), 1.03 (t, 8.4 Hz, 6 H), 1.31 (q, 7.6 Hz, 6 H), 1.50 (q, 8.4 Hz, 6 H), 3.32 (s, 3 H), 3.36 (s, 3 H), 6.87 (s, 1 H) ^{13}C NMR ($CDCl_3$) δ 9.9, 13.8, 27.4, 27.7, 29.1, 36.8, 111.0, 146.7, 152.4, 166.5.

Attempted synthesis of 2,3-dibenzyloxy-5-benzyloxymethyl-1-[4-(1,3-dimethyl-5-pyrimidinyl-2,4-dione)imidazol-1-yl]-1-β-D-ribofuranose (21). In a 50 mL, 3-neck round bottom flask was charged with $Pd(PPh_3)_4$ (15 mg, 0.013 μmol), CuI (5 mg, 0.026 μmol) and **13b** (936 mg, 1.57 mmol) in anhydrous DMF (10 mL) under Ar. To this mixture was added dropwise a solution of **32** (525 mg, 1.22 mmol) in anhydrous DMF (5 mL). The mixture was heated at 80 °C under Ar for 12 h. At suitable time intervals, a part of the reaction mixture was sampled and subjected to TLC analysis. Upon TLC analysis (2% EtOH in CH_2Cl_2), it indicated that the reactions did not show formation of **21**.

Attempted synthesis of 2,3-dibenzyloxy-5-benzyloxymethyl-1-[4-(1,3-dimethyl-5-pyrimidinyl-2,4-dione)imidazol-1-yl]-1-β-D-ribofuranose (21). In a 50 mL, 3-neck round bottom flask was charged with $PdCl_2(PPh_3)_2$ (12.5 mg, 0.018 μmol), CuI (6 mg, 0..036 μmol) and **13b** (750 mg, 1.26 mmol) in anhydrous DMF (10 mL) under Ar. To this mixture was added dropwise a solution of **32** (430 mg, 1.00 mmol) in anhydrous DMF (5 mL). The mixture was heated at 80 °C under Ar for 12 h. At suitable time intervals, a part of the reaction mixture was sampled and subjected to TLC analysis. Upon TLC analysis (2% EtOH in CH_2Cl_2), it indicated that the reactions did not show formation of **21**.

Attempted synthesis of 5-iodozinc-1,3-dimethyluracil (34) to afford 2,3-dibenzyloxy-5-benzyloxymethyl-1-[4-(1,3-dimethyl-5-pyrimidinyl-2,4-dione)imidazol-1-yl]-1-β-D-ribofuranose (21). In a 50 mL, 3-neck round bottom flask was charged with 5-iodo-1,3-dimethyluracil (**20b**) (452 mg, 2.0 mmol), Zn powder (190 mg, 3.0 mmol), *N*,*N*-dimethylacetamide (3 mL) and 1,2-dibromoethane (57 mg, 0.3 mmol). The mixture was heated for 10 min at 80 °C and then cooled to rt. This was followed by the addition of Me_3SiCl (45 μL, 36 mmol) and the mixture was heated to rt. To this mixture was added a solution of **13b** (1.19 g, 2.0 mmol) and $Pd(PPh_3)_4$ (50 mg, 0.043 mmol) in anhydrous DMF (5 mL). The solution was stirred under Ar at rt for 18 h. The solvent was removed under reduced pressure. Upon TLC analysis (3% EtOH in CH_2Cl_2), it was indicative that all of the reactions did not show formation of **21**.

5-Bromo-2,4-dibenzyloxypyrimidine (35).[157] A stirred solution of benzyl alcohol (13.4 mL, 129 mmol) in anhydrous toluene (140 mL) was treated with NaH (60% in mineral oil, 4.84 g, 121 mmol) under Ar. The mixture was warmed to 50 °C to facilitate the formation of the sodium salt, and stirred until all signs of gas evolution had subsided. The suspension was cooled and 5-bromo-2,4-dichloropyrimidine (**24**) (9.1 g, 40 mmol) was added dropwise, while maintaining the temperature below 25 °C. After stirring for 18 h at rt, the reaction was filtered to remove precipitated NaCl, and thoroughly washed with toluene. The filtrate was then evaporated under reduced pressure to give an oil, which solidified upon cooling. The crude solid was then recrystallized in EtOH to afford **35** as a white crystalline solid (16 g, 91%). mp: 88-

90°C. (Lit. 89-91 °C) ^{1}H NMR ($CDCl_3$) δ 5.40 (s, 2 H), 5.48 (s, 2 H), 7.32-8.48 (m, 10 H), 8.35 (s, 1 H). ^{13}C NMR ($CDCl_3$) δ 69.1, 69.7, 98.4, 127.7, 128.0, 128.1, 128.2, 128.5, 128.6, 135.5, 136.1, 159.4, 159.5, 163.5, 166.2.

5-(Dihydroxyboryl)-2,4-bis(benzyloxy)pyrimidine (36). a) sequential method.[151] A solution of 5-bromo-2,4-dibenzyloxypyrimidine (**35**) (1.0 g, 2.7 mmol) in THF (10 mL) was added dropwise to a solution of n-BuLi (1.3 M in hexane, 2.5 mL, 3.2 mmol) in THF (30 mL) at -78°C under Ar. The resulting solution was stirred at -78 °C for 10 min and a solution of $B(O^iPr)_3$ (1.0 mL, 5.3 mmol) in THF (4 mL) was added dropwise. The reaction mixture was stirred at -78 °C for 1 h, warmed to room temperature for 2 h. Then the reaction mixture was quenched with hydrochloric acid (3 M, 9 mL). After 2 h at room temperature, the mixture was diluted with ethyl acetate (30 mL) and phases were separated. The aqueous layer was extracted with ethyl acetate (2 x 30 mL), and the combined organic layers were dried over $MgSO_4$, filtered and concentrated in vacuo. The residue was purified through column chromotography eluting with 3% ethanol in methylene chloride to give comound as a colorless syrup (199 mg, 22%). ^{1}H NMR ($CDCl_3$) δ 5.46 (s, 4 H), 7.25-7.48 (m, 10 H), 8.72 (s, 1H); ^{13}C NMR ($CDCl_3$) δ 118.5, 160.1, 161.4, 165.9. b) **one-pot method.**[157] *N*-Butyllithium (1.3 M in hexane, 2.5 mL, 3.2 mmol) was dropwise added over a 1 h period to a solution of **35** (1.0 g, 2.7 mmol) and $B(O^iPr)_3$ (1.0 mL, 5.3 mmol) in a mixture of anhydrous THF and toluene (1:4 volume ratio, 50 mL total) at –78 °C under Ar. The mixture was stirred for an additional 18 h at rt, followed by addition of dilute HCl (1 M). The residue was then treated with H_2O (50 mL) and

extracted with CH_2Cl_2 (3 x 30 mL). The organic extracts were combined, washed with brine (50 mL), dried over $MgSO_4$ and the solvent removed under reduced pressure to give **36** as a white powder (860 mg, 95%). ^{1}H NMR ($CDCl_3$) δ 5.46 (s, 4 H), 7.25-7.48 (m, 10 H), 8.72 (s, 1H); ^{13}C NMR ($CDCl_3$) δ 118.5, 160.1, 161.4, 165.9.

2,3-Dibenzyloxy-5-benzyloxymethyl-1-[4-(2,4-dibenzyloxy-5-pyrimidinyl)-imidazol-1-yl]-β-D-ribofuranose (37).[158] A mixture of **13b** (1.7 g, 2.9 mmol) and $Pd(PPh_3)_4$ (185 mg, 0.16 mmol) in 40 mL of 1,2-dimethoxyethane (DME) was stirred at rt under Ar for 10 min. To this mixture, 5-(dihydroxyboryl)-2,4-bis(benzyloxy)-pyrimidine (**36**) (3.2 mmol in 20 mL DME) was added. Saturated aqueous $NaHCO_3$ (40 mL) was added, and the mixture refluxed under Ar for 4 h. The solution was cooled to rt, the DME layer separated and set aside. The aqueous layer was then extracted with EtOAc (3 x 50 mL) and the organic extracts combined with the DME layer, washed with brine (100 mL), and dried over $MgSO_4$. The solvent was removed to give a pale brown syrup. Column chromatography eluting with 2% EtOH in CH_2Cl_2 gave **37** as a colorless syrup (1.47 g, 70%). ^{1}H NMR ($CDCl_3$) δ 3.45 (dd, 3.0 Hz, 10.6 Hz, 1 H), 3.56 (dd, 3.3 Hz, 10.6 Hz, 1 H), 4.01-4.48 (m, 1 H), 4.11 (br t, 5.5 Hz, 1 H), 4.31-4.62 (m, 7 H), 5.42-5.52 (m, 4 H), 5.78 (d, 6.0 Hz, 1 H), 7.15-7.54 (m, 26 H), 7.73 (s, 1 H), 9.15 (s, 1 H). ^{13}C NMR ($CDCl_3$) δ 68.3, 68.9, 69.4, 72.1, 72.5, 73.1, 76.5, 81.5, 82.1, 88.7, 109.5, 115.6, 127.3, 127.6, 127.8, 127.9, 128.3, 134.0, 135.6, 136.1, 136.5, 136.7, 137.2, 137.3, 155.9, 162.7, 166.0. Anal. Calcd for $C_{47}H_{44}N_4O_6 \bullet 1H_2O$: C, 72.48; H, 5.95; N, 7.19. Found: C, 72.82; H, 5.75; N, 7.03.

1-[4-(Uracil-5-yl)imidazol-1-yl]-1-β-D-ribofuranose 2,3,5-Triol (6).[115] A mixture of **37** (200 mg, 0.26 mmol), palladium (10% Pd/C, 200 mg) and ammonium formate (300 mg) in EtOH (50 mL) was heated under reflux for 2 h. The solvent was then removed under reduced pressure and the residue purified by column chromatography eluting with EtOAc:acetone:EtOH:H_2O (7:1:1:0.5) to give **6** as a white crystalline solid (72 mg, 88%), mp: 239-242°C. ^{1}H NMR (DMSO-d_6) δ 3.49 (dd, 4.5 Hz, 12.3 Hz, 1 H), 3.55 (dd, 5.0 Hz, 12.3 Hz, 1 H), 3.86 (br d, 3.3 Hz, 1 H), 4.0 (dd, 4.0 Hz, 6.0 Hz, 1 H), 4.11 (br t, 5.1 Hz, 1 H), 5.00 (br t, 4.8 Hz, 1 H), 5.14 (br d, 3.9 Hz, 1 H), 5.36 (br d, 5.7 Hz, 1 H), 5.52 (d, 6.0 Hz, 1 H), 7.67 (s, 1 H), 7.81 (s, 1 H), 7.86 (s, 1 H). 11.0 (s, 1 H), 112.2 (s, 1 H). ^{13}C NMR (DMSO-d_6) δ 61.3, 70.3, 75.1, 85.2, 89.3, 107.3, 114.5, 133.5, 135.7, 136.3, 150.5, 162.2. Anal. Calcd for $C_{12}H_{14}N_4O_6$•0.6H_2O: C, 44.88; H, 4.80; N, 17.38. Found: C, 45.14; H, 4.60; N, 17.03.

Attempted synthesis of 1-[4-(4-aminopyrimidin-5-yl-2-one)imidazol-1-yl]-1-β-D-ribofuranose 2,3,5-Triol (4).[160] 1-[4-(Uracil-5-yl)imidazol-1-yl]-1-β-D-ribofuranose 2,3,5-Triol (**6**) (27.4 mg, 88.3 μmol), formamidine (7.04 μL, 177 μmol), hexamethyldisilazane (280 μL, 1.33 mmol) and ammonium sulfate (13 mg, 98.5 μmol) were combined in a Parr bomb and stirred at 120 °C for 72 h. After cooling to rt, the contents of the bomb were dissolved in methanol and refluxed for 6 h. Upon TLC observation, the reaction failed to afford **6** and no starting material was recovered.

Attempted synthesis of 1-[4-(1,3-Dimethyluracil-5-yl)imidazol-1-yl]-1-β-D-ribofuranose 2,3,5-Triol (38).[161] 1-[4-(Uracil-5-yl)imidazol-1-yl]-1-β-D-ribofuranose 2,3,5-Triol (**6**) (75 mg, 241 μmol) and DMF-dimethylacetal (10 mL) was heated to 80 °C for 6 h. The reaction mixture as cooled to rt, and the solvent was removed under reduced pressure to afford **38** as an off-white powder (39 mg, 48%). The product was used without purification. MS (ESI): Calc'd for $C_{14}H_{18}N_4O_6$: 338. Found: (M+1) 339.

Attempted synthesis of 1-[4-(2-aminopyrimidin-5-yl-4-one)imidazol-1-yl]-1-β-D-ribofuranose 2,3,5-Triol (3).[161] Guanidine HCl (100 mg, 1.05 mmol) was stirred in a 0.7 M sodium ethoxide (20 mL) for 10 min and the NaCl salt was removed by filtration. To the filtrate was added (35 mg, 0.103 mmol) and the reaction was refluxed for 18 h. The solvent was removed under reduced pressure. Upon TLC analysis in a mobile phase of EtOAc:acetone:EtOH:H_2O (4:1:1:0.5), it was indicative that all of the reactions did not show formation of **3**.

2,3-Dibenzyloxy-5-benzyloxymethyl-1-[4-(2,4-diaminopyrimidine)-imidazol-1-yl]-1-β-D-ribofuranose (39).[162] In a Parr bomb, anhydrous ammonia gas was bubbled in an anhydrous methanolic solution of **37** (1.0 g, 1.3 mmol in 50 mL of methanol) at –78 ºC for 5 min. The bomb was sealed and heated at 170 ºC for 96 h. After cooling to 0 ºC, the solvent was removed under reduced pressure. The residue was purified by column chromatography eluting with 8% EtOH in CH_2Cl_2 to give **39** (306 mg, 40%) a colorless syrup. ^{1}H NMR ($CDCl_3$) δ 3.54 (dd, 2.4 Hz, 10.4 Hz, 1 H), 3.70 (dd, 2.8

Hz, 10.4 Hz, 1 H), 4.09 (dd, 2.5 Hz, 4.5 Hz, 1 H), 4.16 (br t, 4.8 Hz, 1 H), 4.33-4.36 (m, 1 H), 4.39 (d, 12.0, 1 H), 4.47-4.68 (m, 6 H), 5.06 (br s, 2 H), 5.66 (br s, 2 H), 5.74 (d, 6.4 Hz, 1 H), 7.01 (s, 1 H), 7.10-7.35 (m, 15 H), 7.60 (s, 1 H), 7.78 (s, 1 H). ^{13}C NMR ($CDCl_3$) δ 70.2, 72.7, 73.0, 74.0, 76.9, 81.7, 82.9, 89.2, 102.6, 110.4, 127.3, 127.8, 128.0, 128.1, 128.2, 128.3, 128.4, 128.5, 128.7, 128.8, 129.0, 135.3, 136.9, 137.4, 137.5, 138.9, 152.3, 161.2, 161.4.

1-[4-(2,4-Diaminopyrimidin-5-yl)imidazol-1-yl]-1-β-D-ribofuranose-2,3,5-triol (5).[115] In a similar fashion as was used to obtain **6**, the desired triol **5** was obtained in 90% yield (159 mg) as a white powder following deprotection of **39** with Pd/C and ammonium formate. Mp: 268-272 °C. ^{1}H NMR (DMSO-d_6) δ 3.72 (dd, 3.6 Hz, 12.0 Hz, 1 H), 3.80 (dd, 3.2 Hz, 12.0 Hz, 1 H), 4.05 (q, 3.2 Hz, 1 H), 4.20, (dd, 3.6 Hz, 4.2 Hz, 1 H), 4.27 (br t, 4.2 Hz, 1 H), 5.64 (d, 5.6 Hz, 1 H), 7.56 (s, 1 H), 7.91 (s, 1 H), 7.96 (s, 1 H). ^{13}C NMR (DMSO-d_6) δ 61.4, 70.4, 75.1, 85.4, 89.4, 100.6, 111.0, 135.5, 137.5, 150.4, 160.3, 160.5. Anal. Calcd for $C_{12}H_{16}N_6O_4 \bullet 1H_2O$: C, 45.42; H, 5.40; N, 26.48. Found: C, 45.71; H, 5.22; N, 26.26.

1-[4-(4-Aminopyrimidin-5-yl-2-one)imidazol-1-yl]-1-β-D-ribofuranose 2,3,5-Triol (4).[162] To a solution of **39** (850 mg, 1.46 mmol) in a 1:1 mixture of THF and H_2O (30 mL) was added sodium nitrite (486 mg, 7.03 mmol), followed by glacial acetic acid (0.62 mL, 10.69 mmol). The mixture was heated to 60 °C and stirred for 2 hours, at which point the TLC showed no traces of starting material. The solution was cooled to rt, neutralized with concentrated NH_4OH (1 mL) and evaporated under reduced

pressure. The crude product was used directly in the next step. In a similar fashion as was used for the deprotection of **37** to get **6**, the benzyl groups were deblocked with Pd/C and ammonium formate in refluxing ethanol, and subsequently purified by column chromatography eluting with EtOAc:acetone:EtOH:H_2O (4:1:1:0.5) to give **4** as a white powder (42 mg, 41% for 2 steps). ^{1}H NMR (D_2O) δ 3.61 (dd, 3.6 Hz, 12.0 Hz, 1 H), 3.71 (dd, 3.2 Hz, 12.0 Hz, 1 H), 4.06 (q, 3.2 Hz, 1 H), 4.19, (dd, 3.6 Hz, 4.2 Hz, 1 H), 4.33 (dd, 1 H), 5.68 (d, 3.9 Hz, 1 H), 7.39 (s, 1 H), 7.56 (s, 1 H), 7.89 (s, 1 H), 8.23 (s, 2H). ^{13}C NMR (D_2O) δ 61.7, 70.3, 75.0, 85.1, 89.5, 101.1, 115.1, 134.2, 137.7, 158.5, 165.1, 171.1.

1-[4-(2-Aminopyrimidin-5-yl-4-one)imidazol-1-yl]-1-β-D-ribofuranose 2,3,5-Triol (3). A solution of **5** (14 mg, 0.05 mmol) and saturated aqueous $NaHSO_3$ (5.0 mL) was heated at 60 ºC for 10 hours. The solution was evaporated under reduced pressure to afford the crude product, which was purified by preparative TLC eluting with EtOAc:acetone:EtOH:H_2O (4:1:1:1) to obtain **3** as a white powder (12.4 mg, 88%). ^{1}H NMR (D_2O): δ 3.70 (dd, 3.3 Hz, 10.2 Hz, 1H), 3.87 (dd, 2.4 Hz, 10.2 Hz, 1H), 4.07-4.16 (m, 2H), 4.29 (dd, 2.4 Hz, 4.5 Hz, 1H), 6.11 (s, 1 H), 6.38 (d, 5.7 Hz, 1 H), 7.84 (d, 1.2 Hz, 1H), 9.14 (dd, 0.6 Hz, 1.5 Hz, 1 H). ^{13}C NMR (D_2O) δ 60.1, 69.0, 75.9, 85.4, 91.6, 105.0, 122.5, 130.0, 135.8, 145.3, 154.0, 163.4. Anal. Calcd for $C_{12}H_{15}N_5O_5$ • 0.75 H_2O: C, 44.65; H, 5.15; N, 21.71. Found: C, 44.53; H, 5.09; N, 21.57.

2,3-Dibenzyloxy-5-benzyloxymethyl-1-[5-(2,4-diaminopyrimid-ine)imidazol-1-yl]-1-β-D-ribofuranose (42).[152] A mixture of **13b** (656 mg, 1.10 mmol) and $PdCl_2$(dppf) (24 mg, 0.03 mmol) in DMF (20 mL) was stirred at room temperature under Ar for 10 min. This was added to a solution of 5-(dihydroxyboryl)pyrimidine (**41**) (124 mg, 1.0 mmol in 20 mL DMF), followed by addition of a saturated aqueous 2M Na_2CO_3 solution (2.5 mL). The mixture was heated at 80 ºC under Ar for 18 h, followed by cooling to rt. The volume was reduced and the residue extracted with EtOAc (3 x 20 mL). The organic extracts were combined, and washed sequentially with H_2O (30 mL), then brine (50 mL), and dried over $MgSO_4$. The solvent was removed under reduced vacuum to give a tan syrup. Column chromatography eluting with 2% EtOH in CH_2Cl_2 gave **42** as a colorless syrup (362 mg, 66%). ^{1}H NMR ($CDCl_3$) δ 3.45 (dd, 3.0 Hz, 10.6 Hz, 1 H), 3.56 (dd, 3.3 Hz, 10.6 Hz, 1 H), 4.01-4.48 (m, 1 H), 4.11 (br t, 5.5 Hz, 1 H), 4.31-4.62 (m, 7 H), 5.42-5.52 (m, 4 H), 5.78 (d, 6.0 Hz, 1 H), 7.15-7.54 (m, 26 H), 7.73 (s, 1 H), 9.15 (s, 1 H). ^{13}C NMR ($CDCl_3$) δ 68.3, 68.9, 69.4, 72.1, 72.5, 73.1, 76.5, 81.5, 82.1, 88.7, 109.5, 115.6, 127.3, 127.6, 127.8, 127.9, 128.3, 134.0, 135.6, 136.1, 136.5, 136.7, 137.2, 137.3, 155.9, 162.7, 166.0. Anal. Calcd for $C_{47}H_{44}N_4O_6$•$1H_2O$: C, 72.48; H, 5.95; N, 7.19. Found: C, 72.82; H, 5.75; N, 7.03.

Attempted synthesis of 2,3-dibenzyloxy-5-benzyloxymethyl-1-[4-(4-aminopyrimidine)-imidazol-1-yl]-1-β-D-ribofuranose (43).[175] To a stirred solution of liquid ammonia (20 mL) containing potassium amide (2.5 eq), the substrate (1-2 mole) was added. After 10 minutes, $KMnO_4$ (3.5 eq) was added portion-wise and

stirring was continued for 20 minutes. The reaction mixture was then quenched with ammonium sulfate (5 equivalents) and after 10 minutes methanol (20 mL) was added through the condenser. The ammonia was evaporated under reduced pressure and according to the TLC and MS showed decomposition of the starting material.

4(5)-Cyanomethylimidazole (45).[165] Commercial bleach Clorox® (active ingredient: sodium hypochlorite, 30 mL, 95 mmol) was added dropwise to a stirred suspension of histidine monohydrochloride monohydrate (10.4 g, 50 mmol) in H_2O (30 mL) at 0 °C. The resulting yellow solution was kept at 10-20 °C for 3 h and the stirring allowed to continue for 18 h at rt. Solid sodium carbonate was added until the pH reached 8.0. The solution was evaporated to dryness, and the residue triturated with refluxing EtOAc (4 x 150 mL). The organic extracts were combined, washed with brine (300 mL), dried over $MgSO_4$ and the solvent removed under vacuum. Recrystallization of the residue in ethanol gave **45** as a yellow crystalline solid (4.5 g, 70%), mp: 135-137 ºC. ^{1}H NMR (DMSO-d_6) δ 3.84 (s, 2 H), 7.05 (s,1 H), 7.64 (s, 1 H), 12.09 (s, 1 H). ^{13}C NMR (DMSO-d_6) δ 16.5, 114.4, 118.8, 129.5, 135.6.

2,3-Diacetoxy-5-acetoxymethyl-1-(4-cyanomethylimidazol-3-yl)-β-D-ribofuranose (46a).[123] A mixture of 4(5)-cyanomethylimidazole (**45**) (2.18 g, 2.03 mmol), 1,2,3,5-tetra-*O*-acetate-β-D-ribofuranose (7.10 g, 2.25 mmol) and BSA (20 mL, 8.1 mmol) in acetonitrile (100 mL) was stirred at rt for 3 h under Ar. The solution was cooled to 0 °C, and TMSOTf (4.3 mL, 2.25 mmol) was added dropwise. The mixture was stirred at 60 °C for 18 h under Ar, then cooled to 0 °C and quenched

with aqueous $NaHCO_3$ (50 mL). The organic solvent was removed, and the residue extracted with CH_2Cl_2 (3 x 50 mL). The organic extracts were combined, washed with brine (100 mL), dried over $MgSO_4$ and the solvent removed under vacuum to give a brown syrup. Column chromatography eluting with 2% ethanol in CH_2Cl_2 gave **45** as a pale yellow syrup (1.6 g, 35%). ^{1}H NMR ($CDCl_3$) δ 2.05 (s, 3 H), 2.08 (s, 3 H), 2.11 (s, 3 H), 3.81 (d, 4.0 Hz, 1 H), 4.36-4.42 (m, 3 H), 5.79 (d, 6.0 Hz, 1 H), 7.16 (s, 1 H), 7.77 (s, 1 H). MS (ESI): Calc'd for $C_{16}H_{19}N_3O_7$: 365. Found: (M+1) 366.

1-[4-(4-Aminopyrimidin-5-yl)imidazol-1-yl]-1)-β-D-ribofuranose 2,3,5-triol (1).[168] A mixture of **11** (1.60 g, 4.38 mmol), sodium methoxide (2 equivalents, made fresh from dissolving 202 mg of sodium metal in 10 mL of anhydrous methanol) and commercially available 1,3,5-triazine (356 mg, 4.38 mmol) was heated under Ar at 40 °C for 18 h. Silica gel was added to the reaction mixture and the solvent was removed under reduced pressure. The silica gel containing the product was loaded on silica gel column and eluted with EtOAc:acetone:EtOH:H_2O (8:1:1:0.5) to give **1** as a hygroscopic foam (272 mg, 15 %). ^{1}H NMR (CD_3OD) δ 3.65 (dd, 3.6 Hz, 12.8 Hz, 1H), 3.72 (dd, 3.2 Hz, 12.8 Hz, 1 H), 3.97 (q, 3.5 Hz, 1 H), 4.15 (dd, 4.0 Hz, 5.2 Hz, 1 H), 4.36 (t, 5.2 Hz, 1 H), 5.36 (d, 6.0 Hz, 1 H), 7.08 (s, 1 H), 8.05 (s, 1 H), 8.22 (s, 1 H), 8.39 (s, 1 H). ^{13}C NMR (CD_3OD) δ 61.5, 70.7, 75.9, 85.7, 89.3, 126.6, 128.7, 137.3, 156.2, 158.1,162.8, 172.9. MS(ESI): Calc'd for $C_{12}H_{15}N_5O_4$: 293. Found: (M+1) 294.

1-[4-(Pyrimidin-5-yl-2-one)imidazol-1-yl]-1)-β-D-ribofuranose 2,3,5-Triol (2).[162] To a solution of **1** (400 mg, 1.36 mmol) in a 1:1 mixture of THF and H_2O (60 mL) was added sodium nitrite (430 mg, 6.23 mmol), followed by glacial acetic acid (0.54 mL, 9.69 mmol). The mixture was heated to 80 °C and stirred for 5 hours, at which point the TLC showed no traces of starting material. The solution was cooled to room temperature, neutralized with concentrated NH_4OH (1 mL) and evaporated under reduced pressure. The crude product was purified by column chromatography eluting with EtOAc:acetone:EtOH:H_2O (8:1:1:0.5) to give **2** as a white powder (272 mg, 68%). ^{1}H NMR (CD_3OD) δ 3.68 (dd, 3.5 Hz, 12.8 Hz, 1 H), 3.75 (dd, 3.2 Hz, 12.8 Hz, 1 H), 4.01 (q, 3.1 Hz, 1 H), 4.11, (dd, 3.8 Hz, 5.1 Hz, 1 H), 4.29 (dd, 2 H), 5.43 (d, 3.6, 1 H), 7.69 (s, 1 H), 7.92 (s, 1 H), 8.01 (s, 1 H), 8.14 (s, 1 H), 8.48 (bs, 1 H). ^{13}C NMR (CD_3OD) δ 60.1, 70.1, 75.6, 85.6, 89.8, 119.1, 123.2, 129.0, 135.7, 158.9, 164.1, 169.7.

REFERENCES

(1) Burger, A. *Burger's Medicinal Chemistry and Drug Discovery*; Wiley-Interscience: New York, 2003.

(2) Silverman, R. B. *The Organic Chemistry of Drug Design and Drug Action*; Academic Press: Evanston, 1992.

(3) Voet, D.; Voet, J. G. *Biochemistry*; 2nd ed.; John Wiley & Sons: Somerset, 1995.

(4) Foye, W. O.; Lemke, T. L.; Williams, D. A. *Princinples of Medicinal Chemistry*; Lippincott Williams & Wilkins: Media, 1995.

(5) Levene, P. A.; Jacobs, W. A. *Ber* **1909***, 42*.

(6) Chu, C. K.; Baker, D. C. *Nucleosides and Nucleotides as Antitumor and Antiviral Agents*; Plenum Press: New York, 1993.

(7) Montgomery, J. A. Studies on the Biologic Activity of Purine and Pyrimidine Analogs. *Medicinal Research Reviews* **1982***, 2*, 271-308.

(8) Mitsuya, H. *Anti-HIV Nucleosides: Past, Present and Future*; R. G. Landes: New York, 1997.

(9) Horwitz, J. P.; Chua, J.; Noel, M. *Journal of Organic Chemistry* **1964***, 29*, 2076-2078.

(10) Zhu, X.-F. The Latest Progress in the Synthesis of Carbocyclic Nucleosides. *Nucleosides, Nucleotides and Nucleic Acids* **2000***, 19*, 651-690.

(11) Simons, C. *Nucleoside Mimetics: Their Chemistry and Biological Properties*; Gordon and Breach: Amsterdam, 2001.

(12) Montgomery, J. A.; Shortnacy, A. T.; Clayton, S. D. A Comparison of Two Methods for the Preparation of 3-Deazapurine Ribonucleosides. *Journal of Heterocyclic Chemistry* **1977***, 14*, 195-197.

(13) Chiang, P. K. Biological Effects of Inhibitors of *S*-Adenosylhomocysteine Hydrolase. *Pharmacol. Ther.* **1998***, 77*, 115-134.

(14) Robins, R. K.; Revankar, G. R. *Advances in Anti Viral Drug Design*; JAI Press: Greenwich, 1993.

(15) Adamson, R. H.; Zaharewitz, D. W.; Johns, D. G. *Pharmacology* **1977***, 15*, 84-87.

(16) Bloch, A.; Leonard, R. J.; Nichol, C. A. *Biochimica et Biophysica Acta* **1967***, 138*, 10-25.

(17) Cristalli, G.; Franchetti, P.; Grifantini, M.; Vittori, S.; Bordoni, T. et al. *Journal of Medicinal Chemistry* **1987***, 30*, 1686-1688.

(18) Cristalli, G.; Grifantini, M.; Vittori, S.; Balduini, W.; Cattabeni, F. *Nucleosides & Nucleotides* **1985***, 4*, 237-242.

(19) Antonini, I.; Cristalli, G.; Franchetti, P.; Grifantini, M.; Martelli, S. et al. *Journal of Pharmaceutical Sciences* **1984***, 1984*, 366-369.

(20) Elliot, R. D.; Montgomery, J. A. *Journal of Medicinal Chemistry* **1977***, 20*, 116-120.

(21) Montgomery, J. A.; Elliot, R. D.; Thomas, H. J. *Ann. N. Y. Acad. Sci.* **1975***, 255*, 292-301.

(22) Franchetti, P.; Messini, L.; Cappellacci, L.; Sheikha, G. A.; Grifantini, M. et al. *Nucleosides & Nucleotides* **1994***, 13*, 1739-1755.

(23) Riggs, A. D.; Jones, P. A. *Adv. Cancer Res.* **1983***, 40*, 1-30.

(24) Momparler, R. L.; Momparler, L. F. *Cancer Chemother. Pharmacol.* **1989***, 25*, 51-54.

(25) Moriconi, W. J.; Slavik, M.; Taylor, S. *Investigational New Drugs* **1986***, 4*, 67-84.

(26) Marquez, V. E. Carbocyclic Nucleosides. *Advances in Antiviral Drug Design*; JAI Press: Greenwich, 1996; pp 89-146.

(27) De Clercq, E. *S*-Adenosylhomocysteine Hydrolase Inhibitors as Broad-Spectrum Antiviral Agents. *Biochemical Pharmacology* **1987***, 36*, 2567-2575.

(28) Chiang, P. K.; Miura, G. A. *S*-Adenosylhomocysteine Hydrolase. *Biological Methylation and Drug Design*; Humana Press: Clifton, NJ, 1986; pp 239-251.

(29) Pauling, L. *Chemical & Engineering News* **1946***, 24*, 1375-1377.

(30) Fischer, E. *Chem. Ber.* **1894***, 27*, 2985.

(31) Koshland, D. E. Application of a Theory of Enzyme Specificity to Protein Synthesis. *Proceedings of the National Academy of Sciences, U.S.A.* **1958***, 44*, 98-104.

(32) Sunderberg, E. J. *Adv. Protein Chem.* **2003***, 61*, 119-160.

(33) Berzofsky, J. A. Intrinsic and Extrinsic Factors in Protein Antigenic Structure. *Science* **1985**, *229*, 932-940.

(34) Foote, J.; Milstein, C. Conformational Isomerism and the Diversity of Antibodies. *Proceedings of the National Academy of Sciences, U.S.A.* **1994**, *91*, 10370-10374.

(35) Ma, B.; Shatsky, M.; Wolfson, H. J.; Nussinov, R. Multiple Diverse Ligands Binding at a Single Protein Site: A Matter of Pre-existing Populations. *Protein Sci.* **2002**, *11*, 184-197.

(36) Bosshard, H. R. Molecular Recognition by Induced Fit: How Fit is the Concept? *News Physiol. Sci.* **2001**, *16*, 171-173.

(37) Leonard, N. J.; Laursen, R. A. Synthesis of 3-β-D-Ribofuranosyladenine and (3-β-D-Ribofuranosyladenine)-5'-phosphate. *Biochemistry* **1965**, *4*, 354-365.

(38) Leonard, N. J.; Morrice, A. G.; Sprecker, M. A. Linear Benzoadenine. A Stretched-Out Analog of Adenine. *Journal of Organic Chemistry* **1975**, *40*, 356-366.

(39) Leonard, N. J.; Hiremath, S. P. Dimensional Probes of Binding and Activity. *Tetrahedron* **1986**, *42*, 1917-1961.

(40) Leonard, N. J. Dimensional Probes of Enzyme-Coenzyme Binding Sites. *Accounts of Chemical Research* **1982**, *15*, 128-135.

(41) Leonard, N. J.; Laursen, R. A. The Synthesis of 3-β-D-Ribofuranosyladenine. *Journal of the American Chemical Society* **1963**, *85*, 2026-2028.

(42) Leonard, N. J.; Scopes, D. I. C.; VanDerLijn, P.; Barrio, J. R. Dimensional Probes of the Enzyme Binding Sites of Adenine Nucleotides. Biological Effects of Widening the Adenine Ring by 2.4 Å. *Biochemistry* **1978**, *17*, 3677-3685.

(43) Ealick, S. E.; Babu, Y. S.; Bugg, C. E.; Erion, M. D.; Guida, W. C. et al. Application of Crystallographic and Modeling Methods in the Design of Purine Nucleoside Phosphorylase Inhibitors. *Proceedings of the National Academy of Sciences, U.S.A.* **1991**, *88*, 11540-11544.

(44) Bugg, C. E.; Carson, W. M.; Montgomery, J. A. Drugs by Design. *Scientific American* **1993**, *269*, 92-98.

(45) Federov, A.; Shi, W.; Kicska, G.; Federov, E.; Tyler, P. C. et al. Transition State Structure of Purine Nucleoside Phosphorylase and Principles of Atomic Motion in Enzymatic Catalysis. *Biochemistry* **2001**, *40*, 853-860.

(46) Montgomery, J. A. Purine Nucleoside Phosphorylase: a Target for Drug Design. *Medicinal Research Reviews* **1993***, 13*, 209-228.

(47) Meyer, E. F.; Swanson, S. M.; Williams, J. A. Molecular Modeling and Drug Design. *Pharmacol. Ther.* **2000***, 85*, 113-121.

(48) Carlson, H. A.; McCammon, J. A. Accommodating Protein Flexibility in Computational Drug Design. *Molecular Pharmacology* **2000***, 57*, 213-218.

(49) Joseph-McCarthy, D. Computational Approaches to Structure-based Ligand Design. *Pharmacol. Ther.* **1999***, 84*, 179-191.

(50) Das, K.; Clark, A. D., Jr.; Lewi, P. J.; Heeres, J.; de Jonge, M. R. et al. Roles of Conformational and Positional Adaptability in Structure-Based Design of TMC125-R165335 (Etravirine) and Related Non-Nucleoside Reverse Transcriptase Inhibitors that are Highly Potent and Effective Against Wild-Type and Drug-Resistant HIV-1 Varients. *Journal of Medicinal Chemistry* **2004***, 47*, 3550-2560.

(51) Lewis, P. J.; de Jonge, M.; Frits, D.; Koymans, L.; Vinkers, M. et al. On the Detection of Multiple-Binding Modes of Ligand to Proteins, From Biological, Structural, and Modeling Data. *Journal of Computer-Aided Molecular Design* **2003***, 17*, 129-134.

(52) Wilson, E. K. Dealing With Flexible Receptors. *Chemical & Engineering News* **2004**, 46-47.

(53) Henry, C. M. Clues for Overcoming HIV Drug Resistance. *Chemical & Engineering News* **2004**, 40-41.

(54) Jimenez, R.; Salazar, G.; Yin, J.; Joo, T.; Romesberg, F. E. Protein Dynamics and the Immunological Evolution of Molecular Recognition. *Proceedings of the National Academy of Sciences, U.S.A.* **2004***, 101*, 3803-3808.

(55) Jimenez, R.; Salazar, G.; Baldridge, K. K.; Romesberg, F. E. Flexibility and Molecular Recognition in the Immune System. *Proceedings of the National Academy of Sciences, U.S.A.* **2002***, 100*, 92-97.

(56) Westheimer, F. H.; Mayer, J. E. *Journal of Chemical Physics* **1946***, 37*, 733.

(57) Hill, T. L. *Journal of Chemical Physics* **1946***, 37*, 465.

(58) Hendrickson, J. B. Molecular Geometry. I. Machine Computation of the Common Rings. *Journal of the American Chemical Society* **1961***, 83*.

(59) Bultinck, P. *Computational Medicinal Chemistry for Drug Discovery*; Marcel Dekker: New York, 2004.

(60) Jiang, F.; -H., K. S. "Soft-docking": Matching of molecular surface cubes. *Journal of Molecular Biology* **1991***, 219*, 79-102.

(61) Holtje, H.-D.; Sippl, W.; Rognan, D.; Folkers, G. *Molecular Modeling. Basic Principles and Applications*; 2nd ed.; Wiley-Vch: Weinheim, 2003.

(62) Zhu, J.; Fan, H.; Liu, H.; Shi, Y. Structure-based ligand design for flexible proteins: Application of new F-DycoBlock. *Journal of Computer-Aided Molecular Design* **2001***, 15*, 979-996.

(63) Knegtel, R. M. D.; Kuntz, I. D.; Oshiro, C. M. Molecular Docking to Ensembles of Protein Structures. *Journal of Molecular Biology* **1997***, 266*, 424-440.

(64) Clauben, H.; Buning, C.; Rarey, M.; Lengauer, T. FlexE: Efficient Molecular Docking Considering Protein Structure Variations. *Journal of Molecular Biology* **2001***, 308*, 377-395.

(65) Bursavich, M. G.; Rich, D. H. Designing Non-peptide Peptidomemetics in the 21st Century: Inhibitors Targeting Conformational Ensembles. *Journal of Medicinal Chemistry* **2002***, 45*, 541-558.

(66) Kastenholz, M. A.; Pastor, M.; Cruciani, G.; Haaksma, E. E. J.; Fox, T. GRID/CPCA: A New Computational Tool to Design Selective Ligands. *Journal of Medicinal Chemistry* **2000***, 43*, 3033-3044.

(67) Martin, Y. C.; Willet, P. *Designing Bioactive Molecules. Three-Dimensional Techniques and Applications*; American Chemical Society: Washington, DC, 1998.

(68) Goldberg, D. E. *Genetic Algorithm in Search, Optimization and Machine Learning*; Addison-Wesley: Reading, 1989.

(69) Apostolakis, J.; Pluckthun, A.; Caflisch, A. Docking Small Ligands in Flexible Binding Sites. *Journal of Computational Chemistry* **1998***, 19*, 21-37.

(70) Carlson, H. A.; Masukawa, K. M.; McCammon, J. A. Method for Inducing the Dynamic Fluctuations of a Protein in Computer Aided-Drug Design. *Journal of Physical Chemistry, A* **1999***, 103*, 10213-10219.

(71) Carlson, H. A. Protein Flexibility and Drug Design: How to Hit a Moving Target. *Current Opinion in Chemical Biology* **2002***, 6*, 447-452.

(72) Carlson, H. A. Protein Flexibility is an Important Component of Structure-Based Drug Discovery. *Current Pharmaceutical Design* **2002***, 8*, 1571-1578.

(73) Huggins, J. W.; Zhang, Z.-X.; Bray, M. Antiviral Drug Therapy of Filovirus Infections: S-Adenosylhomocysteine Hydrolase Inhibits Ebola Virus In Vitro

and in a Lethal Mouse Model. *Journal of Infectous Diseases* **1999***, 179 (Suppl 1)*, S240-S247.

(74) Huggins, J. W. Prospects for Treatment of Viral Hemorrhagic Fevers with Ribavirin, A Broad-Spectrum Antiviral Drug. *Review of Infectious Diseases* **1989***, 11*, S750-S761.

(75) Tuske, S.; Sarafianos, S. G.; Clark, A. D., Jr.; Ding, J.; Naeger, L. K. et al. Structures of HIV-1 RT-DNA Complexes Before and After Incorporation of the Anti-AIDS Drug Tenofovir. *Nature Structural & Molecular Biology* **2004***, 11*, 469-474.

(76) De Clercq, E. Antiviral Activity Spectrum and Target of Action of Different Classes of Nucleoside Analogues. *Nucleosides & Nucleotides* **1994***, 13*, 1271-1295.

(77) Wolfe, M. S.; Borchardt, R. T. *S*-Adenosyl-L-homocysteine Hydrolase as a Target for Antiviral Chemotherapy. *Journal of Medicinal Chemistry* **1991***, 34*, 1521-1530.

(78) Borchardt, R. T. *S*-Adenosyl-L-Methionine-Dependent Macromolecule Methyltransferases: Potential Targets for the Design of Chemotherapeutic Agents. *Journal of Medicinal Chemistry* **1980***, 23*, 347-357.

(79) Borchardt, R. T.; Creveling, C. R.; Ueland, P. M. *Biological Methylation and Drug Design*; Humana Press: Clifton, NJ, 1986.

(80) Cantoni, G. The Centrality of *S*-Adenosylhomocysteinase in the Regulation of the Biological Utilization of S-Adenosylmethionine. *Biological Methylation and Drug Design*; Humana Press: Clifton, NJ, 1986; pp 227-238.

(81) Razin, A.; Cedar, H.; Riggs, A. D. *DNA Methylation. Biochemistry and Biological Significance*; Springer-Verlag Inc.: New York, 1984.

(82) Razin, A.; Szyf, M. DNA Methylation Patterns. Formation and Function. *Biochimica et Biophysica Acta* **1984***, 782*, 331-342.

(83) Banerjee, A. K. 5'-Terminal Cap Structure in Eucaryotic Messenger Ribonucleic Acids. *Microbiological Reviews* **1980***, 44*, 175-205.

(84) Konarska, M.; Padgett, R. A.; Sharp, P. A. Recognition of Cap Structure in Splicing in Vitro of nRNA Precursors. *Cell* **1984***, 38*, 731-736.

(85) Palmer, J. L.; Abeles, R. H. The Mechanism of Action of *S*-Adenosylhomocysteine. *Journal of Biological Chemistry* **1979***, 254*, 1217-1226.

(86) Turner, M. A.; Dole, K.; Yuan, C.-S.; Hershfield, M. S.; Borchardt, R. T. et al. Crystallization and preliminary X-ray analysis of human placental S-adenosylhomocysteine hydrolase. *Acta Cryst.* **1997***, D53*, 339-341.

(87) Turner, M. A.; Yang, X.; Yin, D.; Kuczera, K.; Borchardt, R. T. et al. Structure and Function of *S*-Adenosylhomocysteine Hydrolase. *Cell Biochemistry and Biophysics* **2000***, 33*, 101-125.

(88) Turner, M. A.; Yuan, C.-S.; Borchardt, R. T.; Hershfield, M. S.; Smith, D. G. et al. Structure Determination of Selenomethionyl S-Adenosylhomocysteine Hydrolase Using Data at a Single Wavelength. *Nature Structural Biology* **1998***, 5*, 369-376.

(89) Yaun, C. S.; Yeh, J.; Squier, T. C.; Borchardt, R. T. Ligand-Dependent Changes in Intrinsic Fluorescence of S-adenosylhomocysteine hydrolase: Implications for the Mechanism of Inhibitor-Induced Inhibition. *Biochemistry* **1993***, 32*, 10414-10422.

(90) Yin, D.; Yang, X.; Hu, Y.; Kuczera, K.; Schowen, R. L. et al. Substrate Binding Stabilizes *S*-Adenosylhomocysteine Hydrolase in a Closed Conformation. *Biochemistry* **2000***, 39*, 9811-9818.

(91) Yaun, C. S.; Ault-Riche, D. B.; Borchardt, R. T. Chemical Modification and Site-directed Mutagenesis of Cysteine Residues in Human Placental S-Adenosylhomocysteine Hydrolase. *Journal of Biological Chemistry* **1996***, 271*, 28009-28016.

(92) Hu, Y.; Komoto, J.; Huang, Y.; Gomi, T.; Ogawa, H. et al. Crystal Structure of S-Adenosylhomocysteine Hydrolase from Rat Liver. *Biochemistry* **1999***, 38*, 8323-8333.

(93) Yin, D.; Yang, X.; Squier, T. C.; Borchardt, R. T. *Biophysical Journal* **1999***, 76*, A169.

(94) Howell, P. L.

(95) Keller, B. T.; Borchardt, R. T. *Antiviral Drug Development - A Multidisciplinary Approach*; Plenum Press: New York, 1988.

(96) Hasobe, M.; McKee, J. G.; Borcherding, D. R.; Borchardt, R. T. 9-(*trans*-2', *trans*-3'-Dihydroxycyclopent-4'-enyl)-Adenine and -3-Deazaadenine: Analogs of Neplanocin A Which Retain Potent Antiviral Activity but Exhibit Reduced Cytotoxicity. *Antimicrobial Agents and Chemotherapy* **1987***, 31*, 1849-1851.

(97) Hasobe, M.; McKee, J. G.; Borcherding, D. R.; Keller, B. T.; Borchardt, R. T. Effects of 9-(*trans*-2', *trans*-3'-Dihydroxycyclopent-4'-enyl)-Adenine and -3-Deazaadenine on the Metabolism of *S*-Adenosylhomocysteine in Mouse L929 Cells. *Molecular Pharmacology* **1988***, 33*, 713-720.

(98) Cools, M.; De Clercq, E. Correlation Between the Antiviral Activity of Acyclic and Carbocyclic Adenosine Analogues in Murine L929 cells and Their Inhibitory Effect on L929 cell *S*-Adenosylhomocysteine Hydrolase. *Biochemical Pharmacology* **1989***, 38*, 1061-1067.

(99) Snoeck, R.; Andrei, G.; Neyts, J.; Schols, D.; Cools, M. et al. Inhibitory Activity of *S*-Adenoslhomocysteine Hydrolase Inhibitors Against Human Cytomegalovirus Replication. *Antiviral Research* **1993***, 21*, 197-216.

(100) Yaun, C. S.; Liu, S.; Wnuk, S. F.; Robins, M. J.; Borchardt, R. T. *Advances in Antiviral Drug Design*; Connecticut: Greenwich, 1996.

(101) Paisley, S. D.; Hasobe, M.; Borchardt, R. T. Elucidation of the Mechanism by Which 9-(*trans*-2', *trans*-3'-Dihydroxycyclopent-4'-enyl)-adenine Inactivates *S*-Adenosylhomocysteine Hydrolase and Elevates Cellular Levels of *S*-Adenosylhomocysteine. *Nucleosides & Nucleotides* **1989***, 8*, 689-698.

(102) De Clercq, E.; Cools, M.; Balzarini, J.; Marquez, V. E.; Borcherding, D. R. et al. Broad-Spectrum Antiviral Activities of Neplanocin A, 3-Deazaneplanocin A, and Their 5'-Nor Derivatives. *Antimicrobial Agents and Chemotherapy* **1989***, 33*, 1291-1297.

(103) Yuan, C. S.; Yeh, J.; Liu, S.; Borchardt, R. T. Mechanism of inactivation of *S*-adenosylhomocysteine hydrolase by (Z)-4',5'-didehydro-5'-fluoroadenosine. *J. Biol. Chem.* **1993***, 268*, 17030-17037.

(104) Yuan, C.-S.; Liu, S.; Wnuk, S. F.; Robins, M. J.; Borchardt, R. T. Design and Synthesis of *S*-Adenosylhomocysteine Hydrolase Inhibitors as Broad-Spectrum Antiviral Agents. *Advances in Antiviral Drug Design*; JAI Press, Inc.: Greenwich, 1996; pp 41-88.

(105) Yaun, C.-S.; Wnuk, S. F.; Liu, S.; Robins, M. J.; Borchardt, R. T. (E)-5',6'-Didehydro-6'-deoxy-6'-fluorohomoadenosine: A Substrate That Measures the Hydrolytic Activity of S-Adenosylhomocysteine Hydrolase. *Biochemistry* **1994***, 33*, 12305-12311.

(106) De Clercq, E. Carbocyclic Adenosine Analogues as *S*-Adenosylhomocysteine Hydrolase Inhibitors and Antiviral Agents: Recent Advances. *Nucleosides & Nucleotides* **1998***, 17*, 625-634.

(107) Yaginuma, S.; Muto, N.; Tsujino, M.; Sudate, Y.; Hayashi, M. et al. Studies on Neplanocin A, New Antitumor Antibiotic. I. Producing Organism, Isolation and Characterization. *Journal of Antibiotics* **1981***, 34*, 359-366.

(108) Yaun, C.-S.; Wnuk, S. F.; Robins, M. J.; Borchardt, R. T. A Novel Mechanism-based Inhibitor (6'-Bromo-5',6'-didehydro-6'-deoxy-6'-fluorohomoadenosine) That Covalently Modifies Human Placental S-

Adenosylhomocysteine Hydrolase. *Journal of Biological Chemistry* **1998**, *273*, 18353-18364.

(109) Herdewijn, P. A. M. M. 5-Substituted-2'-deoxyuridines as Anti-HSV-1 Agents: Synthesis and Structure Activity Relationship. *Antiviral Chemistry and Chemotherapy* **1994**, *5*, 131-146.

(110) De Winter, H.; Herdewijn, P. Understanding the Binding of 5-Substituted 2'-Deoxyuridine Subtrates to Thymidine Kinase of Herpes Simplex Virus Type-1. *Journal of Medicinal Chemistry* **1996**, *39*, 4727-4737.

(111) Popescu, A.; Hornfeldt, A.-B.; Gronowitz, S. Catalytic Osmylation and Antiviral Activity of Some Carbocyclic 5-Substituted Uridine and Cytidine Analogues. *Nucleosides & Nucleotides* **1995**, *14*, 1639-1657.

(112) Wang, W.; Purwanto, M. G. M.; Weisz, K. CG Base Pair Recognition by Substituted Phenylimidasole Nucleosides. *Organic and Biomolecular Chemistry* **2004**, *2*, 1194-1198.

(113) Lengeler, D.; Weisz, K. New Nucleobase Analogs for the Extension of the Triple Helix Recognition Code. *Nucleosides & Nucleotides* **1999**, *18*, 1657-1658.

(114) Seley, K. L.; Zhang, L.; Hagos, A. "Fleximers". Design and Synthesis of Two Novel Split Nucleosides. *Organic Letters* **2001**, *3*, 3209-3210.

(115) Seley, K. L.; Zhang, L.; Hagos, A.; Quirk, S. "Fleximers". Design and Synthesis of a New Class of Novel Shape-Modified Nucleosides. *Journal of Organic Chemistry* **2002**, *67*, 3365-3373.

(116) Seley, K. L.; Quirk, S.; Salim, S.; Zhang, L.; Hagos, A. Unexpected Inhibition of *S*-Adenosyl-L-homocysteine Hydrolase by a Guanosine Nucleoside. *Bioorganic & Medicinal Chemistry Letters* **2003**, *13*, 1985-1988.

(117) Hwang, M.-J.; Ni, X.; Waldman, M.; Ewig, C. S.; Hagler, A. T. Derivation of Class II Force Fields. VI. Carbohydrate Compunds and Anomeric Effects. *Biopolymers* **1998**, *45*, 435-468.

(118) Maple, J. R.; Hwang, M.-J.; Jalkanen, K. J.; Stockfisch, T. P.; Hagler, A. T. Derivation of Class II Force Fields: V. Quantum Force Field for Amides, Peptides, and Related Compounds. *Journal of Computational Chemistry* **1998**, *19*, 430-458.

(119) Katritzky, A. R. A General Route to 4-Substituted Imidazoles. *Journal of the Chemical Society Perkins Transactions I* **1989**, 1139-1145.

(120) Li, J. J.; Gribble, G. W. *Palladium in Heterocyclic Chemistry*; Pergamon: Amsterdam, 2000.

(121) Stensiö, K.-E.; Wahlberg, K.; Wahren, R. Synthesis of Brominated Imidazoles. *Acta Chemica Scandinavica* **1973**, *27*, 2179-2183.

(122) Iddon, B. A Convenient Synthesis of 4,5-Mono, 4,5-Di- and 2,4,5-Trisubstituted Imidazoles. *Tetrahedron Letters* **1986**, *27*, 1635-1638.

(123) Koshkin, A. A.; Singh, S. K.; Nielsen, P.; Rajwanshi, V. K.; Kumar, R. et al. LNA (Locked Nucleic Acids): Synthesis of the Adenine, Cytosine, Guanine, 5-Methylcytosine, Thymine and Uracil Bicyclonucleoside Monomers, Oligomerisation, and Unprecedented Nucleic Acid Recognition. *Tetrahedron* **1998**, *54*, 3607-3630.

(124) Vorbruggen, H.; Strehlke, P. Eine Einfache Synthese von 2-Thiopyrimidin-nucleosiden. *Chem. Ber.* **1973**, *106*, 3039-3061.

(125) Czernecki, S.; Georgoulis, C.; Provelenghiou, C. Nouvelle Methode De Benzylation D'Hydroxyles Glucidiques Encombres. *Tetrahedron Letters* **1976**, *17*, 3535-3536.

(126) Stille, J. K. Transition Metals in Organic Synthesis. Principles of Transition Metal Chemistry. *Modern Synthetic Methods*; Springer: Berlin, 1983; pp 2.

(127) Stille, J. K. The Palladium-Catalysed Cross-Coupling Reactions of Organotin Reagents with Organic Electrophiles. *Angew. Chem., Int. Ed. Engl.* **1986**, *25*, 508.

(128) Smith, M. B. *Organic Synthesis*; McGraw-Hill, Inc.: New York, 1994.

(129) Hassan, J.; Sevignon, M.; Gozzi, C.; Schulz, E.; Lemaire, M. Aryl-Aryl Bond Formation One Century After the Discovery of the Ullmann Reaction. *Chemical Reviews* **2002**, *102*, 1359-1470.

(130) March, J. *Advance Organic Chemistry. Reactions, Mechanism and Structure*; Fourth ed.: New York, 1992.

(131) Elschenbroich, C.; Salzer, A. *Organometallics, A Concise Introduction*; 2nd ed.; Wiley-VCH: Weinheim, 1992.

(132) Cliff, M. D.; Pyne, S. G. Palladium Catalyzed Coupling of Imidazoles to Alkynyl and Vinyl Substrates. *Tetrahedron* **1996**, *52*, 13703-13712.

(133) Jetter, M. C.; Reitz, A. B. Synthesis of 4-Substituted Imidazoles via Palladium-Catalyzed Cross-Coupling Reactions. *Synthesis* **1998**, 829-831.

(134) Wang, E.; Koshlap, K. M.; Gillespie, P.; Dervan, P. B.; Feigon, J. Solution Structure of a Pyrimidine-Purine-Pyrimidine Triplex Containing the Sequence-Specific Intercalating Non-natural Base D_3. *Journal of Molecular Biology* **1996**, *257*, 1052-1069.

(135) Kirk, K. L. 4-Lithio-1-tritylimidazole as a Synthetic Intermediate. Synthesis of Imidazole-4-carboxaldehyde. *Journal of Heterocyclic Chemistry* **1985***, 22*, 57-59.

(136) Larsen, A. A. Iodinated 3,5-Diaminobenzoic Acid Derivatives. *Journal of the American Chemical Society* **1956***, 78*, 3210-3216.

(137) Wang, J.; Scott, A. I. A General Synthesis of β-Aryl- and Heteroarylpyrroles by Palladium-Catalyzed Coupling Reaction of β-Tributylstannylpyrrole with Aryl and Heteroaryl Halides. *Tetrahedron Letters* **1996***, 37*, 3247-3250.

(138) Kennedy, G.; Perboni, A. D. The Preparation of Heterobiaryl Phosphonates via theStille Coupling Reaction. *Tetrahedron Letters* **1996***, 37*, 7611-7614.

(139) Hirota, K.; Watanabe, K. A.; Fox, J. J. Pyrimidines. 14. Novel Pyrimidine to Pyrimidine Transformation Reactions and Their Application to *C*-Nucleoside Conversion. A Facile Synthesis of Pseudoisocytidine. *Journal of Organic Chemistry* **1978***, 43*, 1193-1197.

(140) Erdik, E. Transition Metal Catalyzed Reactions of Organozinc Reagents. *Tetrahedron* **1992***, 48*, 9577-9648.

(141) Negishi, E.-I.; Luo, F.-I.; Frisbee, R.; Matsushita, H. *Heterocycles* **1982***, 18*, 117.

(142) Kress, T. J. Chemistry of pyrimidine. II. Synthesis of pyrimidine N-oxides and 4-pyrimidinones by reaction of 5-substituted pyrimidines with peracids. Evidence for covalent hydrates as reaction intermediates. *Journal of Organic Chemistry* **1985***, 50*, 3073-3076.

(143) Santagostino, M.; Palmisano, G. Base-modified Pyrimidine Nucleosides. Efficient Entry to 6-Derivatized Uridines by Sn-Pd Transmetallation-coupling Process. *Tetrahedron* **1993***, 49*, 2533-2542.

(144) Campbell, J. B.; Firor, J. W.; Davenport, T. W. Facile Palladium-Catalyzed Cross-Coupling of Monoorganiczinc Halides with 3-Iodoanthranilonitriles. *Synthetic Communications* **1989***, 19*, 2265-2272.

(145) Bumagin, N. A.; Luzikova, E. V. Palladium Catalyzed Cross-Coupling Reaction of Grignard Reagents with Halobenzoic Acids, Halophenols and Haloanilines. *Journal of Organometallic Chemistry* **1997***, 532*, 271-273.

(146) Hilbert, G. E.; Jansen, E. F. Action of Alkali and Ammonia on 2,4-Dialkoxypyrimidine. *Journal of the American Chemical Society* **1934***, 56*, 134-139.

(147) Whittaker, N. 336. Pyrimidine. *Journal of the Chemical Society, Chemical Communications* **1953**, 1646-1649.

(148) Strekowski, L. Synthesis with Pyrimidine-Lithium Compounds. Part II. 2,6-Bis(methylthio)-4,5-didehydropyrimidine as Intermediate in the Synthesis of Biopyrimidines. *Rocziniki Chem.* **1975***, 49*, 1693-1705.

(149) Strekowski, L. Syntheses with Pyrimidine-Lithium Compound. Further Study on the Formation of Bipyrimidines. *Bulletin De L'Academie Polon Des Sciences. Serie des Sciences Chemiques* **1976***, 24*, 29-35.

(150) Miyura, N.; Suzuki, A. Palladium Catalyzed Cross-Coupling Reactions of Organoboron Compounds. *Chem. Rev.* **1995***, 95*, 2457-2483.

(151) Faul, M. M.; Ratz, A. M.; Sullivan, K. A.; Trankle, W. G.; Winneroski, L. L. Synthesis of Novel Retinoid X Receptor-Selective Retinoids. *Journal of Organic Chemistry* **2001***, 66*, 5772-5782.

(152) Giroux, A.; Han, Y.; Prasit, P. One Pot Biaryl Synthesis via in situ Boronate Formation. *Tetrahedron Letters* **1997***, 38*, 3841-3844.

(153) Ishiyama, T.; Itoh, Y.; Kitano, T.; Miyura, N. Synthesis of Arylboronates via the Palladium(0)-Catalyzed Cross-Coupling Reaction of Tetra(alkoxo)diboranes with Aryl Triflates. *Tetrahedron Letters* **1997***, 38*, 3447-3450.

(154) Hirota, K.; Kitaoka, S.; Shimada, K.; Maki, Y. Pyrimidines. 54. Ring transformation of 5-(2-carbamoylvinyl)uracil derivatives to 5-carbamoylpyridin-2-ones. *Journal of Organic Chemistry* **1985***, 50*, 1512-1516.

(155) Farina, V.; Krishnamurthy, V.; Scott, W. J. The Stille Reaction. *Org. React. (N.Y.)* **1997***, 50*, 1-652.

(156) Rao, C. J.; Knochel, P. A Direct Preparation of Vinylogous Acyl Anion Equivalents. *Journal of Organic Chemistry* **1991***, 56*, 4593-4596.

(157) Schinazi, R. F.; Prusoff, W. H. Synthesis of 5-(Dihdroxyboryl)-2'-deoxyuridine and Related Boron-containing Pyrimidines. *Journal of Organic Chemistry* **1985***, 50*, 841-847.

(158) Wellmar, U.; Hornfeldt, A.-B.; Gronowitz, S. Synthesis of Various 5-(Bromoaryl)-substituted Uracils. *Journal of Heterocyclic Chemistry* **1995***, 32*, 1159-1163.

(159) Koshkin, A. A.; Fensholdt, J.; Pfundheller, H. M.; Lomholt, C. A Simplified and Efficient Route to 2'-O, 4'-C-Methylene-Linked Bicyclic Ribonucleosides (Locked Nucleic Acid). *Journal of Organic Chemistry* **2001***, 66*, 8504-8512.

(160) Krenitsky, T. A.; Freeman, G. A.; Shaver, S. R.; Beacham III, L. M.; Hurlbert, S. et al. 3'-Amino-2'.3'-dideoxyribonucleosides of Some Pyrimidines:

Synthesis and Biological Activities. *Journal of Medicinal Chemistry* **1983***, 26*, 891-895.

(161) Watanabe, K. A.; Su, L. T.; Pankiewicz, K. W.; Harada, K. Novel Ring Transformation Reactions and their Applications to the Synthesis of Potential Anticancer Heterocyclic Compounds. *Heterocycles* **1984***, 21*, 289-307.

(162) Ogilvie, K. K.; Nghe, N.-B.; Gillen, M. F.; Radatus, B. K.; Cheriyan, U. O. et al. Synthesis of a Purine Acyclonucleoside Series Having Pronounced Antiviral Activity. The Glycopurines. *Can. J. Chem.* **1984***, 62*, 241-252.

(163) Watanabe, K. A.

(164) Plavec, J.; Chattopadhyaya, J. Comparative Assessment of Structure and Reactivity of Wyosine by Chemistry, Spectroscopy and *ab initio* Calculations. *Tetrahedron* **1996***, 52*, 1597-1608.

(165) Bauer, H.; Tabor, H. Cyanomethylimidazole and Imidazoleacetic Acid Hydrochloride. *Biochemical Preparations* **1957***, 5*, 97-100.

(166) Bennua-Skalmowski, B.; Krolikiewicz, K.; Vorbruggen, H. A New Simple Nucleoside Synthesis. *Tetrahedron Letters* **1995***, 36*, 7845-7848.

(167) Matthews, H. R.; Rapoport, H. Differential of 1,4- and 1,5-Disubstituted Imidazoles. *Journal of the American Chemical Society* **1973***, 95*, 2297-2303.

(168) Kreutzberger, A.; Wiedemann, D. 5-Substituierte 4-Aminopyrimidine durch Aminomethinylierung von Acetonitrilen. *Liebibs Ann Chem* **1977**, 537-544.

(169) Gacek, M.; Underheim, K. Alkylated 2- and 4-Thiouracils, Synthesis and HPLC Separation. *Acta Chemica Scandinavica B* **1982***, 36*, 15-18.

(170) de Bourguignon, M. J.; Boucly, J. M.; Clinet, J. C.; Uueguiner, G. Chimie Organique - Synthesis de Thienylpyrimidines et Thienylpyrazine. *C. R. Acad. Sc. Paris* **1975***, 281*, 1019-1022.

(171) Palmer, J. L.; Abeles, R. H. Mechanism for enzymatic thioether formation. Mechanism of action of S-adenosylhomocysteinase. *J Biol Chem* **1976***, 251*, 5817-5819.

(172) Riddles, P. W.; Blakeley, R. L.; Zerner, B. Reassessment of Ellman's reagent. *Methods Enzymol.* **1983***, 91*, 49-60.

(173) Nygaard, P.; Duckert, P.; Saxild, H. H. Role of adenine deaminase in purine salvage and nitrogen metabolism and characterization of the ade gene in Bacillus subtilis. *J Bacteriol* **1996***, 178*, 846-853.

(174) Matsui, H.; Shimaoka, M.; Kawasaki, H.; Takenaka, Y.; Kurahashi, O. Adenine deaminase activity of the yicP gene product of Escherichia coli. *Biosci Biotechnol Biochem* **2001***, 65*, 1112-1118.

(175) Hara, H.; van der Plas, H. C. On the Amination of Azaheterocycles. A New Procedure for the Introduction of an Amino Group. *Journal of Heterocyclic Chemistry* **1982***, 19*, 1285-1287.

VITA

Samer Salim, son of Abu Salim and Zarrin Salim, was born in Belfast, Northern Ireland on May 11, 1973. He graduated from Northside High School in Fort Worth, Texas, USA, in 1990. He started his undergraduate career at University of Texas at Austin, in Austin, Texas, USA in 1990-1993. In 1993, he transferred to the University of Houston in Houston, Texas, USA and obtained his Bachelors of Science degree in Chemistry in 1996. He entered the Georgia Institute of Technology in Atlanta, GA, USA in September, 1998 whereby he studied under the direction of Professor Katherine L. Seley.